University of Southern Queensland

Faculty of Health, Engineering & Sciences

Analysis of bridges subjected to flood loadings based on different design standards

A dissertation submitted by

Bradley Jordan

In fulfilment of the requirements of

Course ENG4112 – Research Project

Towards the degree of

Bachelor of Engineering (Honours) (Civil)

Submitted: October, 2015

ABSTRACT

The need to design bridges to withstand flood and debris loads has long been recognised in Australia, however bridges are still failing to live their entire design life when subjected to extreme flooding events. This research project presents a structural evaluation of bridges when subjected to the current flood loadings from design standards around the world. A case study bridge has been selected to apply the flood loads on. The case study bridge chosen is Tenthill Creek Bridge, located within the Lockyer Valley Region.

The flood loadings that were identified from the design standards were drag, lift and debris forces as well as log-impact loads. Static components that were also included in the model were hydrostatic pressure as well as buoyancy. The structural components of the bridge that were identified to be analysed were the piers and superstructures. The structural evaluation has been performed using a finite element analysis (FEA) software package, Strand7. The model was analysed by Strand7's linear static analysis. Displacement and stress concentration results were then produced and analysed. The results indicate that the Australian Standards produced, on average, 20% more adverse effects in comparison to the international standards. The results indicate that no recommendations could be made for the Australian Standards, based on the results produced by the International Standards. Further work will need to be conducted if specific recommendations are to be made for the Australian Standards.

University of Southern Queensland

Faculty of Health, Engineering and Sciences

ENG4111/ENG4112 Research Project

LIMITATIONS OF USE

CERTIFICATION OF DISSERTATION

I certify that the ideas, designs and experimental work, results, analyses and conclusions set out in this dissertation are entirely my own effort, except where otherwise indicated and acknowledged.

I further certify that the work is original and has not been previously submitted for assessment in any other course or institution, except where specifically stated.

Full name: Bradley Jordan

Student Number: 0061033342

ACKNOWLEDGMENTS

I would like to acknowledge my supervisors Weena Lokuge and Karu Karunasena, as well as Buddhi Wahalathrantri, for their constant guidance and support throughout this project. This project would not be possible without their guidance and support.

TABLE OF CONTENTS

LIST OF FIGURES

LIST OF TABLES

LIST OF APPENDICES

CHAPTER 1 INTRODUCTION

1.1 Chapter overview

This chapter provides some background information to introduce the reader to the project topic, explains the relevance importance of this thesis topic and also outline the aims and objective associated with this thesis. This chapter also outlines the structure of the thesis.

1.2 Background

The Lockyer Valley region is a local government area of rich farmlands in the West Moreton region of South East Queensland. It lies to the west of Brisbane, particularly in-between the cities Toowoomba and Ipswich.

Figure 1.1 - Lockyer Valley location

(Queensland 2014)

The Lockyer Valley experiences a sub-humid and subtropical climate with long hot summers and short, mild winters. Rainfall is summer dominant with the average annual rainfall in the valley centre being about 780mm; this makes this the driest part of the South East Queensland region (Galbraith 2009). However, rainfall is highly variable and unpredictable; droughts are experienced regularly however there have been some extreme flooding events, the worst of which occurred in November 2008 and January 2011. As a result, about 85% of council-owned bridges were either completely gone or partially destroyed (Maeseele 2011). This calls for immediate attention to the way in which bridges are being designed and suggests that immediate revisions should be made to ensure that the bridges live for the entire duration of their expected design life.

1.3 Project aim

This project seeks to simulate the behaviour of bridges subjected to flood loadings from different available bridge design standards around the world. In particular, emphasis will be placed on bridges in the Lockyer Valley region. The aim of this project is to simulate the behaviour of a bridge in the Lockyer Valley Region under an extreme flooding event and determine if recommendations can be made for the Australian Bridge Design Standards, AS5100.

1.4 Method of investigation

The main method of investigation for this project is to identify flood loadings from different design standards and perform a detailed simulation. Firstly, the Australian Bridge Design Standards, AS5100, 2004 will be investigated, where flood loadings and traffic loads will be identified as well as the relevant load combinations. These loadings will be simulated on a case study bridge within the Lockyer Valley Region that is prone to extreme flooding events. The simulation will be performed in the Finite Element Analysis Software Package, Strand7. A full, comprehensive analysis will be conducted on the Australian Standards based on different submergence conditions to identify the most critical loading condition. The analysis will be conducted on different types of flooding events, mainly a partial submergence condition (this is to see the effect of traffic loads) and various full submergence conditions (this will be purely flood loads). There will be various full submergence conditions tested to determine if the flood height or velocity has a more adverse effect, the velocity conditions test the dynamic components while the flood height conditions test the static components of a flooding event.

To determine if recommendations can be made to the Australian Standards, an analysis will also be conducted on three International Bridge Design Standards, however they will not be full, comprehensive simulations like the Australian Standards. The analysis for the International Standards will be performed on the most critical loading condition identified from the analysis performed on the Australian Standards. The results will then be analysed and comparisons will be made based off stress concentration and displacement results.

1.5 Project Objectives

The specific objectives of this project are:

1) Research literature and background information relating to the different types of bridges, including the different construction practices used, as well as natural disasters
2) Research and compare bridge design standards from around the world and identify flood loadings and load combinations that need to be taken into consideration for the design of a bridge in areas prone to flooding
3) Simulate the behaviour of a small, simple bridge subjected to the identified flood loadings
4) Identify a more complicated, realistic bridge in the Lockyer Valley Region that is prone to extreme flooding events and collect available data on the bridge
5) Simulate the behaviour of the bridge subjected to different flood loadings from the available design standards
6) Draw appropriate conclusions as to how the Australian Bridge Design Standards perform in a flooding event in comparison to different standards around the world
7) Make recommendations for to the Australian bridge design standards, AS5100 based on these results

1.6 Structure of this thesis

The document is structured as follows:

1) Chapter 1 – Introduction. This chapter introduces the reader to the principle reasons for the commencement of this project.
2) Chapter 2 – Literature review. This chapter introduces the reader to the different types of bridges used around the world and for which particular purpose and specific material bridge is used for. The three main materials of bridges that will be investigated are timber, steel and concrete bridges. Concrete bridges will be the main focus for this project and will be investigated into much more detail. It also introduces the reader to the different types of natural disasters including earthquakes, cyclones, flooding and bushfires. Flooding will be the main focus for this project as it is the

most common and unpredictable natural disaster. Examples of recent flooding events within Australia will also be provided to illustrate how much damage can be done in a flooding event. Also, background information will be given on the general forces exhibited during a flooding event.

3) Chapter 3 – Australian Bridge Design Standards. This chapter outlines the different flood loadings that should be taken into consideration when designing a bridge within a flood prone area by analysing the different flood loads used within the Australian Bridge Design Standards, AS5100, 2004. Flood loads are identified, as well as traffic loads and load combinations.
4) Chapter 4 – International Bridge Design Standards. This chapter outlines the relevant flood loadings from international bridge design standards around the world. The three standards that have been chosen are the British Design Standards, Ba 59/94, the Indian Code of Practice, 2014 as well as the American Design standards, AASHTO LFRD Bridge Design Specifications, 2012. Flood loadings and load combinations will be identified.
5) Chapter 5 – Project Planning – Methodology. This chapter describes the methods that will be used to complete the project as well as the resources required and the associated risks involved. The chapter also identifies the complex bridge, located within the Lockyer Valley Region that will be used for the main simulation of the project. All of the required information to solve for the flood loads are presented such as the location, details, geometry and ground profile of the bridge of interest. Finally, the streamflow data is presented (the flood depths and flood velocities).
6) Chapter 6 – Simulation. This chapter explains the design process of each simulation (the simple bridge deck and the complex bridge) model such as the creation of the model, model restraints, the meshing of the models and what material properties were used to create the models in Strand7. The simple bridge model is shown to demonstrate the learning process of performing detailed analyses in Strand7. These skills were then applied to develop the complex bridge model.
7) Chapter 7 – Results and discussion. This chapter presents the results that were obtained from the detailed simulation and a detailed comparison is performed to determine how the Australian Standards perform in comparison to the International Bridge Design Standards.
8) Chapter 8 – Conclusions and further work. This chapter presents the main conclusions that were drawn from this project and shows how well the project objectives were

achieved. Based on the validity of the results obtained, recommendations are made for future work that can be conducted to build on this project.

CHAPTER 2 LITERATURE REVIEW

2.1 Chapter overview

This chapter outlines the relevant background information that is related to the thesis topic. In this chapter, background information will be presented on the different types of concrete bridges, different materials used, then expanded on concrete bridges as this is the main focus for the project. Information will then be given on natural disasters and then expanded on flooding events as it is the main focus for this thesis. Concrete bridges and flooding events will then linked together; examples of previous flooding event on bridges are given. Finally, the main forces exhibited on bridges during a flooding event are listed as these will be used later on in the simulation process.

2.2 Bridges around the world

A bridge is a structure built to span obstacles such as rivers, gorges, narrows, straits and valleys. Bridges are used worldwide and have always played a vital role in the history of human settlement. Different types of bridges include arch bridges, beam bridges, truss bridges, cantilever bridges, suspension bridges, cable-stayed bridges and many more, each of which have their own advantages. The main materials currently used for the construction of bridges are concrete, steel and timber. Concrete bridges will be the main focus for this project as they are the most common material used for bridge construction.

2.2.1 Concrete

Concrete is an artificial stone made from a mixture of water, sand, gravel and a binder (most commonly cement); the mixture contents depend on the desired properties. Concrete in its original state has a very high compressive strength but very low shear and tensile strength. Two ways to combat this weakness is to add steel reinforcement bars in the pour, also known as reinforced concrete. This method can be taken one step further and involves the method of prestressing the concrete, otherwise known as prestressed concrete.

2.2.1.1 Reinforced Concrete

Most modern small bridges are of reinforced concrete construction and nearly all modern bridges contain some elements of reinforced concrete. Reinforcement is provided by means of steel bars in reinforced concrete construction to provide strength and ductility. The main steel reinforcement bars provide flexural strength while the stirrups provide the shear strength; other reinforcement in the form of lateral ties, spiral reinforcement in the anchorage zone etc. are part of non-prestressing steel present in the structure. Typical properties of these steel vary from country to country. In Australia, grade of 500 MPa (N500) steel bars are commonly used (USQ 2014).

Figure 2.1 - Reinforced concrete slabs

(Pujol 2015)

2.2.1.2 Prestressed Concrete

> "Prestressed concrete is a special category of reinforced concrete where an initial compressive force is applied to the structural elements to eliminate the internal tensile forces. This eliminates the possibility of cracking when subjected to applied loads. With the uncracked cross section, the concrete section can be fully utilised and accordingly, higher strength and stiffness can be obtained from the same section (compared to a RC section)." (USQ 2014)

Pre-stressed concrete is by far the most used construction material in the industry, including bridges over reinforced concrete. The benefits of prestressing are:

- Cracking is virtually non-existing
- Significantly reduces deflection
- Member sections are smaller than reinforced concrete sections for the same imposed loads

(Constructor 2014)

Figure 2.2 - Prestressed concrete girder box

(Hanes 2012)

There are two methods for prestressing concrete, these are:

1. Pre-tensioned concrete
2. Post-tensioned concrete

Pre-tensioning is the process of prestressing the concrete before casting. The method consists of placing steel tendons in anchors and then applying a tensile force. The concrete is then cast and cured and the steel tendons are released from the anchors and the prestress is transferred. The process can be illustrated in the following figure:

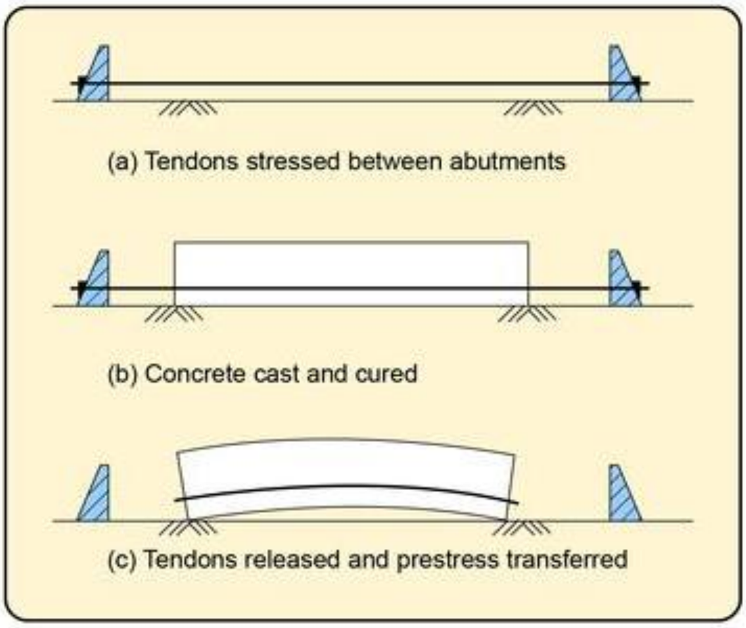

Figure 2.3 - Pre-tensioned concrete

(USQ 2014)

Post-tensioning is the process of prestressing the concrete at some point in time after casting. Hollow ducts are created in the casting process for the steel tendons. When the steel tendons are inserted into the ducts, they are locked with mechanical anchors and stressed. After this is complete, the tendons are normally grouted in place. This method can be illustrated below:

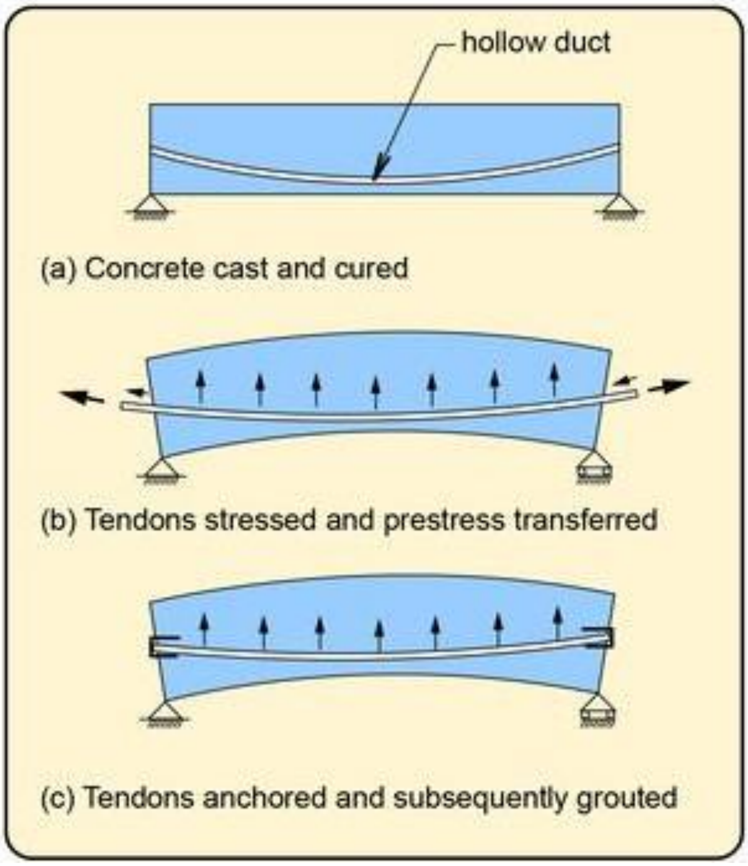

Figure 2.4 - Post-tensioned concrete

(USQ 2014)

The different concrete elements of a bridge can be found in appendix B.

2.2.2 Steel

After concrete, steel bridges are the most commonly constructed bridges, from the very large to the very small. Steel is a highly versatile and effective material for bridge construction, able to carry various loads in tension, compression and shear. Structural steelwork is used in the superstructures of bridges from the smallest to the largest. The different types of steel bridges are: beam bridges, arch bridges, suspension bridges, truss bridges and stayed girder bridges. (Corus 2007).

Listed below are some of the advantages that steel can offer:

- High quality prefabrication
- High strength to weight ratio
- Fast construction
- Versatility

- Easy to modify and repair
- Recyclable
- Durability
- Aesthetically pleasing

(Corus 2007)

Figure 2.5 - A typical steel truss bridge

(REIDsteel 2015)

2.2.3 Timber

> “The strength of wood is highly dependent upon the orientation of the applied load in relation to the grain direction of the wood. This is one of the most important characteristics of wood as an engineering material: the resistances and the elastic properties of wood differ greatly in different directions, thereby classifying wood as an anisotropic material.” (NSW 2008)

Wood is much different to steel and concrete in the way that it is not weak in a specific loading case (mainly tension, compression and shear) but rather its strength depends on the orientation of the fibres within the wood. Wood is at its strongest in the longitudinal direction (grain direction).

Timber bridges are very uncommon at present due to the significant advantages of steel and concrete bridges. Due to the weak structure of timber, it is generally only built in areas with fairly small imposed loads (lightly populated areas).

Figure 2.6 - A typical timber truss bridge

(NSW 2008)

2.3 Concrete Bridges

2.3.1 General terminology

Most of these terminology definitions have been obtained from the Lichtenberger Engineering Library (2015).

Abutment: That part of a pier from which an arch springs. A structure sustaining one end of a bridge span and at the same time supporting the embankment which carries the track or roadway.

Buckle: To bend in a lateral direction by a longitudinal pressure.

Corrosion: The disintegration of a substance by the action of chemical agents.

Creep: The tendency of a solid material to move slowly or deform permanently under the influence of mechanical stresses.

Expansion Bearing: A support at the end of a span where provision is made for the expansion and contraction of the structure.

Expansion Joint: A joint in which movement for expansion and contraction is allowed.

Fatigue: Deformation response over a long period of time caused by repeated cyclic loading.

Foundation: That portion of a structure, usually below the surface of the ground, which distributes the pressure upon its support. Also applied to the supporting material itself.

Girder: A beam or compound structure acting as a beam carrying principally transverse loads which develop normal reactions at the supports.

Pier: A structure, usually composed of masonry, which is used to transmit the loads from a bridge superstructure to the foundation.

Substructure: The part of any construction which supports the superstructure. The piers, pedestals, and abutments of a bridge or trestle.

Superstructure: That portion of a bridge or trestle lying above the piers, pedestals, and abutments. The part of a structure which receives the live load directly (e.g. girders, beams etc.).

Scour: A clearing out or removal of silt and sand in the bed of a stream by a strong current. To remove such material in that manner.

Thermal Shock: Thermal gradient causes different parts of an object to expand by different amounts.

Viaduct: An extended bridge of many spans, mainly over dry ground. Usually consists of alternate towers and open spaces or bays.

Wear: Erosion or sideways displacement from its original position on a solid surface performed by the action of another surface.

Yielding: The stress at which a material begins to deform plastically, unable to return to its original shape.

(Library 2015)

The following figure better illustrates the components of a typical bridge structure.

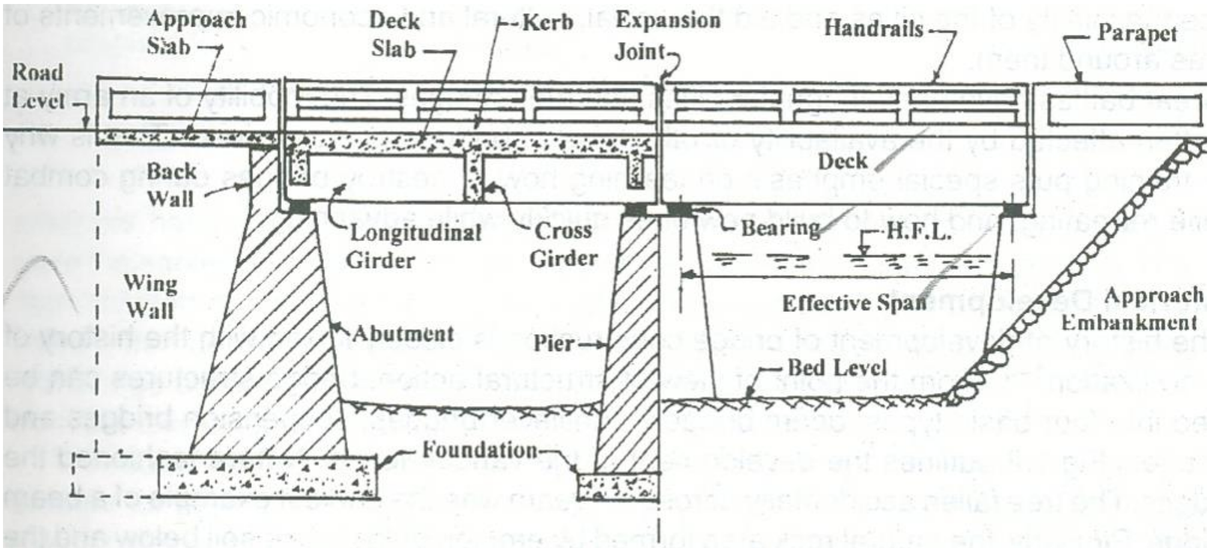

Figure 2.7 - Typical components of a bridge

(CivilDigital.com 2015)

2.3.2 Construction methods used

From the smallest, most simple bridge to inspiring bridges that span enormous gorges, each bridge has unique requirements and challenges faced during the construction process. The same bridge design may require completely different construction methods due to factors such as site restrictions and accessibility. Additionally, there may be more than one construction technique used on a single project to achieve the most efficient construction process. While there is no single construction method used for bridges, there are several broad categories that they fall under.

2.3.2.1 Falsework/staging

There is a common confusion between the difference of formwork and falsework. Groundforce (2015) describes formwork as "A structure which is usually temporary but can be whole of part permanent, it is used to contain poured concrete to mould it into required dimensions and support until it is able to support itself."

Groundforce (2015) also describes falsework as "any temporary structure, in which the main load bearing members are vertical, used to support permanent structures, used to support a permanent structure and associated elements during the erection until it is self-supporting."

These two methods can work together in some situations in which falsework can include temporary support structures for formwork, used to mould concrete to form a desired shape. This method of construction is generally used in spanning or arched elements in bridge construction.

Figure 2.8 - Falsework used for a long spanning concrete bridge

(PERI 2015)

2.3.2.2 Incremental Launching

Bridges have been constructed using the incremental launching method for many years and is a very popular method when constructing bridges over an inaccessible or environmentally protected obstacle. (LaViolette, Wipf, Lee, Bigelow &Phares 2007) describes this method as follows:

> "In this method of construction, the bridge superstructure is assembled on one side of the obstacle to be crossed and then pushed longitudinally (or "launched") into its final position. The launching is typically performed in a series of increments so that additional sections can be added to the rear of the superstructure unit prior to subsequent launches."

The incremental launching method is particularly suited to the construction of continuous post-tensioned multi-span bridges.

Figure 2.9 - Incremental launching of a bridge

(BBR 2015)

2.3.2.3 Span-by-span

Span-by-span bridge construction offers a very high speed of construction. The two different types of this method is precast and in-situ, although precast is by far the most common method of the two. The first step is to erect the segments for the entire span onto a temporary erection girder, spanning between two piers. Then, the Post-tensions tendons are installed and stressed; this allows the segments to span on their own. Finally, the erection girder is advanced into place for the erection of the next span. The most common use of span-by-span construction is to build long viaducts with spans ranging from 25-45m.(BBR 2015)

Figure 2.10 - Span-by-span construction of a bridge

(Rohleder 2015)

2.3.2.4 Balanced cantilever

> "Free cantilevering is a method of construction where a structure is built outward from a fixed point to form a cantilever structure, without temporary support, using staged cast-in-situ construction. When two opposing free cantilever structures are attached as a single structure and erected in the same step, it is known as 'balanced cantilever'." (BBR 2015)

There are two different methods of balanced cantilever bridge construction which are cast-in-situ and precast. Cast-in-situ is the process whereby segments are progressively cast in their final positions on site. However, for precast construction, the segments have already been prefabricated at a casting plant and then transported on-site and erected as a complete unit in their final positions. They can be precast on-site or at a remote facility.

The balanced cantilever method is often appropriate and cost-effective for the construction of long span concrete bridges in situations where height, topography and/or geotechnical conditions render the use of the conventional formwork method uneconomical.

2.3.3 Types of bridges

Throughout history, engineers and architects have devised many ways of building bridges, there are many different designs that all serve a unique purpose, each of which apply to different situations. Bridges may be classified by how the forces of tension, compression, bending, torsion and shear are distributed throughout the structure. Most bridges will employ all of the principal forces to some degree but in most circumstances only a few will be dominant.

2.3.3.1 Arch bridges

Arch bridges are one of the oldest types of bridges and have been around for thousands of years, mainly because of their simplicity and effectiveness. They are still a very common type of bridge used within the industry. Arch bridges derive their strength from the fact that vertical loads on an arch generate compressive forces in the arch ring. This is great for concrete bridges as concrete is very weak in tension. The arch cannot be too long however or the arch may collapse in on itself, this is when several arches should be used.

Figure 2.11 – Long-span arch bridge

(Group 2015)

2.3.3.2 Reinforced slab bridges

For short spans, a reinforced concrete slab, generally cast in-situ rather than precast, is the simplest design. It is also cost-effective, since the flat, level soffit means that falsework and formwork are also simple. The steel reinforcement is also uncomplicated. With larger span bridges, the reinforced slab has to be thicker to carry the extra stresses. This extra self-weight of the slab itself can then become a problem. This can be solved in one of two ways; the first is to use prestressing techniques and the second is to reduce the self-weight of the slab by including voids, often expanded polystyrene cylinders. Voided slabs are generally more economical than prestressed slabs up to about a 25m span. (Group 2015)

Figure 2.12 - Reinforced slab bridge

(Group 2015)

2.3.3.3 Beam and slab bridges

Beam and slab bridges are one of the most common types of concrete bridges thanks to the success of standard precast prestressed concrete beams being developed, which were then later developed to the 'Y' beam. They are simple, economic, quick to erect and are widely available in the industry. The precast beams are placed on the supporting piers or abutments, usually on rubber bearings which are maintenance free. An in-situ reinforced concrete deck slab is then cast on permanent shuttering which spans between the beams. (Group 2015)

Figure 2.13 - Beam and slab bridge in construction

(Group 2015)

2.3.3.4 Box girder bridges

For spans greater than around 45 metres, prestressed concrete box girders are the most common method of concrete bridge construction. The main spans are hollow and the shape of the 'box' will vary from bridge to bridge and along the span, being deeper in cross-section at the abutments and piers because they are taking a considerable amount of the stresses and shallower at the midspan due to the significant increase in stress.

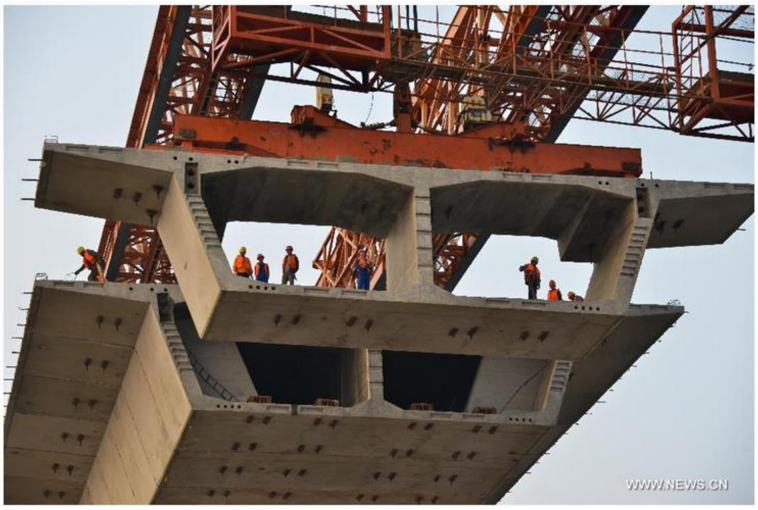

Figure 2.14 - Box girder bridge in construction

(Construction 2015)

2.3.3.5 Integral bridges

One of the difficulties in designing any structure is deciding where to put the joints. These are necessary to allow movement as the structure expands due to the heat in summer and contracts during the cold of winter. Previous expansion joints and bearings used in these type of bridges proved to be very unreliable and not very cost effective, therefore more and more bridges are being built without either. Such structures, called 'integral bridges', can be constructed with all types of concrete deck. They are constructed with their decks connected directly to the supporting piers and abutments. Thermal movement of the deck is accommodated by flexure of the supporting piers and horizontal movements of the abutments, with elastic compression of the surrounding soil. Already used for bridges that span up to 60m, the integral bridge is becoming increasingly popular as engineers and designers find other ways of dealing with thermal movement. (Group 2015)

2.3.3.6 Cable-stayed bridges

For very large span bridges, one solution is the cable-stayed bridge. As characterized by the Dee River Crossing where all elements are concrete, the design consists of supporting towers carrying cables which support the bridge from both sides of the tower. Generally, cable-stayed bridges are built using a form of cantilever construction which can be either in-situ or precast. (Group 2015)

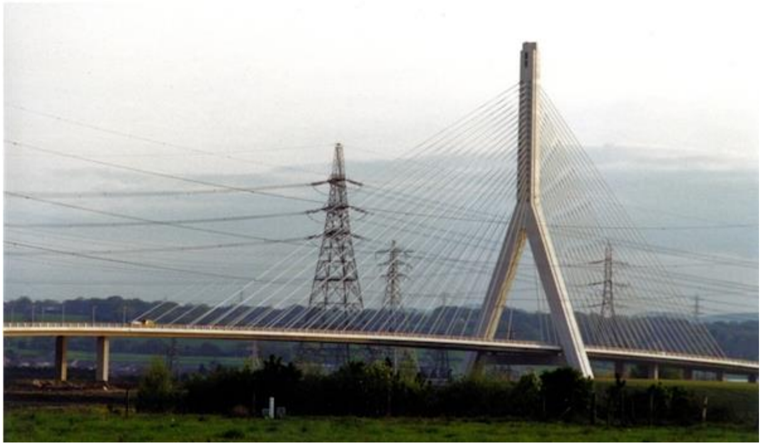

Figure 2.15 - Dee River Crossing cable-stayed bridge

(LUSAS 2013)

2.3.3.7 Suspension bridges

> "A suspension bridge is fundamentally simple in action: two cables are suspended between two supports ('towers' or 'pylons'), hanging in a shallow curve, and a deck is supported from the two cables by a series of hangers along their length. The cables and hangers are in simple tension and the deck spans transversely and longitudinally between the hangers. In most cases the cables are anchored at ground level, either side of the main towers; often the side spans are hung from these portions of the cables." (SteelConstruction.info 2015)

While suspension bridges mainly consist of steel, the concrete used plays a vital role. There will be massive foundations, usually embedded in the ground, that support the weight and cable anchorages. Also, the abutments provide the vital strength and ability to resist the enormous forces. Finally, the superstructures carrying the upper ends of the supporting cables are generally made from reinforced concrete. (Group 2015)

Figure 2.16 - Suspension bridge

(Group 2015)

2.3.4 Design life

As described in the Australian Standards AS 5100.1 - 2004 – *Bridge Design, Part 1: Scope and General Principles*

“The design life of structures covered by this standard shall be 100 years.

Elements such as bearings and expansion joints shall be designed to have a long life, compatible with the design life of the bridge. Provision shall be made for easy removal and replacement of such elements, and any fixings shall be detailed to be reusable.” (Standards 2004a)

2.3.5 Modes of failure

Some of the most expensive engineering projects in history have involved building bridges. Although the fundamentals of bridge-building have been established for thousands of years, every bridge presents complicated factors that must be taken into consideration, such as the geology of the surrounding area, the amount of traffic, weather, construction materials and much more. Occasionally these factors are miscalculated or not taken into account, or something occurs that the bridge designers didn't expect. The result can be tragic. Below are the possible broad failure modes that can occur within concrete bridge structures.

2.3.5.1 Mechanical failure

Mechanical failures often occur due to an overload of stress, causing a component of a bridge to fracture or even fail. Mechanical failure is a common failure mode which generally occur as a result of buckling, corrosion, creep, fatigue, fracture, impact, mechanical overload, cracking, thermal shock, wear and yielding. It is common for mechanical failure to occur due to a combination of these failure modes.

2.3.5.2 Scouring

Iqbal (2013) defines scouring as “a process due to which the particles of the soil or rock around the periphery of the abutment or pier of the bridge spanning over a water body, gets eroded and removed over a certain depth called scour depth”. Scouring generally occurs when the velocity of the flowing water increases beyond the limit that the soil particles can easily handle.

Scouring is a major issue that occurs during a flooding event and is usually initiated at the nose of the piers or at the sharp bends. Scouring can compromise the structural integrity and in some situations cause failure. It has been estimated that over 60 % of the highway bridges are being collapsed due to scouring (Iqbal 2013).

Figure 2.17 - Scouring around a bridge foundation

(Johnson 2015)

2.3.5.3 Deterioration/spalling

Concrete spalling is a form of deterioration within a reinforced or prestressed concrete system. This type of deterioration for a concrete structural component occurs at the surface where concrete will decompose, often leaving any steel reinforcement visible and open to additional corrosion. Spalling is typically a result of reinforcement corrosion or joint failure.

Concrete spalling is a serious and common issue within bridge structures. It begins at either the concrete or steel reinforcement level, where chemical-physical effects will occur. Typical forms of reaction include: calcium chloride with concrete, sulphate attack on concrete, chloride penetration to steel, and the carbonation process (Friend 2013). Certain environments can intensify the process, so appropriate consideration must be taken in the design process.

Figure 2.18 - Deterioration of an overpass

(Friend 2013)

2.3.6 How they are maintained

Concrete structures gradually deteriorate over an extended period of time, requiring maintenance to be performed. It is generally a long-term process as the rate of deterioration is dependent on a number of different variables. These include the amount of time the structure has been in service, the specific function of the structure, the activities that are conducted within/on the structure, the environmental conditions in which the structure is situated in as well as the physical properties of the concrete used (Rashidi et al. 2010).

The most common problems encountered that require maintenance are corrosion of steel reinforcement, structural deficiency, chemical/acid attack, frost damage, fire damage, creep, internal reaction within the concrete, restrained movement, cracking and mechanical damage (Rashidi et al. 2010).These problems can develop suddenly or gradually over a long period of time.

A long, successful bridge program is based on a strategic, systematic and balanced approach. The U.S. Department of Transportation (2011) splits the maintenance of a bridge up into two broad categories, these are:

1. Preventative maintenance
2. Rehabilitation

2.2.3.1 Preventative maintenance

Preventative maintenance is intended to delay the need for costly reconstruction or replacement actions by applying preservation strategies on bridges as long as possible while they are still in good condition. This maintenance is typically applied to elements of components of a bridge with significant remaining useful life. Some examples of preventative maintenance activities are bridge washing/cleaning, sealing deck joints, facilitating drainage, sealing concrete, painting steel, removing channel debris, protecting against scour and lubricating bearings (U.S Department of Transportation 2011).

2.2.3.2 Rehabilitation

Rehabilitation is intended to restore the structural integrity of a bridge and correct major safety defects. Rehabilitation projects provide complete or near complete restoration of bridge elements/components. These projects generally require significant engineering resources, a lengthy completion schedule and are very costly. Some examples of bridge rehabilitation are deck replacement, superstructure replacement and strengthening (U.S Department of Transportation 2011).

2.4 Natural Disasters

2.4.1 Flooding

> "Floods are part of the natural water cycle or a "Hydrologic Cycle". In this natural cycle, the energy of the sun causes water to evaporate and form clouds, which move inland and become rain. This rain will then runoff either directly through the river systems or be absorbed into the soil to later form groundwater flow. Floods happen when the capacity of the rivers is not enough to carry the water that has entered the river network, and the banks overflow. " (BOM 2015)

Flooding is considered a complex, natural phenomenon due to its unpredictable nature. This is mainly due to the different factors that affect the size of flooding. Some examples are rainfall intensity, rainfall duration, how wet or dry the land is, topography and ground cover.

In Australia, the most common forms of flooding are:

- Slow-onset flooding
- Rapid-onset flooding
- Flash flooding

2.4.1.1 Slow-onset flooding

Slow-onset floods usually occur on inland rivers such as those found in central and western New South Wales, central and western Queensland and parts of Western Australia. As the name suggests, these floods are very slow to develop, take at least a week to develop and can persist for months. As heavy rain falls, the river is unable to accommodate the extra water storage and as a result, causes the river to overflow its banks. Slow-onset floods can result in damage to crops, livestock, rail lines, roads and property. (BOM 2015)

2.4.1.2 Rapid-onset flooding

Rapid-onset floods occur more quickly, but they can be more catastrophic since there is less warning than with slow-onset floods. Rapid-onset floods occur on rivers in coastal and mountain. Since these rivers drain more quickly than slow-moving inland rivers, flooding happens more quickly, generally over 2-3 days. (BOM 2015)

2.4.1.3 Flash flooding

Flash floods occur when the local drainage systems, either natural or man-made, cannot accommodate the extreme intensity of the rainfall. These floods occur with little or no warning, and as a result, are far more dangerous than the other two flood types. Flash floods are an increasing problem in cities which have poor drainage (BOM 2015). The 2011 Toowoomba floods is a prime example of how deadly they can be.

2.4.1.4 Bridge failures due to flooding

Floods can cause bridges to collapse in a few different ways. Severe floods, such as rapid-onset and flash flooding, can cause rivers and creeks to overflow, picking up debris such as trees, cars and parts of houses in the process. When the river passes under a bridge, the high water level smashes the debris into the bridge. The shear impact of the debris can cause immediate bridge failure, or the weight of the debris piled up combined with the immense force of the fast-flowing water pushing on it can cause the bridge to fail more gradually.

Flooding can also cause bridges to fail by gradually wearing away the earth around and underneath the bridge piers. This process is known as scouring, and is a serious issue to consider whenever bridge foundations are placed underwater. The natural flow of the water can produce scour over many years, but bridges are designed to withstand this. However, in the event of floods, the enormous increase in force and volume of water affecting the bridge and damage to the foundation soil can cause a bridge to collapse immediately or very gradually.

Figure 2.19 - Bridge collapse cause by Cumbria floods

(BBC 2009)

2.4.2 Earthquake

Earthquakes are caused by the Earth naturally releasing stress within the crust. This release of stress usually occurs when two blocks of earth slip past one another. As these plates move past each other, the stress is released as energy which moves through the Earth in the form of waves, which cause the surrounding surface to vibrate. (Subranami et al. 2014)

Earthquakes occur throughout the world, but the vast majority occurs along narrow belts which can be tens to hundreds of kilometres wide. These belts mark boundaries (also known as plate boundaries) on the planet's surface that are very geologically active. Intraplate earthquakes are less common. These take place in relatively stable areas, away from plate boundaries. This type of earthquakes generally originate at more shallow levels of the Earth's crust. Fortunately, due to the geological position, Australia is only prone to intra-plate earthquakes and hence doesn't have to worry a great deal about a disaster occurring. (Subranami et al. 2014)

Major earthquakes can cause dozens of buildings to collapse, but collapsed bridges are often the most visible signs of the havoc an earthquake can cause. Fortunately, earthquake-triggered bridge collapses are relatively rare. To combat this issue, bridges can be designed in earthquake-prone areas to withstand tremors (for example, Japan), or at least minimize the loss of life when one occurs. The following figure shows the devastating effects that earthquakes can have on bridges.

Figure 2.20 - Complete collapse of a bridge in Santiago due to an earthquake

(Subranami et al. 2014)

2.4.3 Cyclone

Cyclones are low pressure systems that form off the coast over warm tropical waters. They form when there is a combination of warm water (above 26.5°C), high relative humidity and increased precipitation. This in turn drives atmospheric energy to form a cyclone. They are extremely dangerous because they produce destructive winds, heavy rainfall (which can cause major flooding) as well as damaging storm surges that can inundate low-lying coastal areas (which can cause serious erosion of foreshores). Once formed, they can persist for many days and follow unpredictable paths. Cyclones will usually dissipate when they travel inland or across colder oceans as their driving forces decrease. (BOM 2015)

The Bureau of Meteorology (2015) has created five categories for identifying the severity of a cyclone, depending on the wind speed that they exert, these can be seen in table 2.1:

Table 2.1 - Cyclone categories

Category	Maximum wind speed (km/h)	Typical effects (indicative only)
1	<125	Negligible house damage. Damage to some crops, trees and caravans. May drag vessel moorings.
2	125-169	Minor house damage. Significant damage to signs, trees and caravans. Risk of power failure.
3	170-224	Some roof and structural damage. Some caravans destroyed. Power failure likely.
4	225-279	Some roofing loss and structural damage. Many caravans destroyed and blown away. Dangerous airborne debris. Widespread failures.
5	>280	Extremely dangerous with widespread destruction.

(BOM 2015)

The main effects of tropical cyclones include heavy rainfall, strong winds and large storm surges, all of which can lead to major damage to bridges. The sheer force of these strong winds can tear a bridge apart that are not built to withstand this. Furthermore, all of the loose debris that are picked up along the path of destruction can turn these debris into deadly flying projectiles and can cause very large impact damage. Also, the heavy rainfall associated with tropical cyclones can cause major flooding of rivers. The loose debris can also be thrown into these rivers; this accumulation of debris and increased flow rate of water along the channel can cause major damage to bridges. Finally, storm surges along coastal areas are generally the worst effect from cyclones and have the most potential for damage to infrastructure. The quick surge in sea level coupled with the heavy rainfall and strong winds can be lethal. Figure 2.21 shows how destructive cyclones can be to bridges that span cross rivers.

Figure 2.21 - A blown away bridge cause by Cyclone Hudhud

(Navy 2014)

2.4.4 Bushfire

Skwirk (2015) defines a bushfire as “a wildfire that burns out of control spreading across vegetated regions of bushland”. In order for a bushfire to be catastrophic, the right conditions must be present. Most bushfires happen in times when temperatures are high and the conditions are dry. Areas with dense undergrowth, as can be found in south-eastern Australia, are the most vulnerable to bushfire. New South Wales and Victoria experience bushfires more then any other part of Australia. Bushfires often start when dry winds blow inland from central Australia. While the winds bring dry weather, they also provide ventilation for the flames. Dry leaves and bark are especially flammable. Also, trees such as eucalypts are especially prone to fire because their leaves have a highly-flammable oil (Skwirk 2015).

The Queensland Government (2015) has created a rating scale to indicate the potential for danger that a fire poses, these can be seen in table 2.2:

Table 2.2 - Queensland fire danger categories

Category	Description
Low-Moderate	Fires can be easily controlled and pose little threat to people or property.
High	Fires can be controlled but loss of life and damage to property is still a threat.
Very High	Fires can be difficult to control with flames that may burn into treetops. Loss of life and damage to property is still a threat.
Severe	Fires may be uncontrollable and fast-moving with flames that may be higher than rooftops.
Extreme	Fires may be uncontrollable, unpredictable and fast-moving with flames in the treetops, and higher than rooftops.
Catastrophic	Fires are likely to be uncontrollable, unpredictable and very fast-moving with highly aggressive flames extending high above treetops and buildings.

(Government 2015)

Fire might be one of the rarest causes of bridge failure, but given the right circumstances, it may cause a great deal of damage to a bridge. This was a very big issue for bridge design when timber was still a popular choice of material and bushfires present a serious threat for timber bridges. Train bridges were especially susceptible to fire, because the steel wheels of the train on the steel rails of the track frequently sent sparks shooting onto the bridge. If it was very dry or the wind fanned the sparks, the bridge could catch fire and completely burn down.

Bridge fires can still currently cause major damage to bridges. Several modern bridges have also collapsed or been severely damaged due to fire. This is typically due to very large explosions, for example, the crash of a tanker truck carrying a large amount of a highly flammable substance like petrol. The crash may trigger an explosion and a blaze with such a high temperature, it can melt the steel used to build the bridge. In some situations, this can lead to complete failure, as illustrated in figure 2.22 when a 303m bridge in Asia was destroyed by a raging fire.

Figure 2.22 - Destruction of the Feng Yu Bridge in China

(Blake 2013)

2.5 Extreme flood events in Australia

2.5.1 Summer 2010/2011 Queensland flood events

The 2010/2011 summer in Queensland was not the wettest in history but was notable for the fact that over 80% of the state was declared a natural disaster area. The constant heavy rain throughout the summer ended with a climax when the category 5 Cyclone Yasi hammered northern Queensland. Cyclone Yasi had wind gusts up to 285km/h and caused a 5m tidal surge. (Pritchard 2013)

The most critical flooding event occurred on the 13th January 2011. Major flooding occurred throughout most of the Brisbane River catchment but the most severe flooding occurred in Toowoomba and the Lockyer Creek catchment. The flooding caused the loss of 23 lives in the Lockyer Valley and one in Brisbane; an estimated 18000 properties were inundated in the Brisbane CBD, Ipswich and along the Brisbane River Valley. (Honert & McAneney 2011)

The damage to the bridge network included:

- Two timber bridges requiring replacement due to severe flood damage
- One bridge registering 70 mm pier settlement.
- One concrete bridge downstream of the dams on the North Pine River system having 4m scouring at the river piers due to overtopping of the bridge. Subsequent load testing of the bridge showed there was significant reduction in the pile capacity of the bridge. It was determined that replacement of this bridge was the most economical outcome.
- A steel girder bridge on the Mitchell River requiring replacement due to scour of the piers.
- Scouring of numerous abutments spill-through embankments.
- Many bridge approaches being washed out.

(Pritchard 2013)

Lockyer Valley residents identified vegetation and debris remaining in waterways as a major concern should further flooding occur and were a major contributing factor to the damage of the bridge network (n.a). During the January flood, items picked up by the torrents of water were a serious danger to life and property as they were carried at speed downstream, and blocked the escape of water as they were caught against culverts and bridges. This blockage disrupted the natural flow of water and caused water to back up, resulting in further load damage and bridge scouring.

Figure 2.23 - Urban debris being thrown into a bridge

(Pritchard 2013)

Figure 2.24 - Scoured road approach at bridge abutment

(Pritchard 2013)

2.5.2 2013 Queensland flood events (Cyclone Oswald)

In January 2013, Tropical Cyclone Oswald passed over south-east Queensland and parts of New South Wales, resulting in widespread severe storms, flooding and water spouts.

In many places, the total monthly rainfall for January set new records. The damage from the severe weather resulted in a $2.4 billion bill. The flooding event was the highest recorded flood in the Laidley Creek and in the neighbouring catchments of Black Duck and Tenthill Creeks. (Leeson, Fulmer & Heron 2014)

Following this event, Jacobs Engineering Group Incorporated, Australia, undertook an inspection on all of the bridges that had been submerged by flood waters. A total of 28 bridges were inspected. Leeson, Fulmer and Heron (2014) observed two main issues, the first of which being that a majority of the bridges were impassable due to a significant build-up of debris. The other issue was that some the bridge approaches had been compromised and hence left the bridges inaccessible. Below are some examples of damage that was done to the bridge network that was identified by Leeson, Fulmer and Heron (2014):

Liftin Bridge

During the flooding event, it was estimated that approximately four meters of water passed over the Liftin Bridge, almost reaching the top of the banks. Damage to the bridge included stripping of the approach pavement, scouring of the approach embankment, build-up of debris on the bridge as well as substantial silt deposition on the approaches (Leeson, Fulmer & Heron 2014).

Figure 2.25 - Silt deposition on Liftin Bridge approach

(Leeson, Fulmer & Heron 2014)

Murphy Bridge

Murphy Bridge is a crossing of Lockyer Creek, with the bridge deck sitting slightly higher than the surrounding terrain. During the flooding event a flood water depth of approximately two meters was estimated on the northern approach. Damage to the bridge included stripping of the approach pavement, deposition of silt on the approaches as well as a significant build-up of debris on the bridge deck (Leeson, Fulmer & Heron 2014).

Figure 2.26 – Damage to the Murphy Bridge

(Leeson, Fulmer & Heron 2014)

The Willows Bridge

The Willows Bridge is another crossing of Lockyer Creek, with the bridge deck sitting slightly higher than the surrounding flood plain. During the flood event, it was estimated that the flood water depth was approximately two meters above the bridge level. Damage to the bridge included stripping of the approach pavement, complete scour through both abutments, removal of bridge rails and a build-up of debris on the bridge deck.

Figure 2.27 - Damage to the Willows Bridge

(Leeson, Fulmer & Heron 2014)

2.6 Forces exhibited during a flooding event

2.6.1 Hydrostatic pressure

When a solid is submerged in water, water pressure is applied to the object. The pressure at any particular point is a function of the height of the fluid in consideration and the fluid density. The basic pressure equation is:

$$P = \rho g h$$

Where:

ρ = water density (kg/m^3)

g = gravitational acceleration = 9.81 m/s^2

h = height of the fluid

Consider the submerged object below:

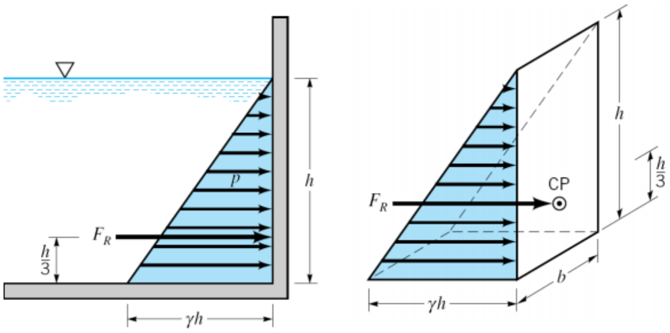

Figure 2.28 - Pressure prism of a submerged object

(Saskatchewan 2015)

The pressure prism can be equated to a resultant force, Fr, which acts through Cp, the centre of pressure. The reason that the pressure prism is represented as a triangle is due to the fact that the least amount of pressure being applied is at the water surface (h=0, P=0). As the distance is increased into the water, pressure is applied to the wall and the pressure above is applied to the point below, therefore the pressure keeps increasing in a linear fashion. The deeper an object in submerged in a fluid, the more pressure will be applied to the object at the deepest point.

2.6.2 Buoyancy

When an object is placed in water, the water exerts an upward force. Buoyancy can be defined as the upward force that an object feels from the water and when compared to the weight of the object, it is what makes an object float, sink or remain neutrally buoyant in the water. When the object floats, the buoyant force is greater than the downward force of the object.

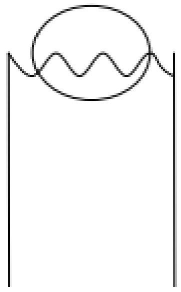

Figure 2.29 - A floating object

(Seaperch 2015)

When an object sinks, the weight of the object overcomes the upward buoyant force.

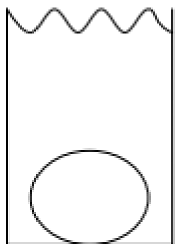

Figure 2.30 - A sinking object

(Seaperch 2015)

When an object is neutrally buoyant, the object has the same density as water and neither floats nor sinks.

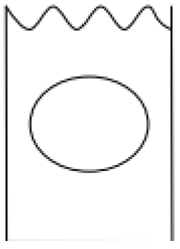

Figure 2.31 - A neutrally buoyant object

(Seaperch 2015)

In the event of a flooding event, due to the immense weight of bridges, the structure will most likely sink. In terms of the debris, these can vary greatly according to the type and size. For example, heavy logs may travel neutrally buoyant through the water and impact somewhere in the middle of a pier, whereas sticks, stones and other small debris will most likely travel along the top water level.

2.6.3 Impact force

In a flooding event, heavy objects such as logs can greatly damage a structure due to the impact force it exerts. The impact force of an object is a function of the mass of the object and the velocity of the moving body. The total impact force can be expressed as a work equation, as seen below:

$$Work = Force * distance$$

Where distance is the slow down distance and the force can be described using the kinematic energy equation:

$$F = \frac{1}{2}mv^2$$

Hence, the final impact force equation can be defined as:

$$F = \frac{\frac{1}{2}mv^2}{s}$$

Where:

m = mass of the object (kg)

v = velocity of the moving object

s = stopping distance before impact (m)

2.6.4 Drag force

When a moving body of fluid flows past a stationary object, the object resists the motion of this fluid. This force is known as drag. This can exist between a fluid and a solid surface. Drag is a function that is dependent on the velocity of the fluid. The following equation represents the typical drag force for a turbulent flowing body of fluid:

$$F_D = \frac{1}{2}\rho v^2 C_D A$$

ρ = fluid density (kg/m^3)

v = fluid velocity (m/s)

C_D = drag coefficient, which varies according to the shape of the object that is resisting the flow of water

A = cross-sectional area of the object that the fluid is acting on

In the event of a flood, there can be a drag force exhibited in more than one direction at a time. In this instance, the “drag force” is the drag force component that acts parallel to the direction of the flow, whereas the drag force component that acts perpendicular to the direction of flow is known as a “lift force”. It should be noted that the lift force can act both horizontally and vertically.

CHAPTER 3 AUSTRALIAN BRIDGE DESIGN STANDARDS

3.1 Chapter overview

This chapter identifies the flood loadings that are outlined in the Australian Bridge Design Standards, AS5100, 2004. Fluid forces will first be identified, for all submergence conditions. This will be followed by traffic loads for the partial submergence case. Finally, the recommended load combinations will be identified from the standards.

3.2 Introduction

The following information throughout this chapter has been extracted from AS 5100.2, 2004.

As described in *AS5100.1 - Part 1: Scope and General Principles* (Standards 2004a):

> *When a bridge crosses a river, stream or any other body of water, it shall be designed to resist the effects of water flow and wave action, as applicable. The design shall include an assessment of how the water forces may vary in an adverse manner under the influence of debris, log impact, scour and buoyancy of the structure.*
>
> *Tidal and wave actions shall be considered on bridges across large bodies of water, estuaries and open sea.*

3.3 Fluid forces on piers

The main forces that need to be taken into consideration in the design of bridge piers are the drag force and lift force, as shown in figure 3.1:

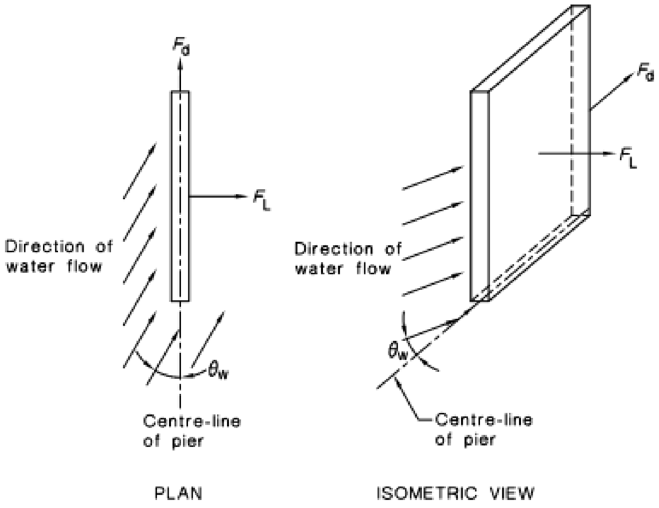

Figure 3.1 - Drag and lift forces on piers

(Standards 2004b)

3.3.1 Drag force

In bridge structures subjected to water flow effects, the design drag forces parallel to the plane containing the pier shall be calculated as follows:

$$F_{du}^{*} = 0.5 C_d V_u^2 A_d$$

Where:

C_d = drag coefficient, depending upon pier shape

In the absence of more exact estimates, C_d shall be calculated as follows:

C_d = 0.7 (semi-circular pier nosing)

= 1.4 (square end pier nosing)

= 0.8 (wedge, sharper than 90°, nosing)

V_u = mean velocity of water flow for ultimate limit states at the level of the superstructure or debris as appropriate

A_d = area,

= (thickness of pier normal to the direction of the water flow) x (height of water flow)

3.3.2 Lift forces

The design lift forces, perpendicular to the plane containing the pier shall be calculated as follows:

$$F_{Lu}^{*} = 0.5 C_L V_u^2 A_L$$

Where:

C_L = lift coefficient, which depends on the angle between the water flow direction and the plane containing the pier. In the absence of more exact estimates, it shall be calculated as follows:

$C_L = 0.9$ for $\theta_w \leq 30°$

$= 1.0$ for $\theta_w > 30°$

Where θ_w is the angle between the direction of the water flow and the transverse centre-line of the pier.

A_L = area,

= (width of the pier parallel to the direction of the water flow) x (height of the flow)

3.3.3 Debris forces

$$F_{du}^{*} = 0.5 C_d V_u^2 A_{deb}$$

Where:

A_{deb} = projected area of debris

C_d = drag coefficient, which can be obtained from figure 3.2:

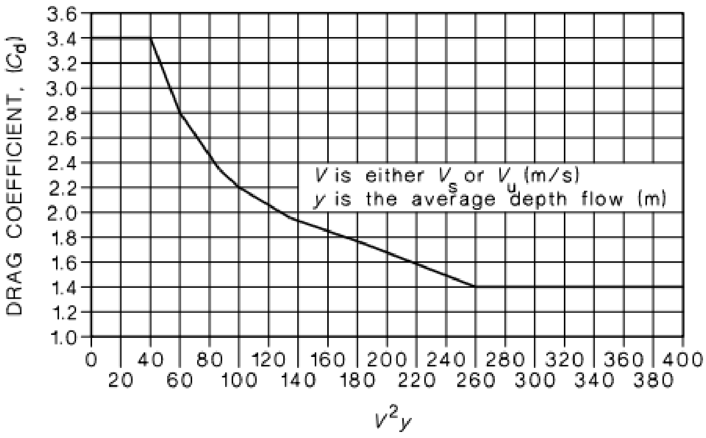

Figure 3.2 - Pier debris C_d

(Standards 2004b)

3.4 Fluid forces on superstructures

The main considerations that need to be taken into consideration for the design of bridge superstructures are drag forces, lift forces and the moment.

3.4.1 Drag force

$$F_{du}^{*} = 0.5 C_d V_u^2 A_s$$

Where:

A_s = wetted area of the superstructure, including any railings or parapets, projected on a plane normal to the water flow

C_d = drag coefficient, which can be obtained from figure 3.3:

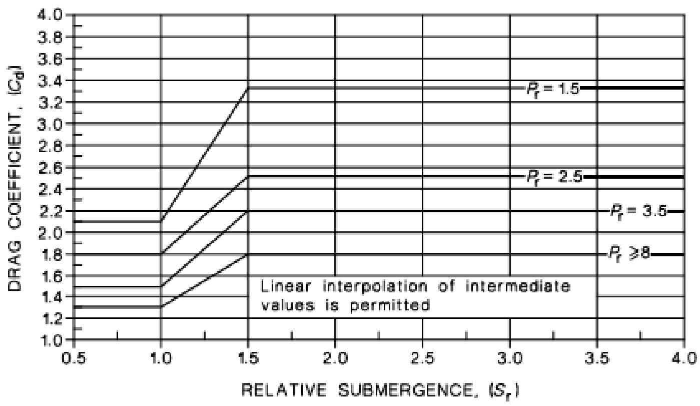

Figure 3.3 - Superstructure C_d

(Standards 2004b)

Relative submergence, $S_r = \frac{d_{wgs}}{d_{sp}}$

Where:

d_{wgs} = vertical distance from the girder soffit of the flood water surface upstream of the bridge

d_{sp} = wetted depth of the superstructure, including any railings or parapets, projected on a plane normal to the water flow

Proximity ratio, $P_r = \frac{y_{gs}}{d_{ss}}$

Where:

y_{gs} = vertical average distance from the girder soffit to the bed assuming no scour at the span under consideration

d_{ss} = wetted depth of the solid superstructure, excluding any railings but including solid parapets, projects on a plane normal to the water flow

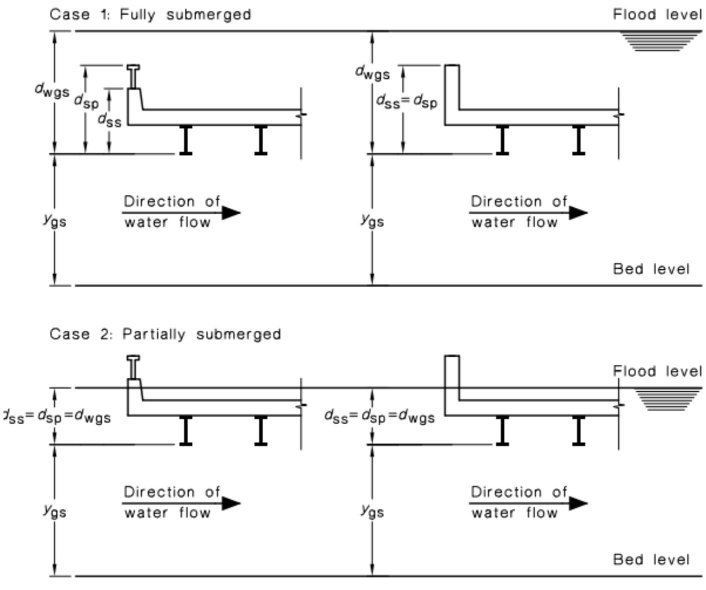

Figure 3.4 - Dimensions required

(Standards 2004b)

3.4.2 Lift force

$$F_{Lu}^{*} = 0.5 C_L V_u^2 A_L$$

Where:

C_L = lift coefficient, which shall be obtained from figure 3.5:

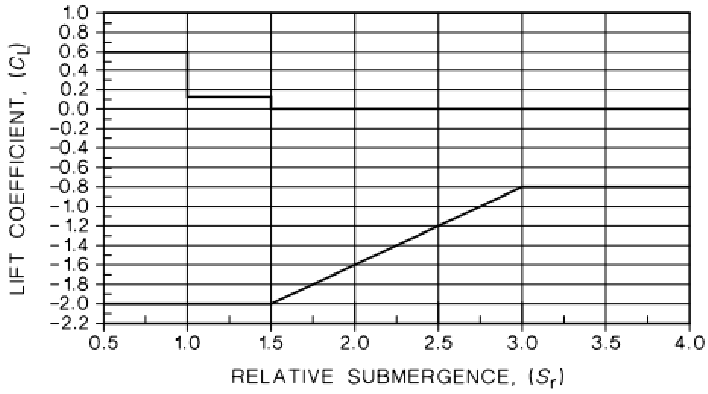

Figure 3.5 - Superstructure C_L

(Standards 2004b)

Two lift forces shall be calculated at each S_r. The upper value of C_L shall be used when determining the resistance of the structure to overturning and the tie down requirements. The lower value of C_L (downward force) will be considered in the design of a deck, girders, substructures and foundations.

3.5 Debris forces

$$F_{du}^{*} = 0.5 C_d V_u^2 A_{deb}$$

Where:

A_{deb} = projected area of debris

C_d = drag coefficient, which can be obtained from figure 3.7:

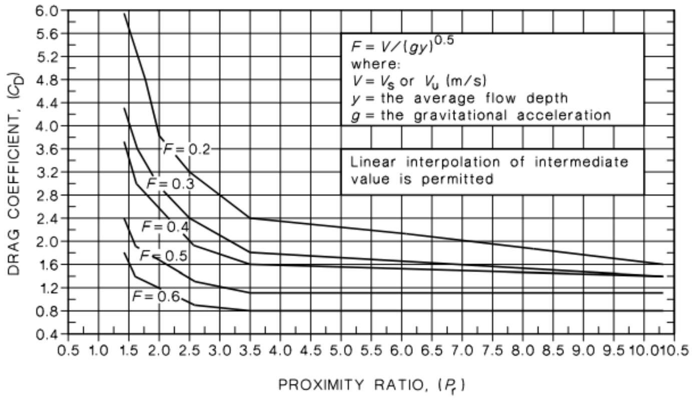

Figure 3.6 - Superstructure debris C_d

3.6 Effects due to logs

Where floating logs are a possibility, the design forces (ultimate and serviceability) exerted by the logs directly hitting piers or superstructures shall be calculated on the assumption that a log has a minimum mass of 2t (2000kg) and will be stopped in a distance of:

1) 150mm for hollow concrete piers
2) 75mm for solid concrete piers

If fender piles or sheathing are placed upstream from the pier to absorb the energy of the blow, the stopping distance shall be increased. The design forces will be calculated using the mean velocity of water flow at flood level V_s for serviceability, or V_u for ultimate limit states.

The forces due to log impact shall not be applied concurrently but they should be applied with other water flow forces as appropriate.

The following equation shall be used to calculate the impact force of a log:

$$F_{Lu}^* = \frac{0.5mV_u^2}{s}$$

Where:

m = mass of the log

s = stopping distance (m)

(Toolbox 2015)

3.7 Effects due to buoyancy

In assessing the effects of buoyancy and lift on bridge structures, the effects of buoyancy and lift on substructures (piling) and superstructures shall be given consideration. Buoyancy shall be applied concurrently with other water flow forces as appropriate.

For beam and slab or box girder bridges, several horizontal bleed holes with a minimum diameter of 75mm will be provided in webs or diaphragms, or both. Similarly, vertical bleed holes with a minimum diameter of 50mm should be provided in the deck to dissipate air which may be trapped between the high water level and the underside of the deck slab.

Where upward lift forces are possible (that is buoyancy is contributing), a positive tie-down system should be provided.

In this case, the ultimate force = $1.5F^*_{Lu} + B - \gamma_g DL$

Where:

B = Bouyancy

DL = dead load

γ_g = lower value given in figure 3.8:

Table 3.1 - Load factors for dead loads

LOAD FACTORS (γ_g) FOR DEAD LOAD OF STRUCTURE

Type of structure	Type of construction	Ultimate limit states where dead load		Serviceability limit states
		Reduces safety	Increases safety	
(a) All structures, except for Items (b) and (c)	Steel Concrete	1.1 1.2	0.9 0.85	1.0 1.0
(b) *Balanced cantilever structures* At a section subjected to approximately equal favourable and unfavourable dead loads	All	1.1	1.0	1.0
(c) *Anchor cantilever structures* At a section subjected to unequal favourable and unfavourable dead loads	All	1.2	1.0	1.0

NOTE: For large segmental cantilever construction, where appropriate control and monitoring are exercised over dimensions, the authority may allow a reduction of γ_g to not less than 1.1 for ultimate limit states, for the case where the dead load reduces safety.

(Standards 2004b)

3.8 Effects due to debris

Debris forces should not be used concurrently with water flow forces except in the case of determining the resistance of the structure to overturning. In this case, an upward lift force shall be assumed when the debris is acting on the superstructure. The upward lift force shall be calculated as follows:

For ultimate design:

$$F_{Lu}^{*} = (0.5C_L V_u^2 A_L) + B$$

Where:

C_L = 0.5

A_L = area,

= (width of the pier parallel to the direction of the water flow) x (height of the flow)

B = Buoyancy force

3.8.1 Depth of debris mat

The depth of a debris mat varies depending on factors such as catchment vegetation, available water flow depth and superstructure span. In the absence of more accurate estimates, the depth shall be estimated somewhere in the range of 1.2 – 3 meters.

3.8.2 Debris acting on piers

A debris load acting on piers shall be considered for bridges where the flood level is below the superstructure. The length of a debris mat shall be taken as:

$L = (0.5 * \sum adjacent\ spans)$, or 20m, whichever is smaller.

The debris load should be applied at mid-height of the debris mat with the assumption that the top of the debris mat is at the same level as to flood level.

3.8.3 Debris acting on superstructures

A debris load acting on superstructures should be considered for bridges where the flood level is above a level of 600mm below the soffit level. The length of the debris mat shall be the projected length of the superstructure. The debris load shall be applied at the mid-height of the superstructure, including any railing or parapets.

3.9 Traffic loads

In the event of partial submergence, traffic loads must be taken into account.

The most likely and most critical traffic scenario is the “M1600 moving traffic load”, provided in clause 6.2.3 of AS5100.

The M1600 moving traffic load accounts for the loads applied by a moving stream of traffic. The load is assumed to act within a standard design lane with a width of 3.2m, as shown in figure 3.9:

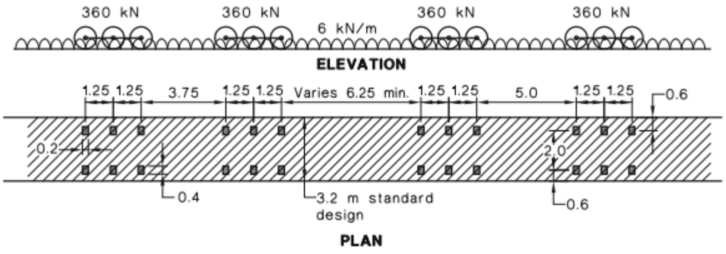

Figure 3.7 - M1600 moving traffic loads

(Standards 2004b)

As shown in figure 3.9, the applied traffic loads can be taken as a 360kN load acting over an area of 2.5m x 2m, as well as a line load of 6kN/m acting through the centre of the lane. For Tenthill Bridge, there are 2 standard design lanes, therefore table 6.6 shall be taken into account.

Table 3.2 - Lane load factors

ACCOMPANYING LANE FACTORS

Standard design lane number, *n*	Accompanying lane factor, ALF_i
1 lane loaded	1.0
2 lanes loaded	1.0 for first lane; and 0.8 for second lane
3 or more lanes loaded	1.0 for first lane; 0.8 for second lane; and 0.4 for third and subsequent lanes

NOTES:

1 First lane—the loaded lane giving the largest effect.

2 Second lane—the loaded lane giving the second largest effect.

(Standards 2004b)

It is more likely that one lane will be loaded, rather than both lanes being loaded simultaneously. Furthermore, the most critical effect that the traffic loading will have on the bridge is when the downstream end is loaded (which will contribute to overturning), hence only the downstream lane will be loaded for the simulation.

Following clause 6.7, a dynamic load allowance shall be taken into consideration to account for the interaction between moving vehicles and the bridge structure. The dynamic load allowance can be obtained from table 6.7.2, as seen below:

Table 3.3 - Dynamic load allowance

DYNAMIC LOAD ALLOWANCE (α)

Loading	Dynamic load allowance (α)
W80 wheel load	0.4
A160 axle load	0.4
M1600 tri-axle group (see Note 2)	0.35
M1600 load (see Note 2)	0.30
S1600 load (see Note 2)	0
HLP loading	0.1

NOTES:

1 Dynamic load allowance is not required for centrifugal forces, braking forces or pedestrian load.

2 Including the UDL component of the traffic load.

(Standards 2004b)

As the M1600 load is the only load being taken into account, $\alpha = 0.3$, hence:

$$M1600\ load = (1 + \alpha) * load\ factor * action\ under\ consideration$$

Where:

Load factor = 1.0, obtained from figure 3.12:

Table 3.4 - Traffic load factors

LOAD FACTORS FOR DESIGN ROAD TRAFFIC LOADS

Traffic load	Limit state	
	Ultimate	Serviceability
W80 wheel load	1.8	1.0
A160 axle load	1.8	1.0
M1600 moving traffic load	1.8	1.0
S1600 stationary traffic load	1.8	1.0
Heavy load platform load	1.5	1.0

(Standards 2004b)

Hence,

$$Total\ traffic\ load = 1.3 * M1600\ load$$

3.10 Load combinations

The ultimate limit state load combinations to be considered for ultimate limit state combinations shall consist of the following factors:

- Permanent effects (PE). This includes the self-weight of the structure. However, due to the immense weight of concrete and the orientation of the structure, it should be noted that the dead load of the structure in fact increases the resistance to overturning, therefore a reduction factor should be applied. The reduction factor can be obtained from figure 3.13.

Table 3.5 - Dead load factors

LOAD FACTORS (γ_g) FOR DEAD LOAD OF STRUCTURE

Type of structure	Type of construction	Ultimate limit states where dead load		Serviceability limit states
		Reduces safety	Increases safety	
(a) All structures, except for Items (b) and (c)	Steel Concrete	1.1 1.2	0.9 0.85	1.0 1.0
(b) *Balanced cantilever structures* At a section subjected to approximately equal favourable and unfavourable dead loads	All	1.1	1.0	1.0
(c) *Anchor cantilever structures* At a section subjected to unequal favourable and unfavourable dead loads	All	1.2	1.0	1.0

NOTE: For large segmental cantilever construction, where appropriate control and monitoring are exercised over dimensions, the authority may allow a reduction of γ_g to not less than 1.1 for ultimate limit states, for the case where the dead load reduces safety.

(Standards 2004b)

Therefore, $\gamma_g = 0.85$

- Ultimate flood loads. This includes a variety of fluid forces applied in conjunction with each other to achieve a specific results. The ultimate flood load factor can be obtained from figure 3.14:

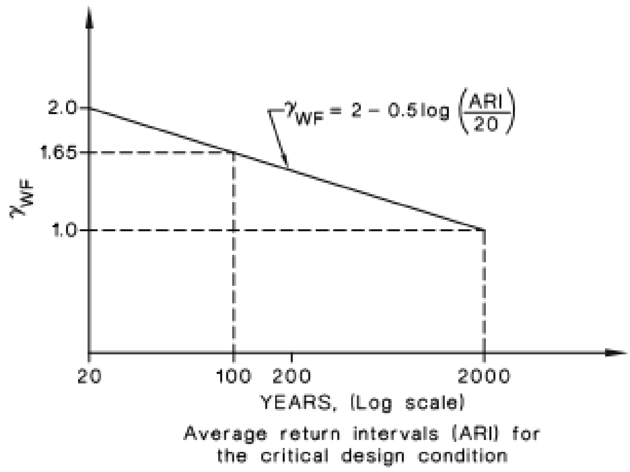

Figure 3.8 - Ultimate flood load factor

(Standards 2004b)

Therefore, the ultimate factors for each ARI is:

Table 3.6 - Ultimate load factors

ARI	Ultimate load factor
50 years	1.8
100 years	1.65
500 years	1.3

For full submergence, the major factors are the permanent effects (structure self-weight) and the flood loads. That is:

$$Full\ submergence = 0.85PE + ultimate\ load\ factor * \ flood\ load$$

For partial submergence, traffic loads need to be taken into account, therefore:

$$Partial\ submergence = 0.85PE + ultimate\ load\ factor * ultimate\ flood\ load + serviceability\ traffic\ load$$

CHAPTER 4 INTERNATIONAL BRIDGE DESIGN STANDARDS

4.1 Chapter overview

This chapter identifies the relevant flood loadings from International Bridge Design Standard. It was determined that a standard would be selected from Europe, Asia and America. Due to limited freely available resources on the internet, the three standards that were chosen was the British Bridge Design Standard, BA 59/94 (the European standard), the Indian Code of Practice, 2014 (the Asian standard) and the American Association of State Highway and Transportation Officials (AASHTO) Load-and-Resistance Factor Design (LFRD) Bridge Design specifications, 2012 (the American standard). The following chapter shows the identified flood loadings from the above Standards.

4.2 European Bridge Design Standards (Ba 59/94)

The following information has been extracted from the British Design Manual for Roads and Bridges, 1994. It should be noted that these standards are fairly old, however this was the only accessible UK standards available to the author.

4.2.1 Hydrodynamic forces on piers

4.2.1.1 Flow pressure

The equation for the hydrodynamic flow pressure can be seen below:

$$P = 0.51KU^2$$

Where:

K is dependent on the pier shape. Recommended K values can be seen in table 4.1:

Table 4.1 - K values

Type	K
Square ended piers	1.5
Circular piers	0.66
Piers with triangular cutwater angle (<30°)	0.5
Piers with triangular cutwater angle (30° to 60°)	0.5 to 0.7
Piers with triangular cutwater angle (60° to 90°)	0.7 to 0.9

(The Highways Agency 1994)

U = velocity of the current at the point where pressure intensity is being calculated. U is assumed to vary linearly from 0 (at the point of deepest scour) to a maximum (at the free water surface).

It should be noted that this method is only applicable for circumstances where the water is flowing perpendicular to the piers. If the current strikes the pier at an angle, the drag and lift coefficients must be used.

4.2.1.2 Drag force

The drag force acting parallel to the direction of flow can be calculated using the equation below:

$$F_D = \frac{C_D \rho U_o^2 y_o L}{2000}$$

Where:

U = approach flow velocity (m/s)

y_o = depth upstream of the pier (m)

L = length of the pier (or pier diameter for single cylindrical pier) (m)

ρ = water density (kg/m^3)

The drag coefficients aren’t provided in this standard, the coefficients are provided in a separate paper in chart form. Since there are only few coefficients for rectangular-faced piers, the charts from the recommended paper cannot be used accurately. However, an example was given for a case study in the standard, therefore the coefficients in this example was used.

Cd = 0.4

4.2.1.3 Lift force

The lift force acting perpendicular to the direction of flow can be calculated using the equation below:

$$F_L = \frac{C_L \rho U_o^2 y_o L}{2000}$$

Where:

C_L = 0.8, as used in the example provided within the standards.

4.2.2 Hydrodynamic forces on submerged bridge superstructures

4.2.2.1 Drag force

The formula for calculating the drag force on a submerged or partially submerged bridge deck can be seen below:

$$F_d = \frac{C_d \rho U_o^2 H}{2000}$$

Where:

F_d = drag force per unit length (kN/m)

C_d = drag coefficient, 2.0 to 2.2 is suggested

ρ = density of water (kg/m^3)

H = depth of submergence (m)

U = velocity of flow (m/s)

4.2.3 Debris forces

4.2.3.1 Impact loads due to logs

In designing against debris forces, the designer should allow for a force equivalent to that exerted by a 2 tonne log, travelling at the stream velocity and detained within distances of 150mm for column type and 75mm for solid type concrete piers. "In the UK, 3 tonne logs travelling at 10mph (4.47m/sec) have been reported in upland areas. If such a log is arrested in 75mm then the force exerted may be estimated from the kinetic energy (The

Highways Agency 1994). The average debris forces on impact is given by the equation below:

$$F = \frac{mv^2}{2d}$$

Where:

F = average collision force (kN)

d = distance before coming to rest (m)

m = mass of moving body (tonnes)

v = velocity of moving body (m/s)

4.2.4 Debris restricting the flow

For the case of the additional hydrodynamic force due to debris restricting the flow, the hydrodynamic force exerted by a minimum debris depth of 1.2m shall be considered. The length of the debris to be applied to a pier should be half of the sum of the adjacent spans up to a maximum of 21 metres. Otherwise, the formula below can be used to calculate the pressure due to trapped debris:

$$P = 0.517U_o^2$$

Where:

P = pressure (kN/m^2)

U_o = approach flow velocity (m/s)

4.2.5 Load combinations and load factors

There are no given load combinations, therefore no load combinations will be used. However, ultimate limit state factors are provided that gives a general indication of the type of load combinations that is expected from the standard, as shown in figure 4.1:

Load	Limit State	γ_{fL} to be considered in combination [2]	[4]
Hydrodynamic forces on bridge supports			
During erection	ULS SLS	1.10 1.00	
With dead load plus superimposed dead load only and for members primarily resisting water forces	ULS SLS	1.40 1.00	
With dead load plus superimposed dead load plus other appropriate Combination 2 loads, excepting wind load	ULS SLS	1.10 1.00	
Relieving effect of water (when relevant)	ULS SLS	1.00 1.00	
Flood debris collision forces on bridge supports			
During erection	ULS SLS	1.40 1.15	
With dead load and superimposed dead load only	ULS SLS	1.50 1.20	
With dead load and superimposed dead load plus other appropriate Combination 2 loads, excepting wind load	ULS SLS	1.50 1.20	

Figure 4.1 - Load combination factors

Where:

ULS = ultimate limit states

SLS = Serviceability limit states

4.3 American Bridge Design Standards (AASHTO, 2012)

The following information has been extracted from the American Association of State Highway and Transportation Officials (AASHTO) Load-and-Resistance Factor Design (LRFD) Bridge Design Specifications, 2012.

4.3.1 Static Pressure

The static pressure of the water shall be assumed to act perpendicular to the surface that is retaining water. The pressure shall be calculated as:

$$\rho_{SP} = Hw$$

Where:

ρ_{sp} = static pressure of water

H = height of water above the point of consideration

w = Specific weight of water

4.3.2 Buoyancy

Buoyancy shall be considered as an uplift force, taken as the sum of the vertical components of static pressure, acting on all components below the design water level, or:

$$B = \sum \rho_{SPy}$$

Where:

B = Buoyancy

ρ_{spy} = vertical static pressure of water

4.3.3 Stream Pressure

4.3.3.1 Longitudinal (drag)

The force of flowing water acting in the longitudinal direction of substructures shall be taken as:

$$F_{du}^{*} = 0.5 C_d V_u^2 A_d$$

Where:

ρ = pressure of flowing water

C_D = drag coefficient for piers as specified in table 4.2

V = design velocity of water for the design flood in strength and service limit states and for the check of the extreme limit state (m/s)

Table 4.2 – Drag Coefficients

Type	C_D
Semicircular-nosed pier	0.7
Square-ended pier	1.4
Debris lodges against the pier	1.4
Wedged-nosed pier with nose angle 90 degrees or less	0.8

4.3.3.2 Lateral (lift)

The lateral, uniformly distributed pressure on a substructure due to water flowing at an angle, θ, to the longitudinal axis of the pier can be illustrated in figure 4.2:

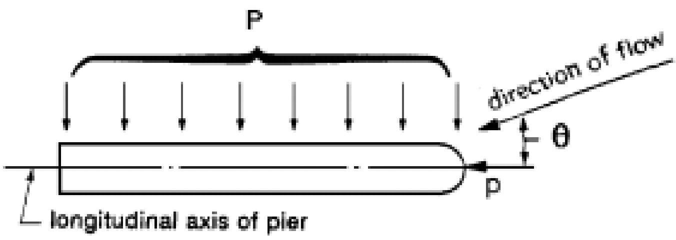

Figure 4.2 – Plan view of pier showing stream flow pressure

(AASHTO 2012)

$$F^*_{Lu} = 0.5 C_L V_u^2 A_L$$

Where:

C_L = lift coefficient, which depends on the angle between the water flow direction and the plane containing the pier, which can be estimated in table 4.3.

θ = angle between the direction of the water flow and the longitudinal axis of the pier.

A_L = area,

= (width of the pier parallel to the direction of the water flow) x (height of the flow)

Table 4.3 - Lift coefficient

θ	C_L
0 degrees	0.0
5 degrees	0.5
10 degrees	0.7
20 degrees	0.9
≥30 degrees	1.0

4.3.4 Effects due to debris

Where a significant amount of driftwood is carried, water pressure shall also be allowed for on a driftwood raft lodged against a pier. The size of the raft is a matter of judgment, but as a guide, figure 4.3 can be used.

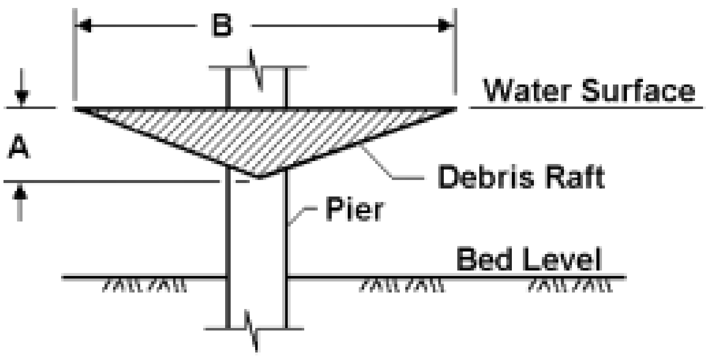

Figure 4.3 - Debris mat

(AASHTO 2012)

As a guide, dimension A should be half of the water depth, but not greater than 10ft (~3m). Dimension B should be half the sum of adjacent span lengths, but not greater than 45 ft (~14m). Finally, C_D should be 0.5.

4.3.5 Load combinations

The given load combinations can be seen in table 4.4:

Table 4.4 – Load combinations

Load Combination Limit State	*DC DD DW EH EV ES EL PS CR SH*	*LL IM CE BR PL LS*	*WA*	*WS*	*WL*	*FR*	*TU*	*TG*	*SE*	Use One of These at a Time				
										EQ	*BL*	*IC*	*CT*	*CV*
Strength I (unless noted)	γ_p	1.75	1.00	—	—	1.00	0.50/1.20	γ_{TG}	γ_{SE}	—	—	—	—	—
Strength II	γ_p	1.35	1.00	—	—	1.00	0.50/1.20	γ_{TG}	γ_{SE}	—	—	—	—	—
Strength III	γ_p	—	1.00	1.40	—	1.00	0.50/1.20	γ_{TG}	γ_{SE}	—	—	—	—	—
Strength IV	γ_p	—	1.00	—	—	1.00	0.50/1.20	—	—	—	—	—	—	—
Strength V	γ_p	1.35	1.00	0.40	1.0	1.00	0.50/1.20	γ_{TG}	γ_{SE}	—	—	—	—	—
Extreme Event I	γ_p	γEQ	1.00	—	—	1.00	—	—	—	1.00	—	—	—	—
Extreme Event II	γ_p	0.50	1.00	—	—	1.00	—	—	—	—	1.00	1.00	1.00	1.00
Service I	1.00	1.00	1.00	0.30	1.0	1.00	1.00/1.20	γ_{TG}	γ_{SE}	—	—	—	—	—
Service II	1.00	1.30	1.00	—	—	1.00	1.00/1.20	—	—	—	—	—	—	—
Service III	1.00	0.80	1.00	—	—	1.00	1.00/1.20	γ_{TG}	γ_{SE}	—	—	—	—	—
Service IV	1.00	—	1.00	0.70	—	1.00	1.00/1.20	—	1.0	—	—	—	—	—
Fatigue I— *LL, IM & CE* only	—	1.50	—	—	—	—	—	—	—	—	—	—	—	—
Fatigue II— *LL, IM & CE* only	—	0.75	—	—	—	—	—	—	—	—	—	—	—	—

(AASHTO 2012)

Where the abbreviations of interest are:

DC = Dead load of structural components and non-structural attachments

WA = water load and stream pressure

The load factors, γ_p can be obtained from table 4.5:

Table 4.5 - Load factors,γ_p

Type of Load, Foundation Type, and Method Used to Calculate Downdrag		Load Factor Maximum	Load Factor Minimum
DC: Component and Attachments		1.25	0.90
DC: Strength IV only		1.50	0.90
DD: Downdrag	Piles, α Tomlinson Method	1.4	0.25
	Piles, λ Method	1.05	0.30
	Drilled shafts, O'Neill and Reese (1999) Method	1.25	0.35
DW: Wearing Surfaces and Utilities		1.50	0.65
EH: Horizontal Earth Pressure			
• Active		1.50	0.90
• At-Rest		1.35	0.90
• *AEP* for anchored walls		1.35	N/A
EL: Locked-in Construction Stresses		1.00	1.00
EV: Vertical Earth Pressure			
• Overall Stability		1.00	N/A
• Retaining Walls and Abutments		1.35	1.00
• Rigid Buried Structure		1.30	0.90
• Rigid Frames		1.35	0.90
• Flexible Buried Structures			
o Metal Box Culverts and Structural Plate Culverts with Deep Corrugations		1.5	0.9
o Thermoplastic culverts		1.3	0.9
o All others		1.95	0.9
ES: Earth Surcharge		1.50	0.75

(BOM 2015)

Hence, the final load combination that will be used is:

$$Load\ combination = 0.9DC + WA$$

4.4 Asian Bridge Design Standards (Indian code of practice)

The following information has been extracted from the Indian Standard Specifications and Code of Practice for Road Bridges, Section two.

4.4.1 Pier forces due to water currents

As specified, "Any part of a road bridge which may be submerged in running water shall be designed to sustain safely the horizontal pressure due to the force of the current". (Congress 2014)

4.4.1.1 Water flowing parallel to the direction of the pier

On piers parallel to the direction of the flowing water, the pressure shall be calculated as follows:

$$P = 52KV^2 * \frac{9.81}{1000}$$

Where:

P = intensity of pressure due to the water current (kN/m^2)

V = velocity of the current at the point of contact (m/s). The value of V^2 shall be assumed to vary linearly from zero at the point where the deepest scour occurs to the maximum velocity at the free surface of water. The maximum velocity shall be assumed to be $\sqrt{2}$ times the maximum velocity of the current. This can better be illustrated in figure 4.4:

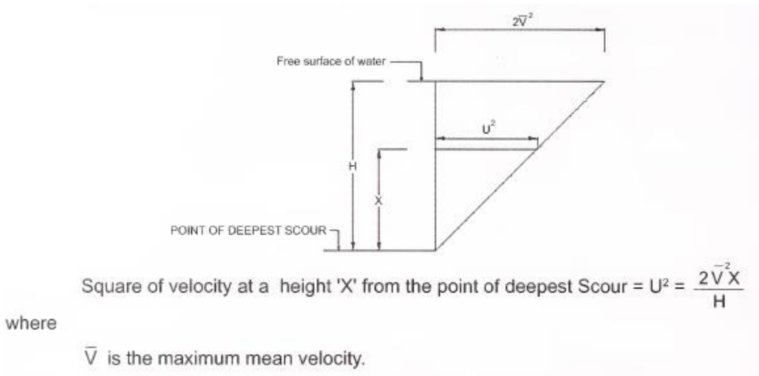

Figure 4.4 - Velocity diagram

(Congress 2014)

K = constant having the following values for different shapes of piers, illustrated in figure 4.5 and table 4.6:

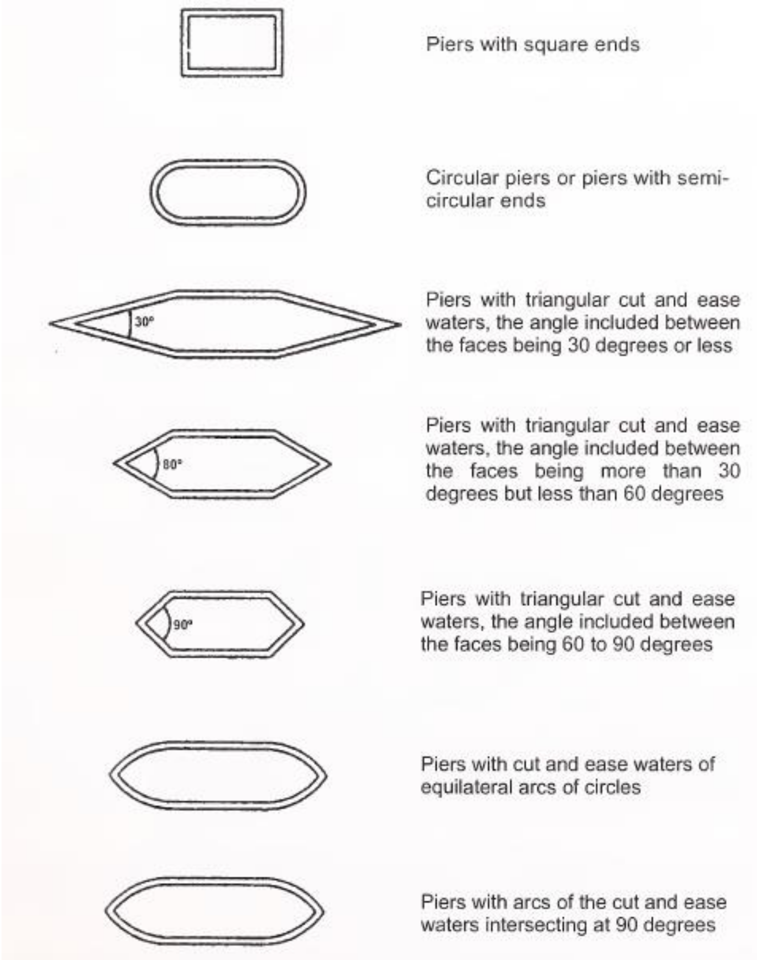

Figure 4.5 - Classification of different shaped bridge piers

(Congress 2014)

Table 4.6 - K values

Bridge pier shape	**K**
Square ended piers (and for the superstructure)	1.5
Circular piers or piers with semi-circular ends	0.66
Piers with triangular cut and ease waters, the angle included between the faces being 30° or less	0.5
Piers with triangular cut and ease waters, the angle included between the faces being between 30° and 60°	0.5 to 0.7
Piers with triangular cut and ease waters, the angle included between the faces being between 60° and 90°	0.7 to 0.9
Piers with cut and ease waters of equilateral arcs of circles	0.45
Piers with arcs of the cut and ease waters intersecting at 90°	0.5

(Congress 2014)

4.4.1.2 Water flowing at an angle to the pier

When the current strikes the pier at an angle, the velocity of the current shall be resolved into two components – one parallel (defined in the previous section) and one normal to the pier. When calculating the pressure of the current normal to the pier, the same equation as used in section 4.3.1.1 shall be used:

$$P = 52KV^2 * \frac{9.81}{1000}$$

Where:

P = intensity of pressure due to the water current (kN/m^2)

V = velocity of the current at the point of contact (m/s).

K = constant having the following values for different shapes of piers

= 1.5, except in the case of circular piers where the constant shall be taken as 0.66

To design against possible variations in the direction of flow from the direction assumed, allowances shall be made for an extra variation in the current direction of 20 degrees, therefore piers that are intended to be parallel to the direction of flow shall be designed considering for a variation of 20 degrees from the normal direction of current and piers that were intended to be design at an angle already shall be design at an angle of (20 + θ) degrees to the length of the pier.

4.4.2 Buoyancy

In the design of abutments (especially those of submerged bridges), the effects of buoyancy shall also be considered, assuming that the fill behind the abutments has been removed by scouring. To allow for full buoyancy, a reduction shall be made in the gross weight of the member being affected by reducing its own density by the density of the displaced water. That is:

$$\rho = \rho_m - \rho_w$$

Where:

ρ = equivalent density of the member

ρ_m = original density of the member

ρ_w = density of water which can be taken as 1000kg/m^3

For artesian condition, high flood level (HFL) or actual water head, whichever is higher, shall be considered for calculating the uplift. In the design of submerged masonry or concrete structures, the buoyancy effect through pore pressure may be limited to 15 percent of full buoyancy.

In the case of submersible bridges, it shall be assumed that the full buoyancy effect will act on the structure.

4.4.3 Load combinations

Table 4.7 - Various load combinations

1	2	3	4	5	6	7	8	9	10			11	12	13	14	15	16	17	18	19	20	21	22
	G	Q	G_s	Q_{im}	F_{im}	V_c	W	F_{wc}	(F_a or F_b) & /or F_f			F_{cf}	G_b	F_{ep}	F_{te}	F_d	F_s	F_{er}	F_{eq}	F_{wp}	G_e	%	
	Dead Load (G)	Live Load (Q)	Snow Load (G_s)	Vehicle Impact (Q_{im})	Impact Floating Bodies (F_{im})	Vehicle Collision Load (V_c)	Wind (W)	Water Current (F_{wc})	Tractive (F_a)	Braking (F_b)	Bearing Friction (F_f)	Centrifugal Force (F_{cf})	Buyancy (G_b)	Earth Pressure (F_{ep})	Temperature (F_{te})	Deformation Effects (F_d)	Secondry effects (Fs)	Erection Effects (F_{er})	Seismic (F_{eq})	Wave Pressure (F_{wp})	Grade Effect (G_e)	Permissible Stresses (%)	Remarks
I	1	1	*	1				1	1	1	1	1	1	1							1	100	Service Condition
II A	1	1	*	1				1	1	1	1	1	1	1	1	1	1				1	115	
II B	1	0.5		1				1	0.5	0.5	1	0.5	1	1	1	1	1				1	115	
III A	1	1	*	1			1	1	1	1	1	1	1	1	1	1	1			1	1	133	
III B	1	0.5		1			1	1	0.5	0.5	1	0.5	1	1	1	1	1			1	1	133	
IV	1	1	*	1			1	1	1	1	1	1	1	1		1	1			1	1	133	
V	1					1																150	
VI	1	0.2		1				1	0.2	0.2	1	0.2	1	1	1	1	1		1	1	1	150	
VII	1	1	*	1	1		1	1	1	1	1	1	1	1	1	1	1				1	133	
VIII	1						1	1			1		1	1				1			1	133	Construction Condition
IX	1							1			1		1	1				1	0.5		1	150	

(Congress 2014)

It can be seen in table 4.7 that in each of the cases where there would be loads in an extreme flooding event, each of the relevant terms have a weighting of “1” applied to themselves, except for the event of traffic loads being applied. This load combination will only be taken into consideration if partial submergence is to be taken into consideration. In the event of a full submergence flooding event, the load combination shall be taken as the sum of the ultimate flood loads.

CHAPTER 5 PROJECT PLANNING – METHODOLOGY

5.1 Chapter overview

This chapter presents the general methodology that was used for this project. Firstly, the methodology process is outlined, then the complex bridge that was used as a case study is identified. The details required for the load calculations are laid out with appropriate assumptions documented during the simplification process. Next, information is supplied about the simulation including which software that will be used for the project as well as how the results will be obtained. Finally, the resource requirements and risk associated with this project are laid out.

5.2 Methodology outline

The general methodology outline used was as follows:

1. Investigate different bridge design standards around the world, identifying the design flood loadings, as well as approximates for the relevant coefficients
2. Identify a small, simple concrete bridge that will be fairly easy to simulate
3. Simulate a flooding event with a single flood loading in Strand7 on the simple bridge identified
4. Identify a more complex, realistic concrete bridge within the Lockyer Valley Region that was damaged in a flooding event within the past 5 years
5. Using the same method as the simple bridge, simulate a flooding event with the identified flood loadings for each different design standard in Strand7 on the complex bridge identified
6. Analyse and discuss the results obtained from the simulations of each different design standard
7. Perform a comparison on the different bridge design standards based off these results
8. Draw appropriate conclusions as to how the complex bridge performs when subjected to Australian bridge design flood loadings, compared to different standards from around the world

5.3 Identification of a Complex Bridge

5.3.1 Location of the bridge

The complex bridge that has been selected to perform the simulations on for this project is Tenthill Creek Bridge. Tenthill Creek Bridge is located within the Lockyer Valley Region in Gatton, Queensland, Australia. The bridge is situated along State Route 80 (Gatton-Helidon Road) between Toowoomba and Ipswich, spanning Tenthill Creek. The location can be seen in figure 5.2:

Figure 5.1 - Location of Tenthill Creek Bridge

(QDMR 2003)

The bridge can be seen in figures 5.2 and 5.3:

Figure 5.2 - Tenthill Creek Bridge

(QDMR 2003)

Figure 5.3 - Cross-sectional view

(QDMR 2003)

5.3.2 Bridge details

Tenthill Creek Bridge is a simple spanning reinforced concrete, pre-stressed beam structure that was built in the 1970's. The bridge spans a total of 82.15 metres in length (which is split into three spans of 27.83 metres) and approximately 9.2 metres in width. The simplified version of the bridge contains the following components:

- Two spread footings

- Four piers, which are supported by the footings
- Two headstocks, which are supported by the piers
- Three spans of four simply supported girders, giving a total of 12 girders, which are supported by the headstocks and the abutments
- One deck, cast monolithically with the girders

5.3.3 Geometry of the structure

The dimensions of the model can be seen in figures 5.4-5.7:

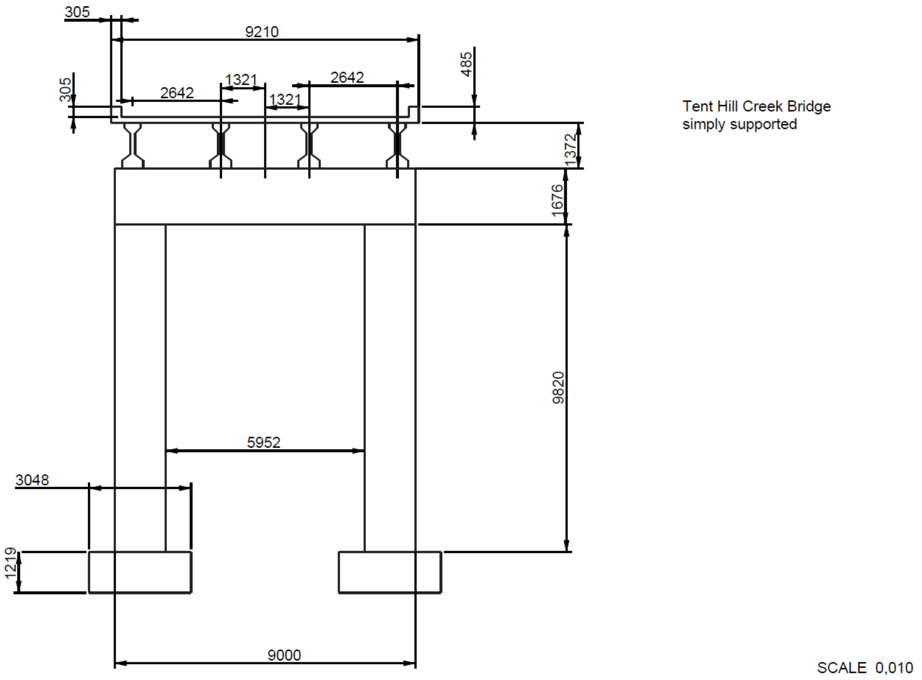

Figure 5.4 - Cross-sectional view

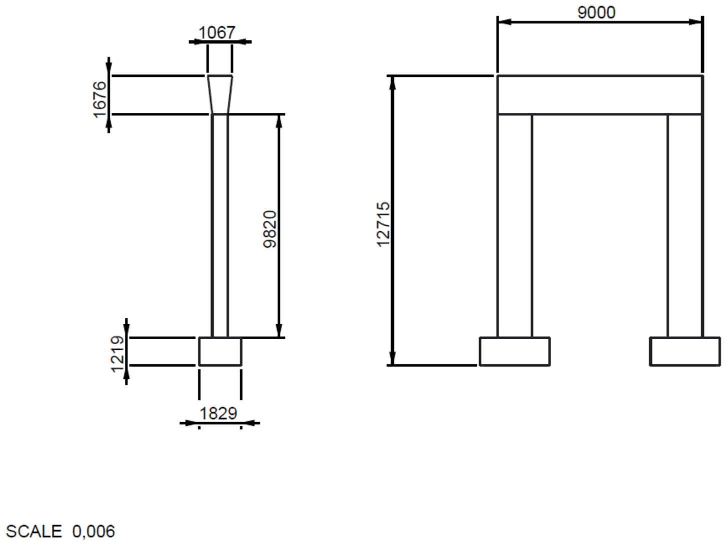

Figure 5.5 - Front and side views of the piers

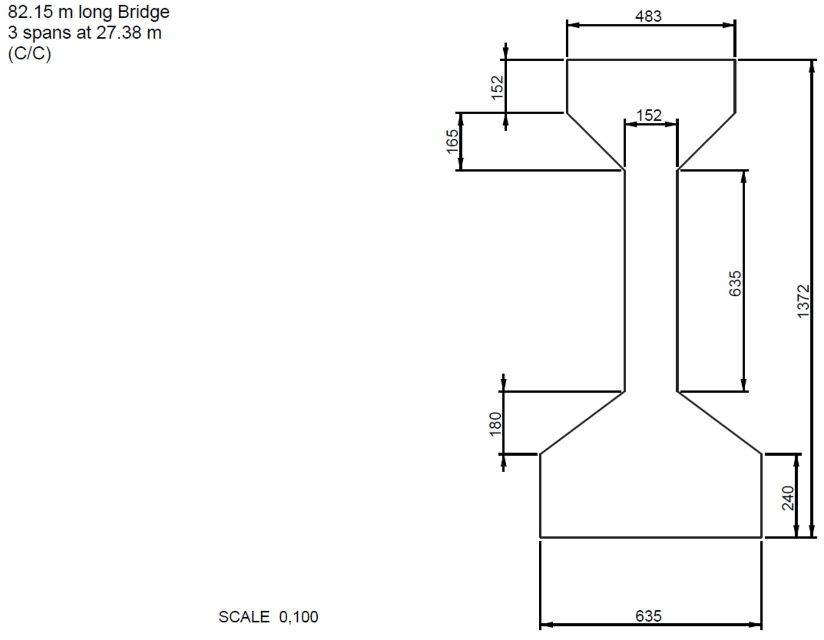

Figure 5.6 Girder dimensions

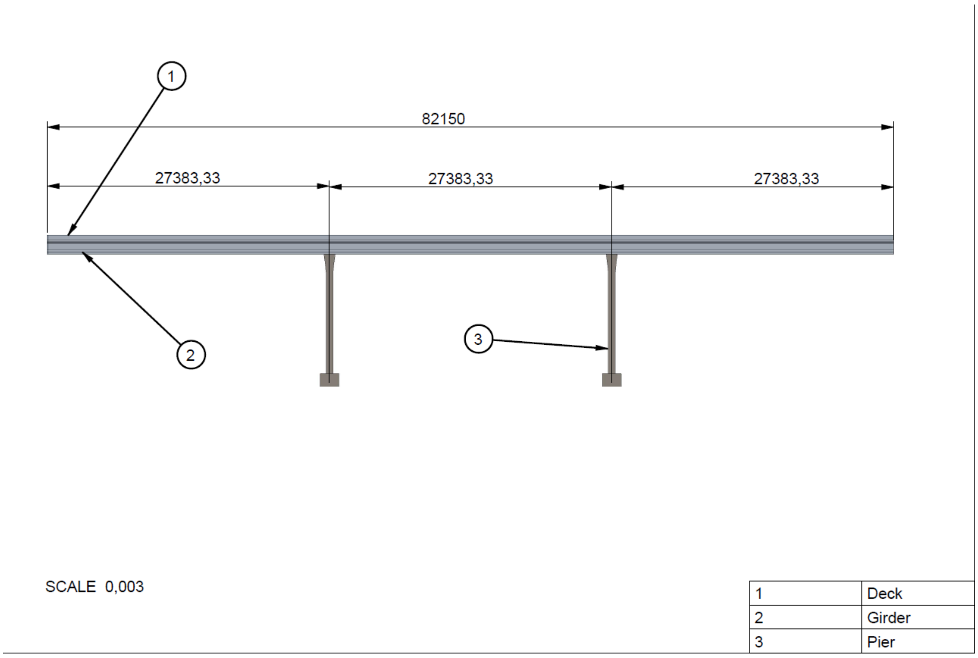

Figure 5.7 - Side view of the bridge

5.3.4 Ground profile

The topographical map below has been used to determine the necessary reduced levels (RL's) to complete the simulation:

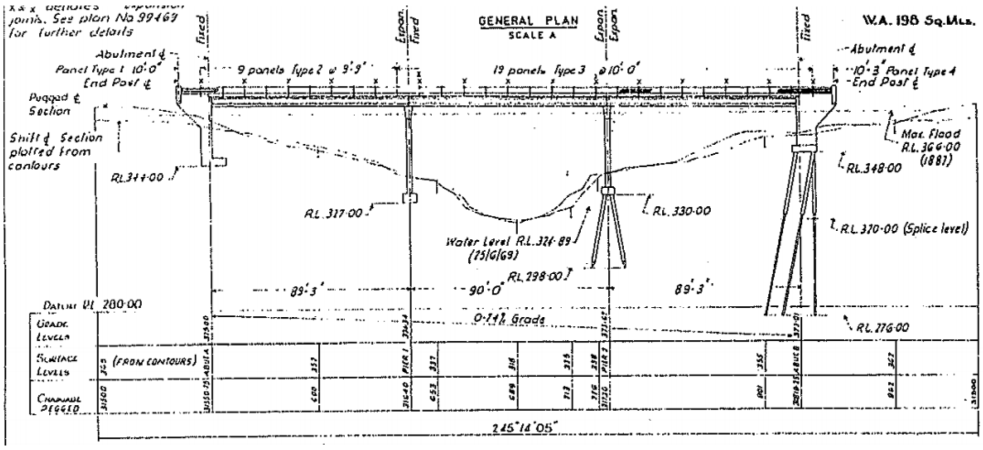

Figure 5.8 - Ground profile provided by the Queensland Department of Transport and Main Roads

(QDMR 2003)

By making appropriate assumptions, scaling and conversions, the following sketch illustrates the ground profile of the bridge:

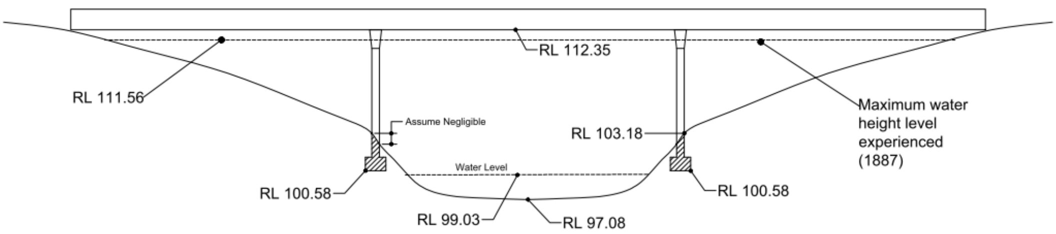

Figure 5.9 - Simplified ground profile with appropriate conversions

The following assumptions were made for the above figure:

- Both piers are fixed into the ground at the same heights
- Assume the difference in height between the two ground levels is negligible, therefore both piers are fixed into the ground for a height of 2.60 metres from the base of the footings

5.3.5 Parameters required

The parameters of the channel required for the parametric study are given below. Refer to appendix C for detailed calculations.

Table 5.1 - Details of channel

Detail	**Value**
Channel Area (m^2)	670.41
Channel slope (%)	4.24
Manning's coefficient, n (dimensionless)	0.03

According to the department of Transport and Main Roads, the maximum recorded flooding event (as indicated in figure 5.10) has the following details:

Table 5.2 - Details of maximum flooding event experienced by the bridge

Detail	**Value**
AEP	1 in 50
Submergence	Partial submergence
Velocity (m/s)	2.32
Cross-sectional area (m^2)	605.16
Discharge (m^3/s)	1403.97

Now that the 50 year ARI has been determined, the next step was to calculate the flowrates for the 100 and 500 year ARI. Realistically, as the bridge was almost completely submerged in the 1887 flooding event, in the event of a 100 or 500 year ARI flood, the bridge would most likely be completely submerged and hence the channel would begin overflowing. This would make it extremely difficult to calculate the new cross-sectional area and hence the velocities could not be determined. Therefore, to determine the absolute maximum velocities in a 100 and 500 year ARI, it is assumed this will occur when the bridge is fully submerged, before the channel has begun overflowing. Before the velocities can be determined, the discharges for these events must be determined. To obtain these discharges, an annual flood frequency analysis (FFA) was conducted. The details of this are shown below.

Annual flood frequency analysis

A flood frequency analysis was able to be performed as there was a gauge station positioned nearby within Tenthill Creek. The Department of Natural Resources and Mines' water monitoring portal provided rainfall data for Tenthill Creek from 1968 to 2015, which was a reasonably good range of data. The details of the gauge station are given below:

Table 5.3 - Site details

Site number	143212A
Zone number	56
Latitude	27°38'03.5''S
Longitude	152°12'55.5''E
Site commenced	18/03/1968
Zero gauge	123.734m RL
Datum	Australian Height Datum (AHD)
Gauging's	166 gauging's between 07/03/1968 and 05/02/2014

(DNRM 2015)

Figure 5.10 - Upstream view of the gauge station

(DNRM 2015)

The annual rainfall data was then extracted into excel where a flood frequency analysis could be performed. Based on the available data, there was 34 years of annual stream discharge data. According to AR&R, 100 year ARI events are generally the largest event that should be estimated by direct frequency analysis for important work, however the absolute maximum that should be estimated using extrapolation methods is a 500 year ARI event, hence this method is suitable for the desired results. Refer to appendix B for the full frequency analysis tables. The final result of the flood frequency analysis can be seen below:

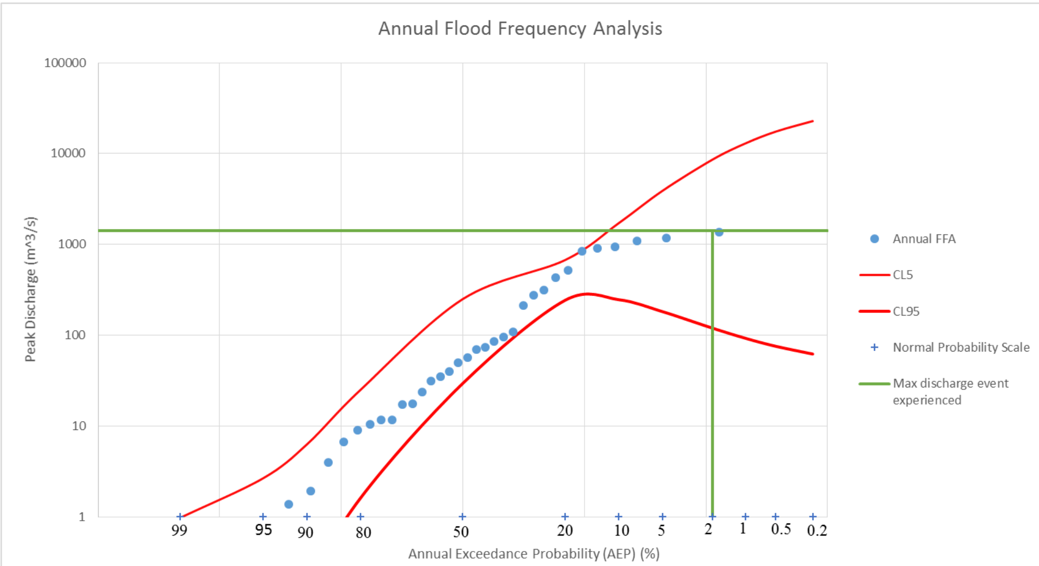

Figure 5.11 - Annual flood frequency analysis for Tenthill Creek

It can be seen in figure 3.14 that the data isn't of a very high standard to perform "neat" results, however this was the only data available. To verify that the method was correct, the maximum discharge that was experienced (the 1887 event) was plotted and the point was located right in the middle of the confidence limits. A fitted Log-Pearson 3 (LP3) curve was not sufficient enough to provide an accurate extrapolation of the 100 and 500 year ARI discharges. Therefore, a manual best line of fit was drawn and the values were drawn off. It was determined that the approximate 100 and 500 year ARI discharges were:

- Q (100 year ARI) = 1900 m^3/s
- Q (500 year ARI) = 2200 m^3/s

Now that the discharges for the major and extreme flooding events have been determined, the velocities can be determined. Since the discharge is dependent on the cross-sectional area as well as the flow velocity, two velocities were determined for each flooding event, one velocity was the worst case velocity scenario and the other was the worst case flood height scenario. The worst case velocity scenario assumes the bridge is fully submerged, however the flood height does not increase above the top deck level, therefore this gives the maximum possible velocities for each flooding event. The worst case flood height velocities give the relevant velocities in the situation that the flood level exceeds the top level of the deck, therefore the increase in cross-sectional area means that there will be an associated decrease in the velocities.

Table 5.4 - Summary of velocities and flood heights

Flooding event	Flood level (based on figure 5.10)	Submergence and location	Relevant flow velocity
50 year ARI	111.56m RL	Partially submerged, TWL is situated around the middle of the headstock	2.32m/s
100 year ARI (worst-case velocity scenario)	114.207m RL	Fully submerged, TWL is situated at the top level of the deck	2.834m/s
100 year ARI (worst case flood height scenario)	115.207m RL	Fully submerged, TWL is situated 1 metre above the top of the deck	2.525m/s
500 year ARI (worst-case velocity scenario)	114.207m RL	Fully submerged, TWL is situated at the top level of the deck	3.43m/s
500 year ARI (worst-case flood height scenario)	116.707m RL	Fully submerged, TWL is situated 2.5 metres above the top of the deck	2.512m/s

3.5.4 Assumptions

The following assumptions were made in the simplification of the bridge:

- The railings were neglected. This is due to the fact that the structural integrity of the entire bridge is being investigated and the railings will have very little effect on the failure of a bridge. It should be noted that in reality, the railings could have an effect on the flow when the flood level exceeds the top level of the deck. Debris are most likely to get lodged within the railings, which in addition with the railings themselves, can disturb the flow above the deck level by creating vortices. However this is outside the scope of this project as CFD modelling would be required to simulate these effects and the extra time is simply not worth it as the structural integrity of the entire bridge is the main concern.

- The abutments were neglected. The girders are assumed as simply supported so simple restraints will be applied to the girders in Strand7 to replace the abutments
- The steel reinforcement within the concrete has been neglected. This is because it is very complex to model steel reinforcement of that level within Strand7 and it is outside the scope of this project
- The piles below the footings have been neglected. The footings are assumed to be completely fixed into the ground so the piles will have no effect during the simulation process
- All other small components of the bridge have been neglected. All other small components will have minimal effect on the performance of the bridge during a flooding event, therefore these have been neglected to save time during the simulation process

5.4 Simulation Method

As the simulation process will consist of a bridge model with simple hydrodynamic forces being applied, the simulation of the flood loadings on the identified bridge models will be performed using the Strand7 software package. Strand7 is a Finite Element Analysis (FEA) software product developed by Strand 7 Pty. Ltd. Strand7 is most commonly used for the construction and mechanical engineering sectors, but also has seen use in other areas of engineering including aeronautical, marine and mining. Strand7 includes solvers such as linear static, natural frequency, buckling, nonlinear static, linear and nonlinear transient dynamic, spectral and harmonic response, linear and nonlinear steady-state heat transfer, linear and nonlinear transient heat transfer (Strand7 2015). As the loading is not very complicated, the linear static solver will be used throughout this project.

The linear static solver performs the following steps:

- Calculates and assembles element stiffness matrices, equivalent element force vectors and external nodal force vectors. In the stiffness calculation, material temperature dependency is considered through the user nominated temperature case. Either consistent or lumped element equivalent load vectors can be calculated according to the option setting. Constraints are also assembled in this process.
- Solves the equations of equilibrium for the unknown nodal displacements.
- Calculates element strains, stresses, stress resultants and strain energy densities as requested.

(Strand7 2015)

CHAPTER 6 SIMULATION

6.1 Chapter Overview

The following chapter will present the simulation section of the report. Firstly, a simple bridge deck model will be analysed in Strand7. The simple bridge deck model was intended to be a learning exercise for the author, these skills will then be used to model the Tenthill Creek Bridge, as introduced in chapter 5, section 5.3 of this report. The purpose of this chapter is to illustrate the development of the bridge models in Strand7. The Tenthill Creek Bridge model results will then be presented and analysed in chapter 7.

6.2 Simple bridge deck model

6.2.1 Model development

The first simulation was on a very simple model, consisting of a bridge deck with supports at each end. The geometry of the structure can be seen in figure 6.1:

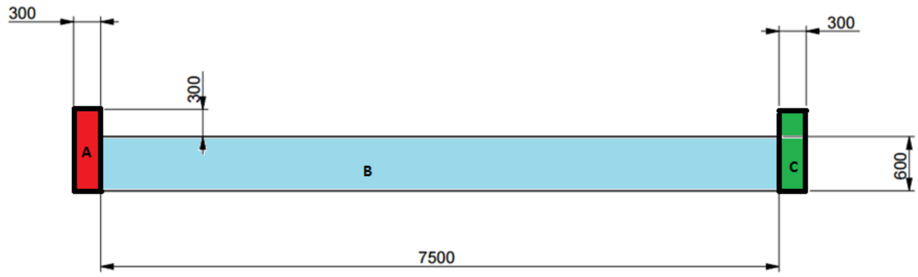

Figure 6.1 - Cross sectional view of the structure

6.2.2 Simulation parameters

As shown in figure 6.1, the model was divided into three elements for simple and accurate meshing, the dimensions can be seen in table 6.1:

Table 6.1 - Element dimensions

Element	**Direction**		
	X	**Y**	**Z**
A	0.3m	0.9m	15.4m
B	7.5m	0.6m	15.4m
C	0.3m	0.9m	15.4m

This was then drawn up in Strand7 and the model was extruded 15.4 metres in the long (Z) direction. Once this was done a mesh was applied using the subdivide function. Three meshes were applied to the model – coarse, medium and fine. Table 6.2 illustrates the subdivision of the model.

Table 6.2 - Subdivision of model

Element	**Coarse**			**Medium**			**Fine**		
	X	**Y**	**Z**	**X**	**Y**	**Z**	**X**	**Y**	**Z**
A	3	9	15	3	18	30	6	36	60
B	8	6	15	8	12	30	16	24	60
C	3	9	15	3	18	30	6	36	60

This resulting model consisted of 2064 nodes and 1530 bricks. The brick dimensions can be seen in table 6.3:

Table 6.3 - Brick sizes

Element	**Coarse**			**Medium**			**Fine**		
	X	**Y**	**Z**	**X**	**Y**	**Z**	**X**	**Y**	**Z**
A	0.3/3 = 0.1m	0.9/9 = 0.1m	15.4/15 = 0.513m	0.3/3 = 0.1m	0.9/18 = 0.05m	15.4/30 = 0.513m	0.3/6 = 0.05m	0.9/36 = 0.025m	15.4/60 = 0.257m
B	7.5/8 = 0.94m	0.6/6 = 0.1m	15.4/15 = 0.513m	7.5/8 = 0.94m	0.6/12 = 0.05m	15.4/30 = 0.513m	7.5/16 = 0.47m	0.6/24 = 0.025m	15.4/60 = 0.257m
C	0.3/3 = 0.1m	0.9/9 = 0.1m	15.4/15 = 0.513m	0.3/3 = 0.1m	0.9/18 = 0.05m	15.4/30 = 0.513m	0.3/6 = 0.05m	0.9/36 = 0.025m	15.4/60 = 0.257m

Table 6.4 shows the number of nodes and bricks for each model:

Table 6.4 - Number of nodes and bricks for each model

Model	**Number of nodes**	**Number of bricks**
Coarse	2064	1530
Medium	7533	6120
Fine	54473	48960

It was assumed that the deck was supported in the typical 'pin and roller' form, which can be better illustrated in figure 6.2:

Figure 6.2 - Typical pin and roller support

Using this form, the restraints of the model were defined as:

Table 6.5 - Boundary conditions for the model

	Degrees of freedom					
Support type	**X-translation**	**Y-translation**	**Z-translation**	**X-rotation**	**Y-rotation**	**Z-rotation**
Pin	Fixed	Fixed	Fixed	Free	Fixed	Fixed
Roller	Fixed	Fixed	Free	Free	Fixed	Fixed

The model development using the three different mesh sizes are shown in figures 6.3-6.5:

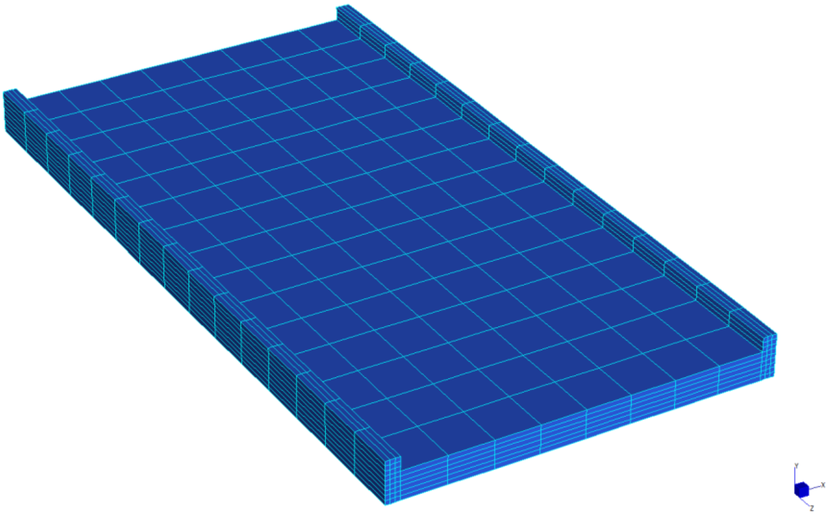

Figure 6.3 - Coarse simulation model

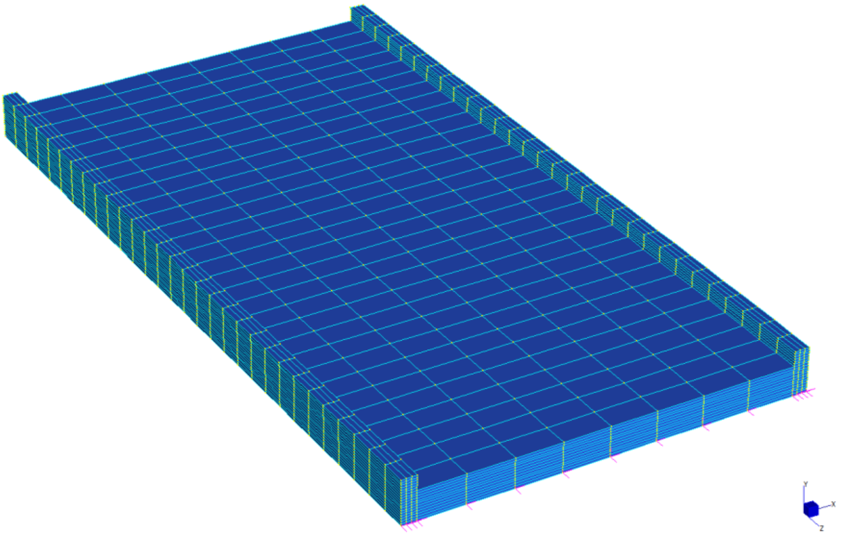

Figure 6.4 - Medium simulation model

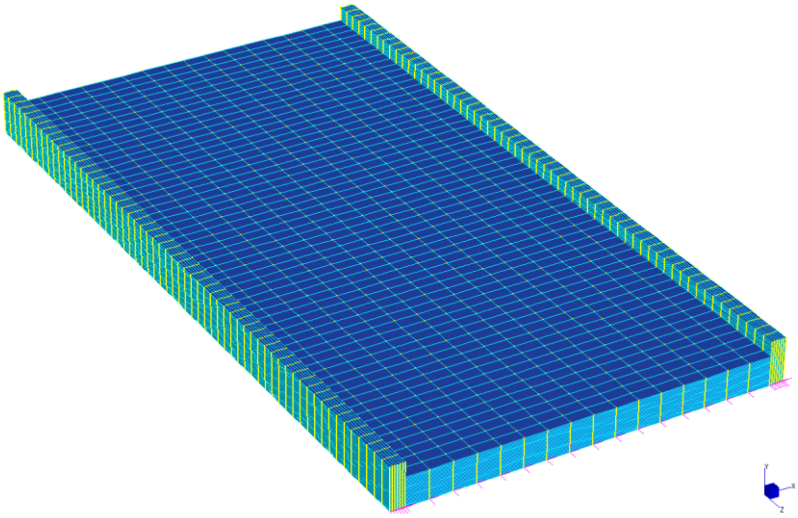

Figure 6.5 - Fine simulation model

6.2.3 Input parameters

Since it is only a bridge deck being analysed in this situation, the major contributing force is drag force. The following drag force equation that was extracted from BA 59/94 (section 5.2) will be used:

$$F_d = \frac{C_d \rho U_o^2 H}{2000}$$

The following parameters have been assumed:

- $C_d = 2.0$
- $\rho = 1000 kg/m^3$

- U_o = 2-10m/s. Since a case study will not be used for this project, a range has been chosen. Three velocities will be chosen, these are 3m/s, 6m/s and 9m/s.
- H = 3.9m (assuming the deck is situated 3m above the bed floor level + 0.9m deck height)
- f'_c = 32MPa

Inputting these variables into the above equation and converting to MPa we get:

$$F_{d1} = 0.009\ MPa$$

$$F_{d2} = 0.036\ MPa$$

$$F_{d3} = 0.081\ MPa$$

6.2.4 Simulation results

The run time for each model can be seen in table 6.6:

Table 6.6 – Run times for the models

Model	Run time
Coarse	0 minutes, 4 seconds
Medium	0 minutes, 12 seconds
Fine	9 minutes, 48 seconds

The maximum displacements and stresses of the coarse model can be seen in table 6.7:

Table 6.7 - Coarse model results

	Max x-displacement	Max y-displacement	Max z-displacement	Max x-stress	Max y-stress	Max z-stress
V1	0.014 mm	0.020 mm	0.0064 mm	0.045 MPa	0.09 MPa	0.15 MPa
V2	0.06 mm	0.079 mm	0.026 mm	0.18 MPa	0.36 MPa	0.61 MPa
V3	0.126 mm	0.178 mm	0.058 mm	0.41 MPa	0.81 MPa	1.38 MPa

The maximum displacements and stresses of the medium model can be seen in table 6.8:

Table 6.8 - Medium model results

	Max x-displacement	Max y-displacement	Max z-displacement	Max x-stress	Max y-stress	Max z-stress
V1	0.015 mm	0.021 mm	0.0069 mm	0.08 MPa	0.16 MPa	0.29 MPa
V2	0.058 mm	0.084 mm	0.028 mm	0.33 MPa	0.64 MPa	1.16 MPa
V3	0.131 mm	0.189 mm	0.062 mm	0.75 MPa	1.44 MPa	2.60 MPa

The maximum displacements and stresses of the fine model can be seen in table 6.9:

Table 6.9 - Fine model results

	Max x-displacement	Max y-displacement	Max z-displacement	Max x-stress	Max y-stress	Max z-stress
V1	0.015 mm	0.022 mm	0.0074 mm	0.17 MPa	0.32 MPa	0.60 MPa
V2	0.060 mm	0.088 mm	0.030 mm	0.69 MPa	1.29 MPa	2.39 MPa
V3	0.136 mm	0.200 mm	0.067 mm	1.56 MPa	2.90 MPa	5.37 MPa

The results in tables 6.7-6.9 give an indication of the changes in results between the different qualities of meshes. The displacement results have very little changes, therefore the coarse model does an adequate job of predicting the behaviour of the model. The stress concentration results appear to double in size for each mesh, this is expected because a smaller mesh size means the same force acting over a smaller area which means a greater pressure. Since the mesh sizes were being decreased by half the previous amount each time, this will result in twice the stress concentration.

Figure 6.6 illustrates the displacement of the model set at 5% scale:

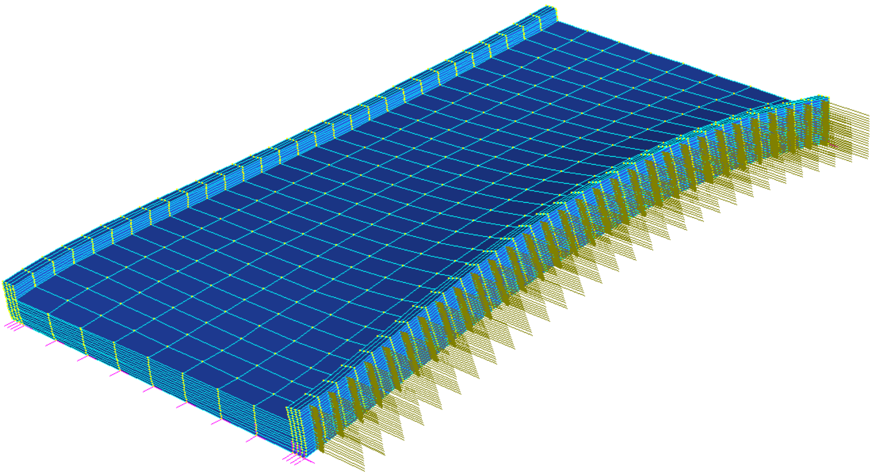

Figure 6.6 - Deformed model set a 5% displacement scale

6.2.5 Discussion

The simple bridge model was intended as a learning exercise for the author. The simple bridge deck model successfully assisted the author in the following ways:

1. Use of the "extrusion" tool in Strand7 to create three dimensional elements. The process is to essentially create one (or more if needed) cross sections, the extrusion tool gives the cross-section the required length and hence converts the model from two dimensional to three dimensional

2. Application of restraints for three dimensional models. As explained in section 6.1.2 of this chapter, supports vary in the degrees of freedom for two and three dimensional supports. This is essential to understand and the model will not work if the proper restraints aren't assigned.
3. Application of a manual mesh by use of the "subdivide" function. This is another essential component of setting up a 3D model in Strand7. As shown in section 6.1.4 of this chapter, the results can vary greatly depending on the size of the mesh. If the mesh is too coarse, the results can be very inaccurate and give misleading results. On the other hand, a fine model can give much more accurate results, however the computation time can greatly increase and begin to take many hours. It all depends on how accurate results are required and how much the results vary depending on the mesh size. Also, the different shape sizes that make up the model are a big factor when determining a suitable mesh size. For example, rectangular blocks do not need a very small mesh size because convergence is not an issue and the model will not have much difficulty distributing the stress, however rounded surfaces or sharp edges where stress concentration could be a very big issue requires a very fine mesh size, or else the model could provide very misleading results. It is ultimately a judgement call.

Overall, the simple bridge deck model proved to be a very good learning exercise and made the author much more proficient in performing 3D modelling in Strand7. These skills could then be applied to a more complex, realistic bridge within the Lockyer Valley.

6.3 Tenthill Creek Bridge

6.3.1 Creating the geometric model

Using the dimensions from the engineering drawings presented in chapter 3, the geometric model could be modelled in Strand7. Firstly, nodes were created at specific cross sections to define the boundary of each element, then tri3 (where appropriate) and quad4 elements were created, this defined the cross-section for each element, then these two-dimensional elements were extruded in the relevant direction, thereby creating the required three-dimensional elements. Different elements had to be extruded in different directions, depending on the orientation of the cross-sections created. For example, the superstructures were extruded in the Z-direction because there is no change in shape along the Z-axis, however this is not the case for the headstocks, and therefore the headstocks had to be extruded in the X-direction instead. The final geometric model can be seen in figure 6.7:

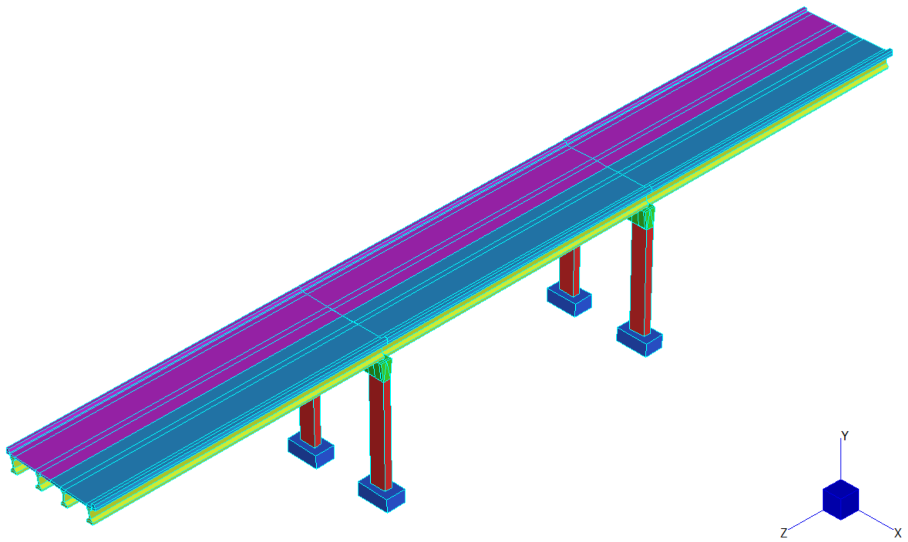

Figure 6.7 - Final geometric model

It can be seen in figure 6.7 that there have been different brick properties assigned to each component of the bridge, this was done to allow each component to be isolated when needed, which would assist in the load application and meshing of the model. Table 6.10 shows the classification of each different section.

Bridge section	Brick property type	Associated colour
Footings	1	
Pier	2	
Headstock	3	
Girder	4	
Deck	5	
Deck	6	

Table 6.10 - Property types for the model

6.3.2 Material properties

According to the Department of Transport and Main Roads, the entire bridge consists of concrete with a characteristic strength of 20MPa. The rest of the material properties were obtained from the Strand7 library. The material properties are presented in table 6.11:

Table 6.11 - Material properties

	Material	E MPa	ν	ρ kg/mm^3
1: Brick Property 1	AS3600 (1994) Concrete - Compressive Strength f'c = 20 Mpa	25000.0	0.2	2.4×10^{-6}
2: Brick Property 2	AS3600 (1994) Concrete - Compressive Strength f'c = 20 Mpa	25000.0	0.2	2.4×10^{-6}
3: Brick Property 3	AS3600 (1994) Concrete - Compressive Strength f'c = 20 Mpa	25000.0	0.2	2.4×10^{-6}
4: Brick Property 4	AS3600 (1994) Concrete - Compressive Strength f'c = 20 Mpa	25000.0	0.2	2.4×10^{-6}
5: Brick Property 5	AS3600 (1994) Concrete - Compressive Strength f'c = 20 Mpa	25000.0	0.2	2.4×10^{-6}
6: Brick Property 6	AS3600 (1994) Concrete - Compressive Strength f'c = 20 Mpa	25000.0	0.2	2.4×10^{-6}

Where:

E = Modulus of elasticity

ν = Poison's Ratio

ρ = density

6.3.3 Restraints of the model

The model was restrained in the following manner:

- The footings have been modelled as being cast monolithically with the piers.
- The piers have been modelled as being cast monolithically with the headstock.

- The deck has been modelled as being cast monolithically with the girders as well as pinned supports on either end.
- The three spans of girders have been assumed to be simply supported.

The freedom conditions can be seen in table 6.12:

Table 6.12 - Degrees of freedom used for each type of support

	Degrees of freedom					
Support type	**x-translation**	**y-translation**	**z-translation**	**x-rotation**	**y-rotation**	**z-rotation**
Fixed	Fixed	Fixed	Fixed	Fixed	Fixed	Fixed
Pin	Fixed	Fixed	Fixed	Free	Fixed	Fixed
Roller	Fixed	Fixed	Free	Free	Fixed	Fixed

To model the segments as being monolithically cast, this was done by assigning the intersecting points of each segments the same node number, thereby creating a rigid joint. For example, where the top of the girder meets the bottom of the deck, the girders were first created and then the deck was created using the top nodes at each girder. The main problem with assigning the restraints was restraining the girders to the headstock. To do this, links were created between the bottom level of the girders and the top level of the headstock. To allow this, the headstock had to be created in such a way that there were nodes situated directly below the bottom level nodes of the girder (a gap of 200mm was made between the girders and the headstock). The master-slave option was used for this. The Master-Slave links are used to force nodes to share degrees of freedom.

The degrees of freedom defined in table 6.12 were used. This can be better illustrated in figure 6.8:

Figure 6.8 - Degrees of freedom for fixed (left), pinned (middle) and roller (right) links

6.3.4 Meshing of the model

An initial mesh of 500mm was chosen to be applied to the model. Since Strand7 doesn't have a function that auto-meshes a model built manually in the program, the Subdivide function was used. It should be noted that a fine mesh is not required for this model, this is because we are looking at the overall structural integrity of the structure. It was shown in in section 6.1.4 of this chapter that the displacement results had very little changes between the different quality meshes, this is because the structure consisted of simple rectangular bricks, therefore convergence was not an issue in the solving process; it is a similar case for this model. Furthermore, due to the size of the model, a fine mesh was simply not worth the extra run time. The purpose of this simulation is to be able to compare the results obtained from the different design standards, however when a fine mesh was applied to the model, the relative increase in accuracy between the results of each model was the same, therefore the model still produced the same comparative results. Hence, the 500mm mesh size was deemed feasible for the simulation. The subdivision of each element of the model can be seen in table 6.13:

Table 6.13 - Model meshing

Section of the model	Subdivision direction		
	X-direction	Y-direction	Z-direction
Footing	7	3	4
Pier (section fixed into the ground)	4	3	2
Pier (free section)	4	17	2
Headstock (section 1)	0	4	n/a
Headstock (sections 2 and 3)	2	4	n/a
Headstock (section 4)	3	4	n/a
Girders (sections 1 and 2)	2	0	55
Girders (section 3)	0	2	55
Girders (sections 4 and 5)	0	0	55
Deck (sections 1-4)	0	0	55
Deck (section 5)	5	0	55
Deck (section 6)	3	0	55

It should be noted that the tri6 elements could only be subdivided in 2 directions, rather than 3; that is why “n/a” was placed in the “Z-direction” column. Also, the pier, headstock, girders and deck was split into a different number of sections based on their associated dimension. Figures 6.9-6.11 illustrate the different sections of the model used in table 6.13.

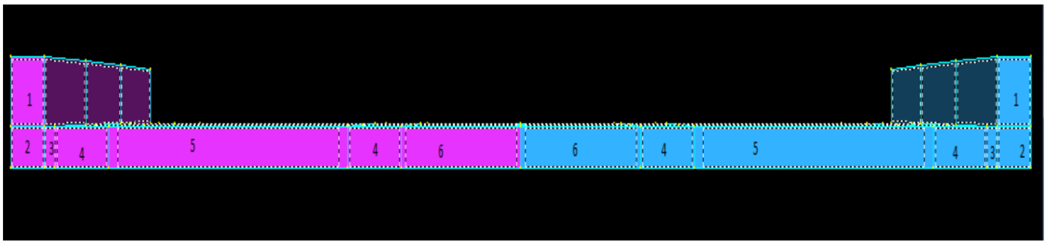

Figure 6.9 - Deck sections

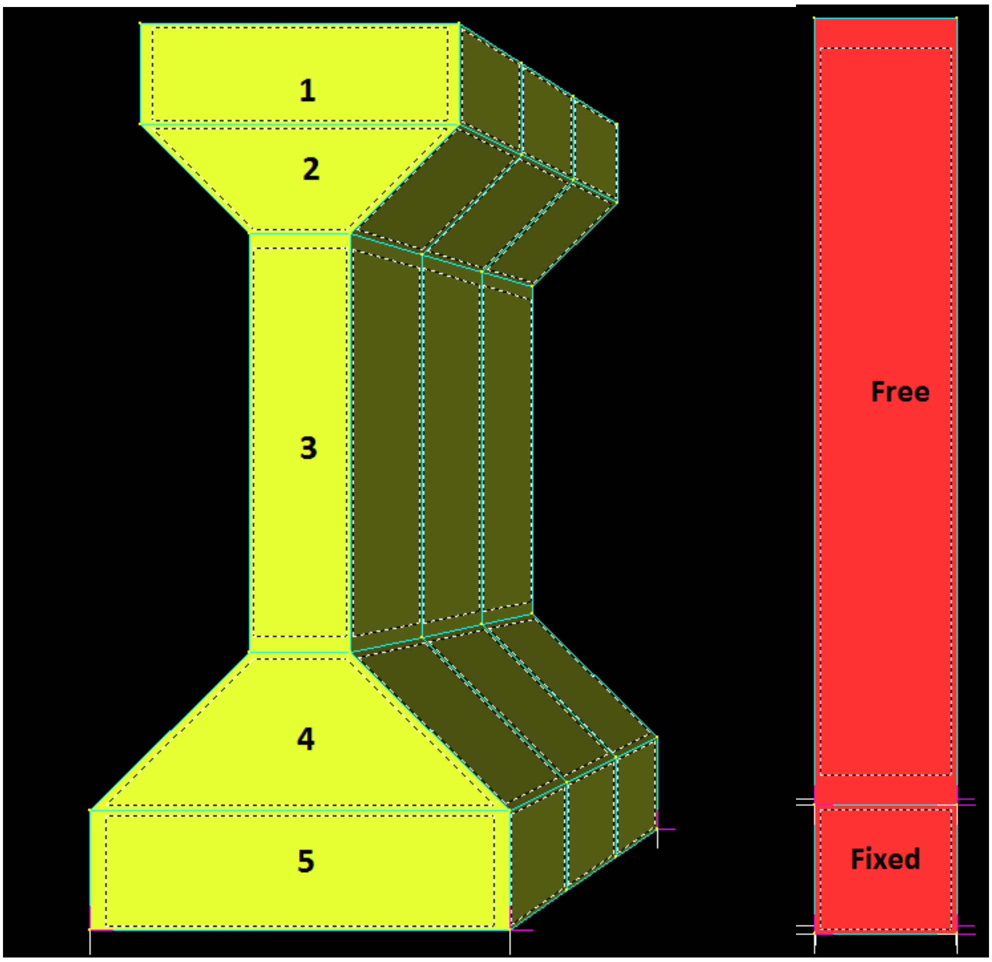

Figure 6.10 – Girder (left) and pier (right) sections

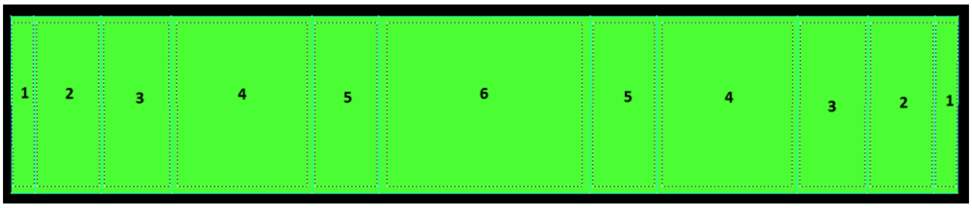

Figure 6.11 - Headstock sections

The final meshed model is shown in figure 6.12:

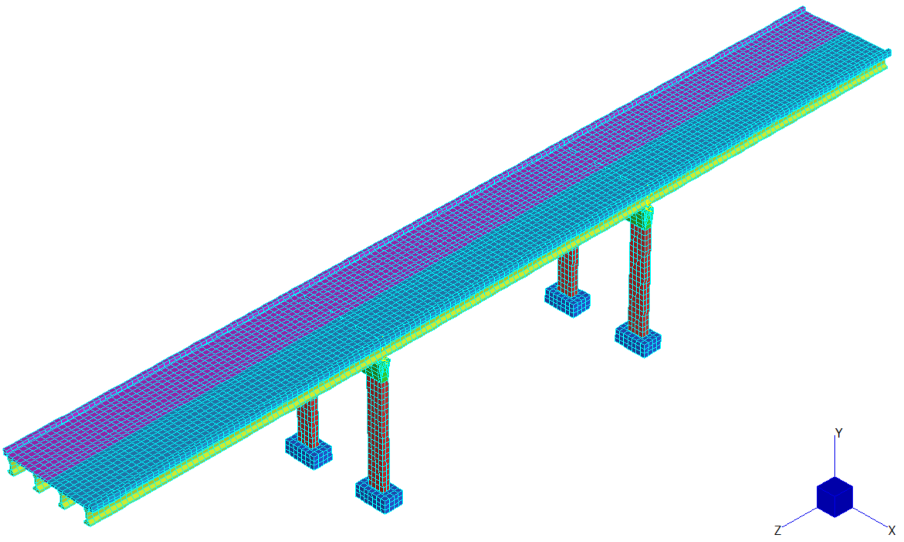

Figure 6.12 - Meshed model

CHAPTER 7 RESULTS AND DISCUSSION

7.1 Chapter overview

This chapter presents the results for the different Bridge Design Standards around the world. This was done by using the "Tenthill Creek Bridge" Strand7 model. Displacement and stress-concentration results were analysed and used to compare The Australian Bridge Design Standards (AS5100, 2004) to the International Bridge Design Standards. A full, comprehensive analysis will be conducted on AS5100, then the most critical flooding event will be used to analyse the International Standards and determine how the Australian Standards perform in comparison.

7.2 AS5100

7.2.1 Load cases and load combinations

The load cases used for the AS5100 model are shown in table 7.1:

Table 7.1 - Load cases

Load case	Contributing force	Force type used
1	Self-weight	Gravity function in Strand7
2	Drag force (partial submergence)	1kPa unit load
3	Drag force (piers, full submergence)	1kPa unit load
4	Drag force (superstructures, full submergence)	1kPa unit load
5	Lift force (partial submergence)	1kPa unit load
6	Lift force (piers, full submergence)	1kPa unit load
7	Lift force (up-lift, superstructures, full submergence)	1kPa unit load
8	Lift force (down-lift, superstructures, full submergence)	1kPa unit load
9	Debris force (partial submergence)	1kPa unit load
10	Debris force (piers, full submergence)	1kPa unit load
11	Debris force (superstructures, full submergence)	1kPa unit load
12	Debris force (piers, full submergence + 1m)	1kPa unit load
13	Debris force (superstructures, full submergence + 1m)	1kPa unit load
14	Debris force (superstructures, full submergence + 2.5m)	1kPa unit load
15	Log force (partial submergence)	1kPa unit load
16	Log force (full submergence)	1kPa unit load
17	Buoyancy (partial submergence)	Refer appendix D
18	Buoyancy (full submergence)	Refer appendix D
19	Hydrostatic thrust (partial submergence)	Refer appendix D
20	Hydrostatic thrust (full submergence)	Refer appendix D
21	Hydrostatic thrust (full submergence + 1m)	Refer appendix D
22	Hydrostatic thrust (full submergence + 2.5m)	Refer appendix D
23	Traffic loads	Refer appendix D

It should be noted that 1kPa unit loads were applied for the dynamic components of the model (drag, lift and debris forces) to facilitate the change in velocity for each different load combination. For example, the drag force for the full submergence condition acts on the same area of each bridge component, however the drag values change between the different flooding events due to a change in velocity, therefore a single drag force load case can be used for all 8 full submergence load combinations, saving a total of 7 load cases being created in Strand7, which in turn reduces the run time of the model.

The load cases now need to be combined in an appropriate manner. The load combinations, obtained from chapter 3, are shown below:

1. 50 year ARI – 0.85*PE + ULF*FF + TL + D

2. 50 year ARI – 0.85*PE + ULF*FF + TL + LI
3. 100 year ARI, worse-case velocity scenario - 0.85*PE + ULF*FF + D
4. 100 year ARI, worse-case velocity scenario – 0.85*PE + ULF*FF + LI
5. 100 year ARI, worse-case flood height scenario - 0.85*PE + ULF*FF + D
6. 100 year ARI, worse-case flood height scenario – 0.85*PE + ULF*FF + LI
7. 500 year ARI, worse-case velocity scenario - 0.85*PE + ULF*FF + D
8. 500 year ARI, worse-case velocity scenario – 0.85*PE + ULF*FF + LI
9. 500 year ARI, worse-case flood height scenario - 0.85*PE + ULF*FF + D
10. 500 year ARI, worse-case flood height scenario – 0.85*PE + ULF*FF + LI

Where:

PE = Permanent effects (self-weight)

ULF = ultimate load factor, as seen in table 7.2:

Table 7.2 - Ultimate load factors

ARI	Ultimate load factor
50	1.8
100	1.65
500	1.3

FF = Fluid forces

TL = Traffic loads

D = Debris forces

LI = Log-impact forces

The load combination factors are shown in table 7.3:

Table 7.3 - Load case factors (AS5100)

	Load combination									
Load case	1	2	3	4	5	6	7	8	9	10
1	0.85	0.85	0.85	0.85	0.85	0.85	0.85	0.85	0.85	0.85
2	6.78	6.78	0	0	0	0	0	0	0	0
3	0	0	9.27	9.27	7.359	7.359	10.71	10.71	5.74	5.74
4	0	0	8.61	8.61	9.47	9.47	9.94	9.94	7.38	7.38
5	4.35	4.35	0	0	0	0	0	0	0	0
6	0	0	5.95	5.95	4.73	4.73	6.87	6.87	3.69	3.69
7	0	0	0.66	0.66	0.528	0.528	0.76	0.76	0	0
8	0	0	0	0	10.52	10.52	0	0	5.33	5.33
9	11.86	0	0	0	0	0	0	0	0	0
10	0	0	16.23	0	0	0	18.733	0	0	0
11	0	0	11.92	0	0	0	12.62	0	0	0
12	0	0	0	0	11.03	0	0	0	0	0
13	0	0	0	0	9.99	0	0	0	0	0
14	0	0	0	0	0	0	0	0	7.8	0
15	0	186.5	0	0	0	0	0	0	0	0
16	0	0	0	278.3	0	220.91	0	407.65	0	218.65
17	1	1	0	0	0	0	0	0	0	0
18	0	0	1	1	1	1	1	1	1	1
19	1	1	0	0	0	0	0	0	0	0
20	0	0	1	1	0	0	1	1	0	0
21	0	0	0	0	1	1	0	0	0	0
22	0	0	0	0	0	0	0	0	1	1
23	1	1	0	0	0	0	0	0	0	0

7.2.2 Simulation results

The same type of results as presented in section 6.1.4 of chapter 6 were obtained for this model, that being X, Y and Z displacement and stress concentration results, with the addition of resultant XYZ displacement and stress concentration results being obtained. While the Z, Y and Z displacement and stress concentration results illustrates the behaviour of the model, it does not take into account "cancelling out" components, hence that is why XYZ results have also been obtained. The X, Y and Z displacement results for the AS5100 model are shown in table 7.4 and figure 7.1:

Table 7.4 - X, Y and Z displacement results

Load combination	Maximum X-displacement (mm)	Maximum Y-displacement (mm)	Maximum Z-displacement (mm)
1	1.909	-8.443	-1.091
2	1.835	-8.407	-1.090
3	-9.739	9.347	-1.389
4	-7.468	9.069	-1.361
5	-9.105	-29.874	-4.699
6	-7.421	-30.009	-4.582
7	-10.623	9.716	-1.504
8	-9.192	9.624	-1.490
9	-9.502	-49.690	-7.391
10	-9.493	-49.258	-7.334

These can be better illustrated in figure 7.1:

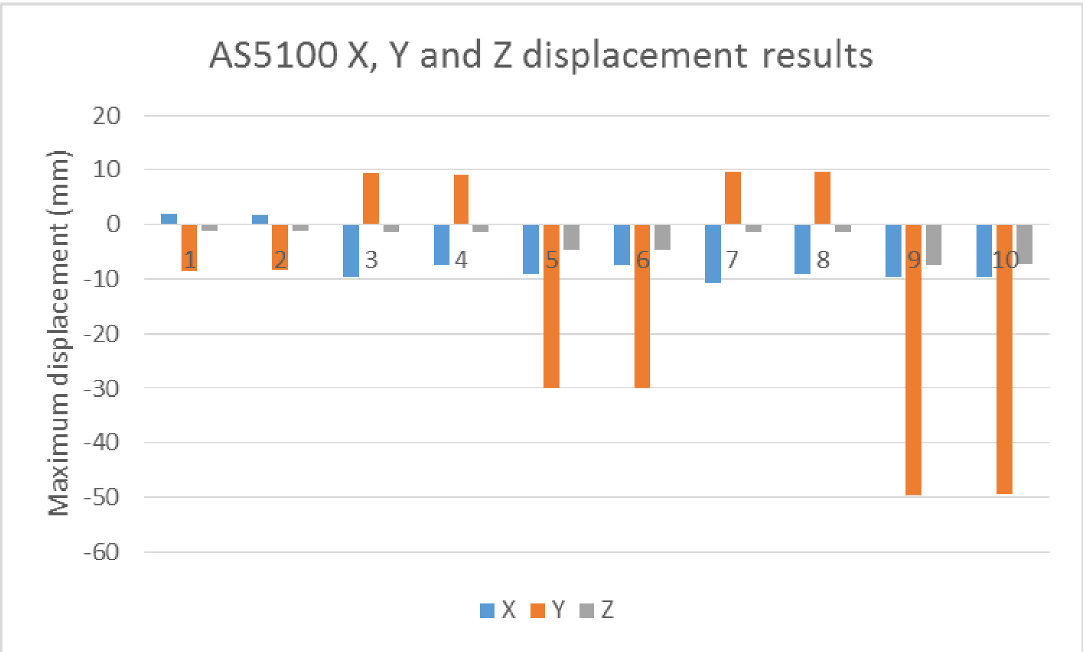

Figure 7.1 - Bar chart of X, Y and Z displacement results

It can be seen in table 7.4 that the results are within a reasonable range. The X-displacement results are a representation of the deflection of the girders. This is assumed because, although the other components can deflect in this manner, however they are prevented from major displacement by being monolithically cast with other components. For example, the piers would have a very large amount of X-displacement, however this is not the case due having a rigid connection with the headstock. This is also illustrated in figure 7.2 for load combination 10:

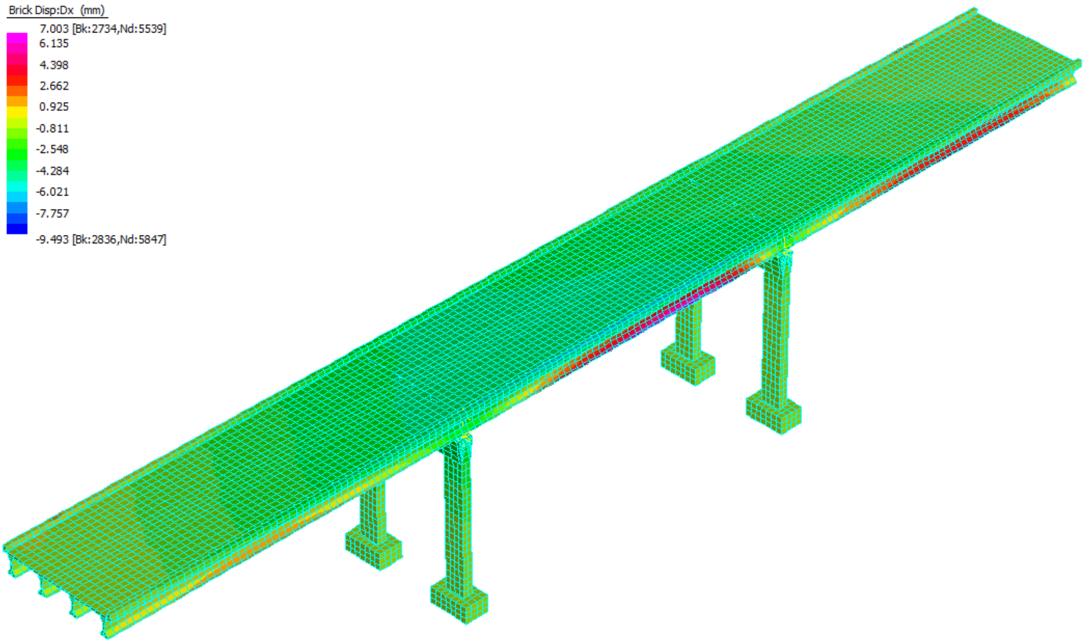

Figure 7.2 - X-displacement contour plot

Using the "find" function in Strand7, the brick with the maximum X-displacement was located and is shown in figure 7.3:

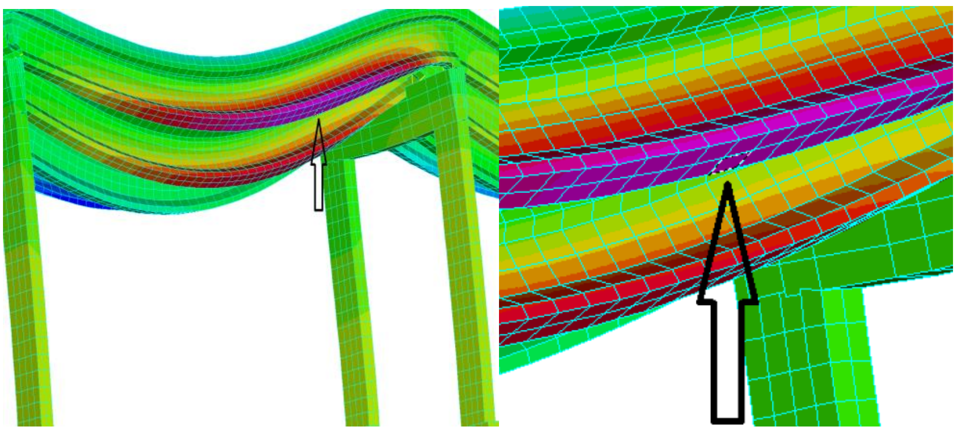

Figure 7.3 - Location of maximum X-displacement in the positive X-direction

It can be seen that the maximum displacement in the positive X-direction occurred at the centre, upstream girder, which indicates the maximum point of overturning on the upstream end of the bridge. Similarly, the maximum X-displacement in the negative X-direction is located at the left (looking downstream), downstream girder, which indicates the maximum point of overturning on the downstream end of the bridge.

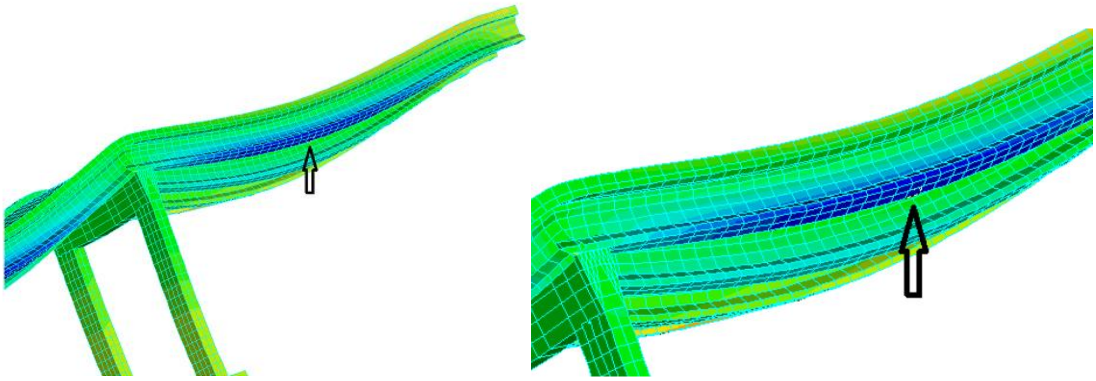

Figure 7.4 - Location of maximum X-displacement in the negative X-direction

The model was set at 5% displacement scale for figure 7.4 to further illustrate this.

The Y-displacement illustrates the deflection of the deck and the girders. Although the Headstock can deflect in the Y-direction as well, the size of it stops it from having much deflection, however the deck is very thin and can therefore deflect much more. This is shown in figure 7.5:

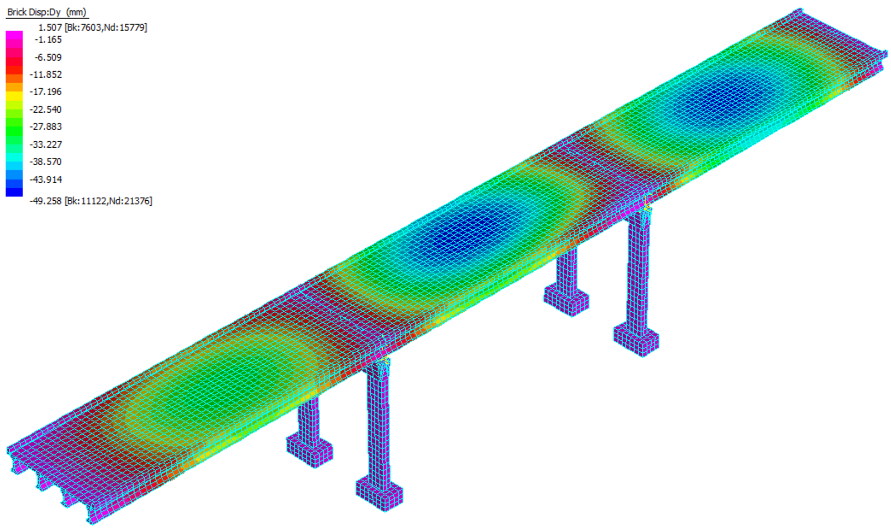

Figure 7.5 - Y-displacement contour plot

Again, the find function was used to locate the brick with the maximum Y-displacement. This is shown in figure 7.6:

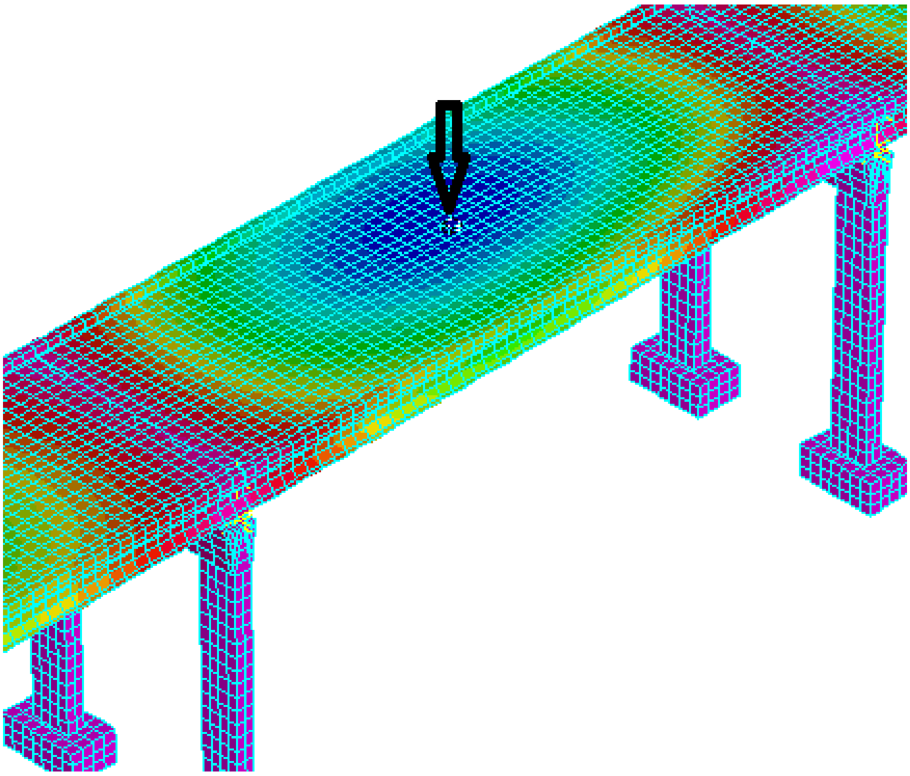

Figure 7.6 - Location of maximum Y-displacement

The Z-displacement represents the deflection of the piers and headstock, as well as the translation of the girders. This is because the deck allows very little displacement in the Z-direction. This can be seen in figure 7.7:

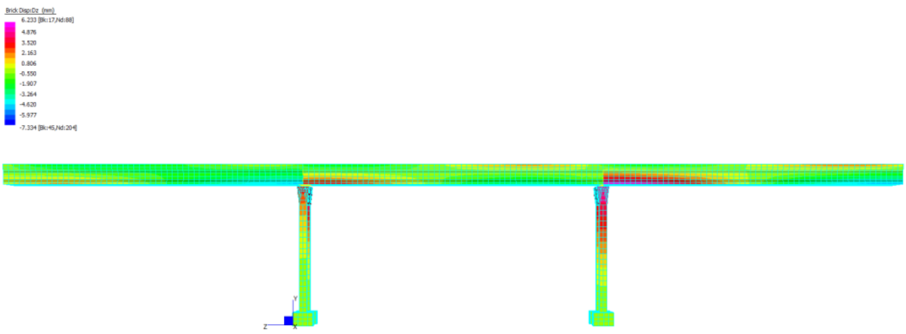

Figure 7.7 - Z-displacement of the AS5100 model

The location of the brick with the maximum Z-direction was found to be located on the 3 girder (looking downstream), shown in figure 7.8:

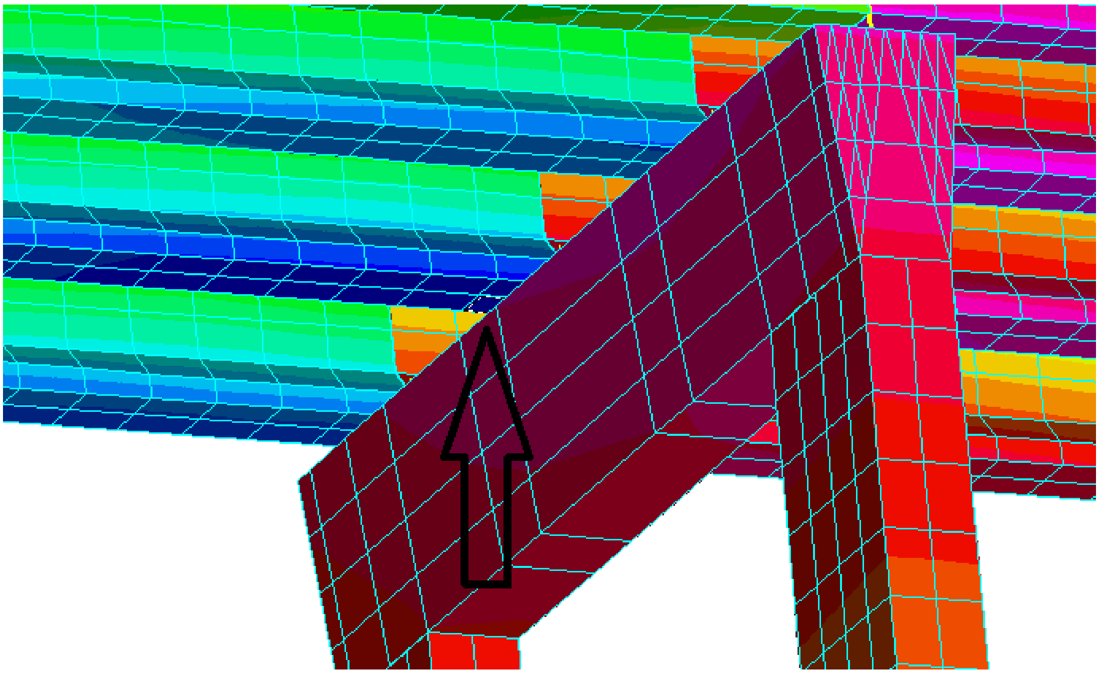

Figure 7.8 - Location of maximum Z-displacement

A slight error in the model was found here; there was a gap of 5mm assumed between the girder faces, however the displacement for this brick was -7.33mm. Furthermore, the brick on the opposing girder had a displacement of around 5-6mm, therefore a total gap of 12-14mm would be needed between the girders to make these results realistic. This indicates that the model isn't telling the girders to stop displacing after they come in contact. Upon further investigation, it appears that this error in the model doesn't actually effect the results, when referring to figure 5.2 of this report, the gap between the girders appears to be greater than 5mm, however this dimension could not be found in any of the engineering drawings provided by the Department of Transport and Main Roads (hence the initial assumption of a 5mm gap).

Overall, it can be seen table 7.4 that the X and Z-displacements are fairly reasonable (below 10mm), however the Y-displacement results are much larger than expected. This can be attributed to the steel reinforcement not being incorporated into the model. Since the spans of the deck and girders are quite long (27.383m), there will be very large bending moments being generated about the midspans, hence there will be a great deal of tensile forces being developed, which is why the steel reinforcement bars are an essential part of concrete structures design, this is because concrete is very weak in tension (refer to section 2.2.1 of chapter 2 for more information). It can also be seen from figure 7.1 that the most critical load combination in terms of deflection is load combination 9.

The stress concentration results were also analysed to give an indication of how the supports behave. The stress concentration results for the AS5100 model are shown in Table 7.5:

Table 7.5 - X, Y and Z stress concentration results

Load combination	Maximum X-stress (MPa)	Maximum Y-stress (MPa)	Maximum Z-stress (MPa)
1	4.64	-6.13	-18.15
2	4.60	-6.13	-17.73
3	-14.170	20.37	36.51
4	-8.97	14.24	29.83
5	-14.38	-39.38	-52.07
6	14.55	-34.96	-57.62
7	-15.48	-18.72	38.87
8	-10.59	15.79	32.77
9	25.70	-50.05	-103.31
10	25.62	-50.13	-102.52

This is better illustrated in figure 7.9:

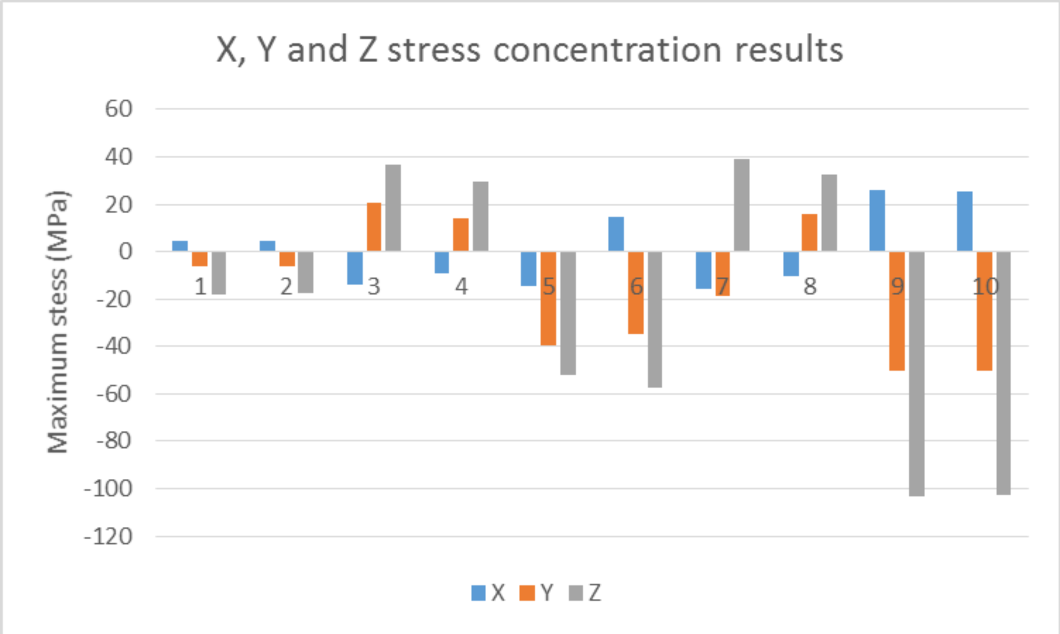

Figure 7.9 - Bar chart of X, Y and Z stress concentrations

It can again be seen in table 7.5 that the results are within a reasonable range. Figure 7.9 shows that the Z-stress is by far the most contributing stress. This is because the girders and deck span in the Z-direction. When the forces are applied to the deck and girders, the stresses are transferred to the supports, which move in the "Z" direction to get to these supports. As explained above, the superstructures are much smaller and weaker in comparison to the substructures, therefore more stress is generated at the superstructure supports.

Table 7.6 shows the overall XYZ displacement and stress concentration results.

Table 7.6 - XYZ stress and displacement results

Load combination	Maximum absolute XYZ displacement (mm)	Maximum absolute mean stress (MPa)
1	8.446	7.99
2	8.412	7.83
3	10.522	15.86
4	9.498	12.94
5	30.378	24.99
6	30.244	25.35
7	11.084	16.87
8	10.237	14.19
9	49.821	45.29
10	49.409	44.99

This is better illustrated in figure 7.10:

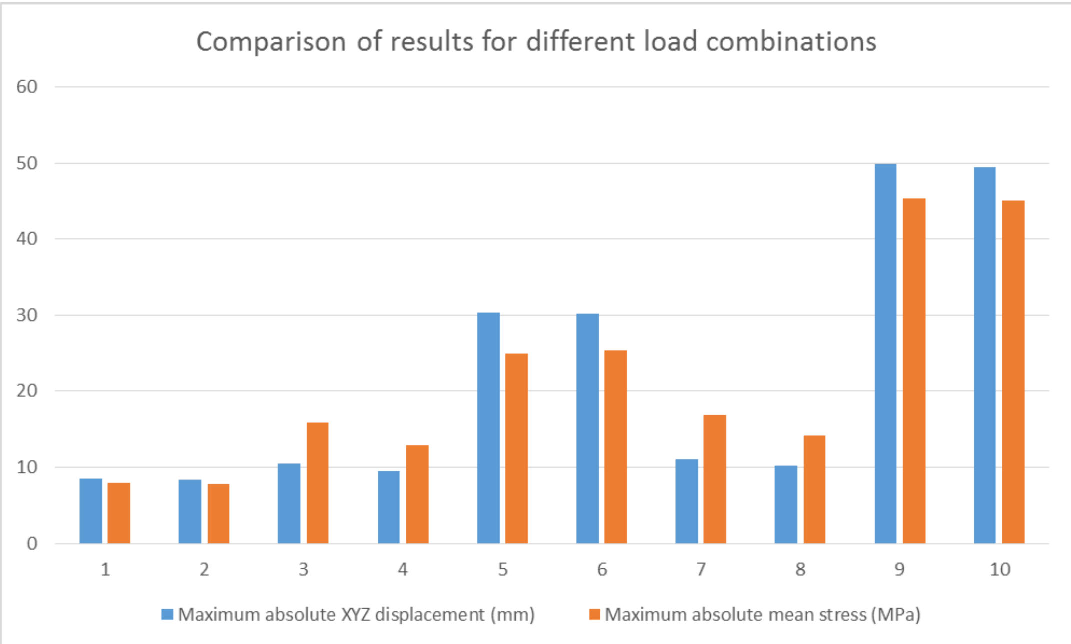

Figure 7.10 - Bar chart of XYZ stress and displacement results

The "XYZ displacement" shows the overall maximum displacement experienced at a node in terms of all directions, not just on a single plane. Similarly, the "mean stress" shows the maximum stress experienced at a brick in any direction, not just a single plane direction. That is why the values in table 7.6 are smaller than the individual stress components. This is because, while there is a great deal of stress experienced in the Z-direction, some of the X and Y-stresses "cancel out" a portion of the Z-stresses and hence yields an overall smaller stress concentration result. The above results are a more realistic representation of the behaviour of the model, therefore these results will be used for the international bridge design standards and a comparison will be made based off these results.

7.3 International Design Standards

As shown in section 7.2 of this chapter, the most critical flooding scenario for the bridge is the 500 year ARI discharge, also the worse-case flood height scenario governs over the worse-case velocity scenario. Hence, this flooding event was chosen to be used in comparing the International Bridge Design Standards to the Australian Standards.

7.3.1 BA 59/94

7.3.1.1 Load cases and load combinations

The load cases for the BA59/94 model are shown in table 7.7:

Table 7.7 - Load cases

Load case	Contributing force	Force type used
1	Self-weight	Gravity function in Strand7
2	Drag force (piers)	1kPa unit load
3	Drag force (superstructures)	1kPa unit load
4	Lift force (piers)	1kPa unit load
5	Debris force (superstructures, full submergence + 2.5m)	1kPa unit load
6	Log force (full submergence)	1kPa unit load
7	Buoyancy (full submergence)	Refer appendix D
8	Hydrostatic thrust (full submergence + 2.5m)	Refer appendix D

The load combinations which were used are:

1. G + 1.4*FF + 1.5*D
2. G + 1.4*FF + 1.5*LI

Where:

G = dead loads (self-weight)

FF = fluid forces (drag and lift)

D = Debris forces

LI = log-impact forces

The corresponding load case factors are shown in table 7.8:

Table 7.8 - Load case factors

Load case	Load combination 1	Load combination 2
1	1.0	1.0
2	1.77	1.77
3	9.72	9.72
4	3.53	3.53
5	4.89	0
6	0.00	184.24
7	1.00	1.00
8	1.00	1.00

7.3.1.2 Simulation results

The displacement results are shown below:

Table 7.9 - X, Y and Z displacement results

Load combination	Maximum X-displacement (mm)	Maximum Y-displacement (mm)	Maximum Z-displacement (mm)
1	-8.22	-39.46	-5.93
2	-8.41	-39.11	-5.89

The stress concentration results are shown in table 7.10:

Table 7.10 - X, Y and Z stress concentration results

Load combination	Maximum X-stress (MPa)	Maximum Y- stress (MPa)	Maximum Z- stress (MPa)
1	19.87	-41.75	-79.95
2	19.75	-42.02	-79.04

The XYZ stress and displacement results obtained are shown in table 7.11:

Table 7.11 - XYZ stress and displacement results (BA59/94)

Load combination	Maximum absolute XYZ displacement (mm)	Maximum absolute mean stress (MPa)
1	39.62	35.05
2	39.29	34.69

7.3.2 AASHTO

7.3.2.1 Load cases and load combinations

As shown in section 7.2 of this chapter, the most critical flooding scenario for the bridge is the 500 year ARI discharge, also the worse-case flood height scenario governs over the worse-case velocity scenario. Hence, there will be six load cases required for Strand7 modelling. The load cases are shown in table 7.12:

Table 7.12 - Load cases

Load case	Contributing force	Force type used
1	Self-weight	Gravity function in Strand7
2	Drag force (piers)	1kPa unit load
3	Lift force (piers)	1kPa unit load
4	Debris force (superstructures, full submergence, +2.5m)	1kPa unit load
5	Buoyancy (full submergence)	Refer appendix D
6	Hydrostatic thrust (full submergence + 2.5m)	Refer appendix D

The load combination which will be used are:

1. 0.9G + FF + D

Where:

G = dead loads (self-weight)

FF = fluid forces (drag and lift)

D = Debris forces

The corresponding load case factors are:

Table 7.13 - Load case factors

Load case	Load combination 1
1	0.9
2	4.42
3	3.15
4	1.58
7	1.00
8	1.00

7.3.2.2 Simulation results

The displacement and stress concentration results for the AASHTO model are shown in tables 7.14 and 7.15, respectively:

Table 7.14 - X, Y and Z displacement results

Load combination	Maximum X-displacement (mm)	Maximum Y-displacement (mm)	Maximum Z-displacement (mm)
1	8.74	-39.95	-5.81

Table 7.15 - X, Y and Z stress concentration results

Load combination	Maximum X-stress (MPa)	Maximum Y- stress (MPa)	Maximum Z- stress (MPa)
1	21.66	-36.01	-87.49

The XYZ stress and displacement results obtained can be found in table 7.16:

Table 7.16 - XYZ stress and displacement results

Load combination	Maximum absolute XYZ displacement (mm)	Maximum absolute mean stress (MPa)
1	39.97	38.32

7.3.3 Indian code of practice

7.3.3.1 Load cases and load combinations

As shown in section 7.2 of this chapter, the most critical flooding scenario for the bridge is the 500 year ARI discharge, also the worse-case flood height scenario governs over the worse-case velocity scenario. Hence, there will be five load cases required for Strand7 modelling. The load cases are tabulated below:

Table 7.17 - Load cases

Load case	Contributing force	Force type used
1	Self-weight	Gravity function in Strand7
2	Drag force (piers)	1kPa unit load
3	Lift force (piers)	1kPa unit load
4	Buoyancy (full submergence)	Refer appendix D
5	Hydrostatic thrust (full submergence + 2.5m)	Refer appendix D

There are no load factors that increase or decrease any of the load cases, therefore the load combination will simply be the sum of the ultimate flood loads.

The corresponding load case factors are:

Table 7.18 - Load case factors

Load case	Load combination 1
1	1
2	8.37
3	4.83
4	1.00
5	1.00

7.3.3.2 Simulation results

The displacement results are shown below:

Table 7.19 - X, Y and Z displacement results

Load combination	Maximum X-displacement (mm)	Maximum Y-displacement (mm)	Maximum Z-displacement (mm)
1	8.66	-39.90	-5.81

The stress concentration results are shown below:

Table 7.20 - X, Y and Z stress concentration results

Load combination	Maximum X-stress (MPa)	Maximum Y- stress (MPa)	Maximum Z- stress (MPa)
1	21.54	-36.87	-86.74

The XYZ stress and displacement results obtained were:

Table 7.21 - XYZ stress and displacement results

Load combination	Maximum absolute XYZ displacement (mm)	Maximum absolute mean stress (MPa)
1	39.92	38.01

7.4 Comparison of the standards

Now that the results have been obtained, a basic comparative analysis can be performed. As explained above, the XYZ displacement and mean stress results have been obtained as they are the best indicator of the behaviour of the bridge, they are also much more convenient for a comparative analysis. Table 7.22 and figure 7.11 summarises the results for the most critical flooding scenario:

Table 7.22 - XYZ stress and displacement results for all standards

Bridge design standard	Maximum absolute XYZ displacement (mm)	Maximum absolute mean stress (MPa)
AS5100	49.82	45.29
BA 59/94	39.62	35.05
AASHTO	39.97	38.32
Indian Code of Practice	39.92	38.01

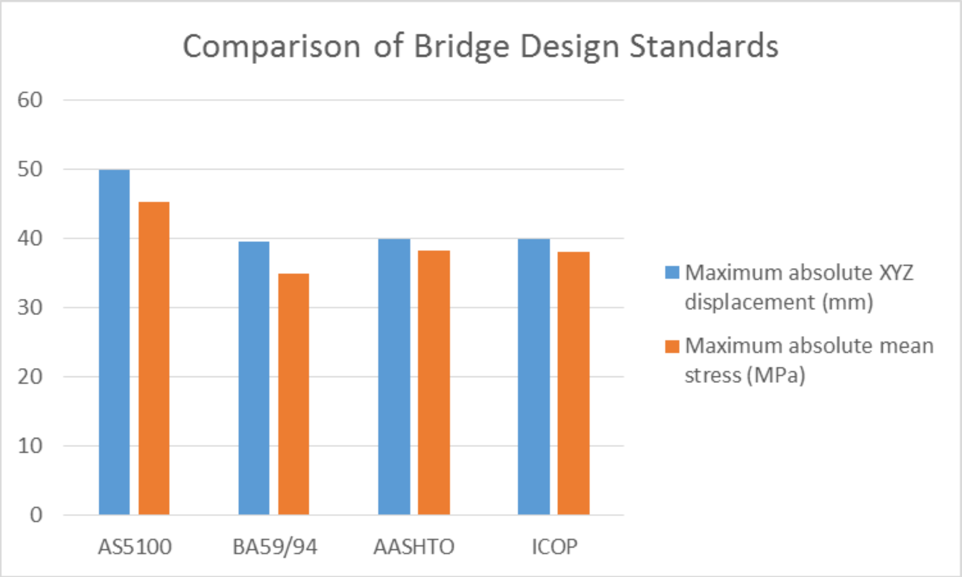

Figure 7.11 - Bar chart stress and displacement results

The results in table 7.22 indicate that the Australian Standards produce much more severe results in comparison to the international bridge design standards. These results shows that the Australian Standards have a higher factor of safety when designing bridges to resist flooding events. A more detailed comparative analysis is shown below.

The X, Y and Z displacement results for all Design Standards are shown in table 7.23 and figure 7.12.

Table 7.23 - X, Y and Z displacement results for all standards

Bridge design standard	Maximum X-displacement (mm)	Maximum Y-displacement (mm)	Maximum Z-displacement (mm)
AS5100 (Fluid forces + debris)	-9.50	-49.69	-7.39
AS5100 (Fluid forces + logs)	-9.49	-49.25	-7.33
BA 59/94 (Fluid forces + debris)	-8.21	-39.46	-5.93
BA 59/94 (Fluid forces + logs)	-8.40	-39.10	-5.89
AASHTO (fluid forces +debris)	8.74	-39.95	-5.81
Indian Code of Practice (fluid forces only)	8.66	-39.90	-5.81

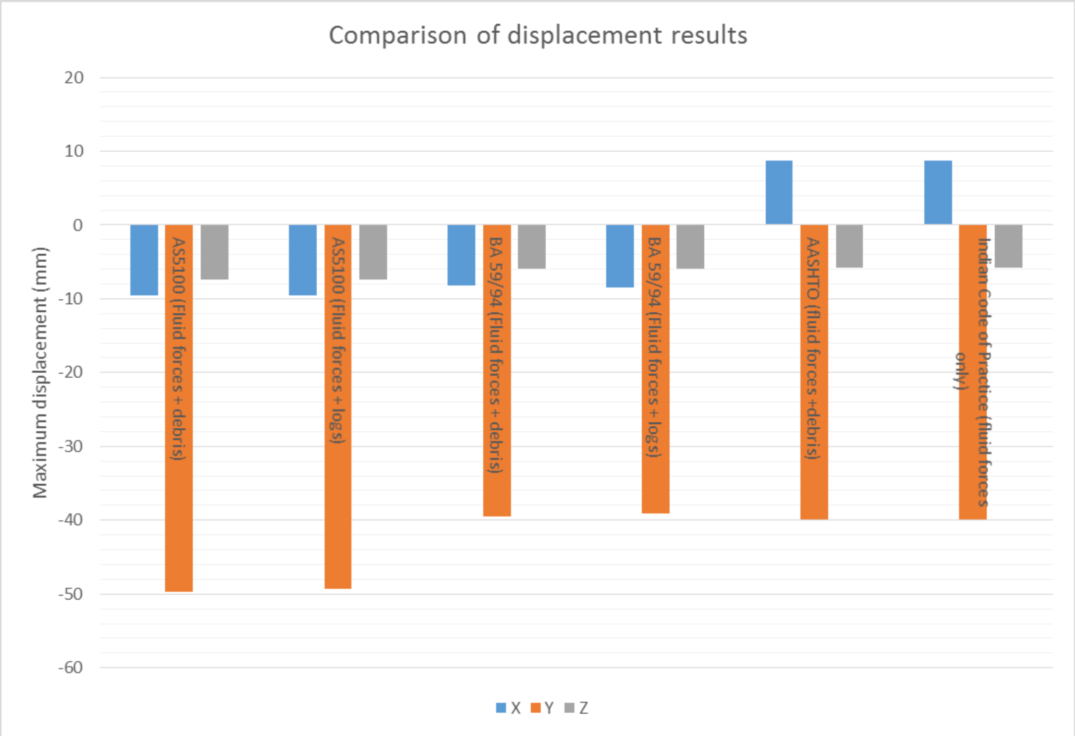

Figure 7.12 - Bar chart comparing displacement results

It can be seen from table 7.23 that, again, the Australian Standards overall produce the most adverse effects. This validates that it provides more conservative results all around, and not just in a single direction. For example, if the Y and Z-displacement results were similar but there was only a large variation in the X-displacement results, then this could simply mean that the Australian Standards provide a safer design against drag or debris forces but provide similar results for the lift (up and down-lift for Y-displacement and side-lift for Z-displacement) forces.

For the X-displacement, the maximum deflections for AS5100 and BA59/94 are in the negative X-direction, while AASHTO and the Indian code of Practice' results are in the positive X-direction. This indicates that the latter two produce a greater overturning result of the bridge, which would be desirable, however this can be attributed to a lack of missing forces not being accounted for in these standards. For example, debris forces are not taken into account in the Indian Code of Practice, which would resist overturning of the structure. Also, downward and up-lift forces aren't taken into account, which also increase the resistance to overturning. The Y and Z-displacements are all reasonable and expected results.

The stress concentration results for all of the standards are shown in table 7.24 and figure 7.13

Table 7.24 - X, Y and Z stress concentration results for all standards

Bridge design standard	Maximum X-stress (MPa)	Maximum Y-stress (MPa)	Maximum Z-stress (MPa)
AS5100 (Fluid forces + debris)	25.69	-50.05	-103.31
AS5100 (Fluid forces + logs)	25.61	-50.12	-102.52
BA 59/94 (Fluid forces + debris)	19.87	-41.75	-79.95
BA 59/94 (Fluid forces + logs)	19.75	-42.02	-79.04
AASHTO (fluid forces +debris)	21.65	-36.01	-87.49
Indian Code of Practice (fluid forces only)	21.53	-36.87	-86.74

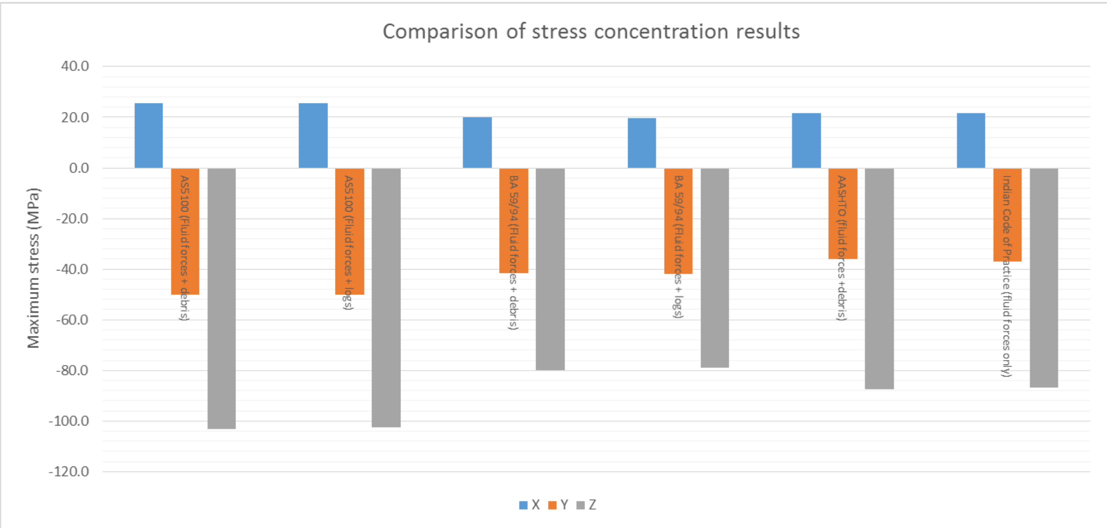

Figure 7.13 - Bar chart of X, Y and Z stress concentration results

The results above again indicate that the Australian Standards produce more adverse effects overall in terms of stress concentration. To compare each standard to the Australian Standard, the relative difference between the Australian Standard and the International Standard of interest was calculated for the most critical load combinations in X, Y and Z stress-concentration. From this, the average relative change was found to give an overall indicator of the difference in results.

Table 7.25 - Relative difference of the International Standards vs Australian Standard

International Standard	Relative difference in X-stress	Relative difference in Y-stress	Relative difference in Z-stress	Average relative difference
BA 59/94	22.65%	16.58%	22.61%	20.62%
AASHTO	15.73%	28.05%	15.31%	19.70%
Indian Code of Practice	16.19%	26.33%	16.04%	19.52%

It can be concluded from table 7.25 that, in comparison to the Australian Standards, the British Standard (BA 59/94) produces the least adverse effect for the 500 year ARI flooding event. This is then followed by the American Standard and finally the Indian Code of Practice.

Overall, the results indicate that there is no recommendations that can be made to the Australian Standards, based on the results produced by the international standards.

CHAPTER 8 CONCLUSIONS AND FUTHER WORK

8.1 Summary

This research project has successfully analysed the behaviour of bridges subjected to flood loadings based on different design standards from around the world. Flood loadings, traffic loadings and load combinations were identified from the Australian Bridge Design Standard, AS5100, 2004. Flood loadings and load combinations were also identified from an American standard, AASHTO LFRD Bridge Design Specifications, 2012, a European standard, BA59/94 as well as an Asian standard, Indian code of Practice, 2014. As a learning process, a simple bridge deck model was simulated in Strand7 with a simple flood loading applied to it to understand the core skills required. A complex bridge (Tenthill Creek Bridge) was successfully identified within the Lockyer Valley Region that is prone to extreme flooding events and data was gathered on the bridges details, however simplifications had to be made to assist in the simulation. The skills obtained from the simple bridge deck model were applied successfully to the complex bridge model. Various submergence conditions were identified and a full, comprehensive analysis was conducted on AS5100 to determine the most critical loading condition. It was determined that a flood height scenario gave the most adverse effects in comparison to the velocity scenarios. The most critical submergence case was identified and this submergence case was used for the modelling of the bridge subjected to the flood loadings from international standards. It was determined that AS5100 produced the most adverse effects in terms of stress concentration and displacement. Based on the results, it was determined that no recommendations could be made to AS5100, based off the results produced by the international standards.

8.2 Achievement of Project Objectives

The following project objectives have been addressed:

1) Research literature and background information relating to the different types of bridges, including the different construction practices used, as well as natural disasters

This has been addressed in chapter two of the report. Basic concepts relating to bridges, bridge construction as well as natural disasters (mainly flooding) have been introduced and linked together via example events. Also, the basic concepts relating to the different types of forces have been outlined.

2) Research and compare bridge design standards from around the world and identify flood loadings and load combinations that need to be taken into consideration for the design of a bridge in areas prone to flooding

This has been addressed in chapters three and four of this report. Chapter three successfully identified the flood loadings, traffic loads and load combinations that are outlined in the standards when designing bridges in flood prone areas. Chapter four outlines the flood loadings and load combinations recommended within the International standards. The comparison between the standards was performed in chapter 7.

3) Simulate the behaviour of a small, simple bridge subjected to the identified flood loadings

This has been addressed in chapter 6, section 6.2 of the report. This section shows the model development as well as some example results with a simple flood loading applied. This section was intended as a learning exercise for the author.

4) Identify a more complicated, realistic bridge in the Lockyer Valley Region that is prone to extreme flooding events and collect available data on the bridge

This has been successfully addressed in section 5.3 of this report. This section gives the bridge details and flooding parameters required to successfully perform the simulation. Simplifications were made to the bridge structure to assist in the simulation process as accurate results were not a number one priority for this simulation.

5) Simulate the behaviour of the bridge subjected to different flood loadings from the available design standards

This has been addressed in section 6.3 and chapter 7 of the report. Section 6.3 presents the development process of the model such as the geometric model creation, the model restraints as well as the meshing of the model. The simulation results were displayed by means of bar charts and tables and discussed in chapter 7

6) Draw appropriate conclusions as to how the Australian Bridge Design Standards perform in a flooding event in comparison to different standards around the world

This has been addressed in chapter 7 and section 8.1 of this report.

7) Make recommendations for the Australian bridge design standards, AS5100 based on these results

This has been addressed in section 8.1 of the report. The results from the international standards did not “out-perform” the Australian Standards in any aspects of the simulation, therefore specific recommendations could not be made to the Australian Standards based off the results from the international standards, however general suggestions have been made in section 8.1.

8.3 Conclusions

In conclusion, it the project aim was successfully achieved. The results indicate that there were no recommendations that could be made to the Australian Bridge Design Standards based on the results produced by the International Standards. In fact, the results indicate that international standards could make a great deal of improvements to their flood loadings, based on the Australian Standards. Further work would need to be conducted to determine if specific recommendations could be made to the current Australian Bridge Design Standards.

8.4 Recommendations for future work

As previously mentioned, the model results are very crude, therefore there is a great deal of future work that can be performed on this project if specific recommendations are to be made to the Australian Standards. Recommendations for future work are:

1. Prepare a model of Tenthill Creek Bridge that incorporates the steel reinforcement layers into the structural components of the bridge.
2. Prepare a 3D or Computational Fluid Dynamics (CFD) model of Tenthill Creek Bridge that accurately describes the behaviour of the fluid during a flooding event.

8.4.1 Incorporation of steel reinforcement

As mentioned in section 3.5.4 of the report, the steel reinforcement has been neglected from the simulation due to time limitations of the project. As it was shown in chapter 7, this had a significant effect on the Y-displacement results, giving deflections of almost 50mm. Including steel reinforcement would have a significant improvement on the results and give a much more accurate indicator of the structural behaviour of the bridge. Due to the complexity of the steel reinforcement of Tenthill Creek Bridge structural components, it was simply not an option for this simulation. However, steel reinforcement can be performed in Strand7 but it is very difficult to model, even for a simple layer of steel reinforcement. Furthermore, the model would need to be processed by Strand7's non-linear analysis solver, which has a very long computational time in comparison to the linear static solver. Due to the size of the bridge, performing a non-linear analysis in Strand7 would take extremely long, so a possible option would be to produce a scaled down model in Strand7. This could make the incorporation of the steel reinforcement layers even more complicated as they too would need to be scaled down. Furthermore, the flood loadings would also need to be scaled down.

8.4.2 Accurate modelling of the flow behaviour

Preparing a 3D or CFD model would also have a fairly significant change in the application of the flood loadings as the current Strand7 model has neglected the water flow behaviour. For example when the flowing water comes in contact with the pier, the water will "split" and there will be variable flow distribution around the piers, which will result in possible "pockets" of stagnant water around the piers as well as vortices being created by the turbulence. The fluid behaviour will also determine the submergence condition of the bridge. It has been assumed that the water level does not change with distance along the structure (from the upstream end to the downstream end), which, unless water was flowing at a very slow velocity, is not the case. Figures 8.1-8.3 show the different possible submergence conditions for a bridge in the event of a flooding event.

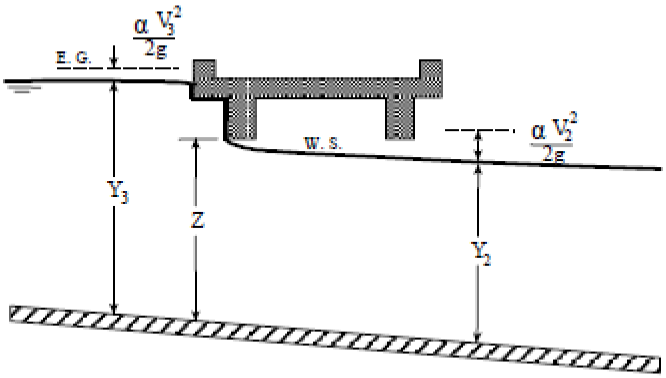

Figure 0.1 - Sluice gate type of pressure flow

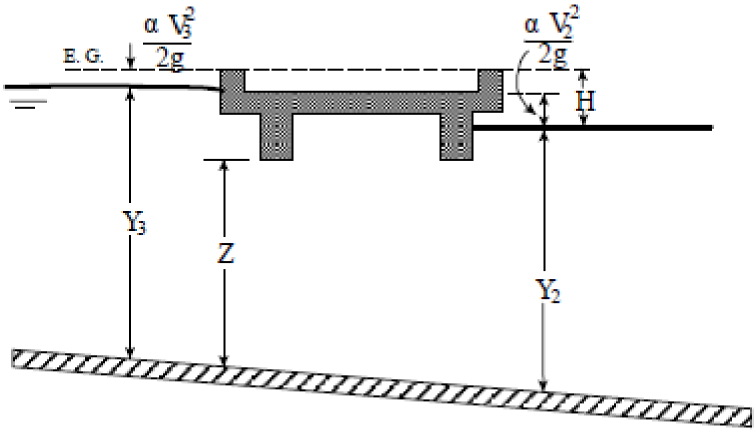

Figure 0.2 - Fully submerged pressure flow

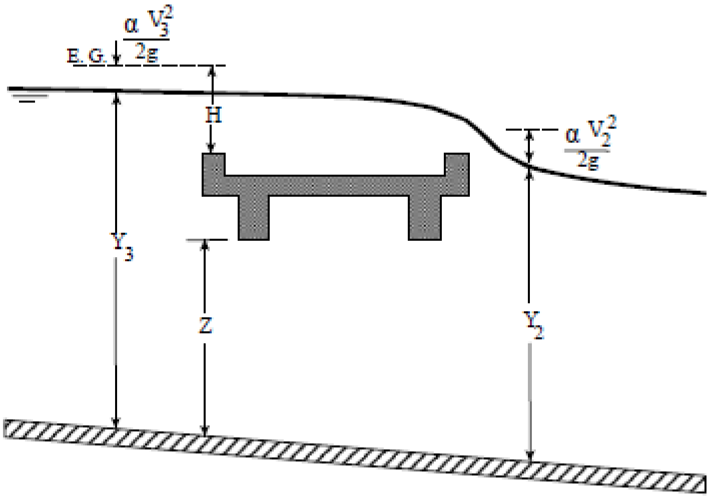

Figure 0.3 - Pressure and weir flow behaviour

(Brunner 2010)

Based on figures 8.1-8.3, for the Tenthill Creek Bridge model, fully submerged pressure flow has been assumed, however it has been assumed that $\frac{\alpha V_3^2}{2g} = \frac{\alpha V_2^2}{2g}$. This has been assumed to simplify the load application process, however this is not realistic fluid behaviour. For example, for the full submergence condition where the flood height level is equal to the top level of the deck, there could be a sluice gate type of pressure flow, depending on the flow velocity; this could cause air pockets between the girders and hence there will be no hydrostatic pressure or buoyancy confining the girders, which could result in more deflection. When the flow velocity is higher, there will be more flow separation, which could result in the submergence condition changing from fully submerged pressure flow to sluice gate, which would result in different structural behaviour by the superstructures.

Finally, if the complex bridge was analysed in a CFD or 3D fluid modelling software package, the effects of scouring could be taken into account.

If the above recommendations for future work were to be performed then the model results could be deemed more reliable and further work could then be performed on investigating finer details and making specific recommendations to the Australian standards. An example of this could be to make a recommendation to the standards to change the drag and lift coefficients depending on the submergence conditions (refer figures 8.1-8.3); there would be a larger down-lift for a fully submerged pressure flow condition compared to a pressure and weir flow behaviour.

REFERENCES

Australian Standards 2004, *AS 5100.1 - 2004*, Bridge Design, Part 1: Scope and General Principles, Standards Australia, Australia, viewed 09/03/2015, <http://www.saiglobal.com/PDFTemp/osu-2015-03-09/8267909466/5100.1-2004(+A1).pdf>.

AASHTO 2012, *AASHTO LFRD Bridge Design Specifications*, American Association of State Highway and Transport Officials, viewed 28/06/2015, <

BBC 2009, *Body found in Cumbria flood is missing Pc, say police*, BBC News, UK, viewed 16/04/2015, <http://news.bbc.co.uk/2/hi/uk_news/8370865.stm>

BBR 2015, *Engineering excellence in bridge construction and heavy lifting*, BBR VT International Ltd, Switzerland, viewed 14/04/2015, <http://www.bbrnetwork.com/technologies/construction-methods.html>

Blake, M 2013, *Longest covered bridge in Asia is destroyed after massive fire ripped through the 303-metre wooden structure*, Associated Newspapers Ltd, viewed 16/04/2015, <http://www.dailymail.co.uk/news/article-2515693/Longest-covered-bridge-Asia-destroyed-massive-ripped-303-metre-wooden-structure.html>

BOM 2015, *FLOODS - Warning, Preparedness & Safety*, Australian Government - Berau of Meteorology, viewed 11/03/2015, <http://www.bom.gov.au/>

Brunner, G 2010, *HEC-RAS, River Analysis System Hydraulic Reference Manual*, CPD-69, Hydrologic Engineering Center (HEC), USA,

CivilDigital.com 2015, *Bridge Engineering – Components of Bridge Structures*, CivilDigital, viewed 16/04/2015, <http://civildigital.com/bridge-engineering-components-classification-bridges/>

Congress, IR 2014, *Standard Specifications and Code of Practice*, Loads and Stresses, Indian Roads Congress, India, viewed 1/08/15, <

Construction, PC 2015, *Very Big Box Girder*, viewed 13/04/2015, <http://www.precastconcreteconstruction.com/32/very-big-box-girder>

Constructor, T 2014, *COMPARISON BETWEEN PRESTRESSED CONCRETE, RCC AND ARCH*, The Constructor, viewed 06/03/2015,

<http://theconstructor.org/others/prestressed-concrete-over-reinforced-concrete-and-arch/6255/>

Corus 2007, *Student guide to steel bridge design*, Corus Construction Services & Development, viewed 06/03/2015, <http://discus.steel-sci.org/Content/documents/student-guide-steel-bridge-design.pdf>

DNRM 2015, *Water monitoring portal*, Department of Natural Resources and Mines, viewed 16/09/2015, <https://www.dnrm.qld.gov.au/water/water-monitoring-and-data/portal>

efunda 2015, *General trapezoid*, EFunda, Inc, viewed 21/10/15, <http://www.efunda.com/math/areas/Trapezoid.cfm>

Friend, C 2013, *Concrete Bridge Failures - Deterioration and Spalling*, Tangient LLC, The Pennsylvania State University, viewed 17/04/2015, <http://failures.wikispaces.com/Concrete+Bridge+Failures+-+Deterioration+and+Spalling>

Galbraith, R 2009, *Living in the Landscape: the Lockyer Valley. A guide to property and landscape management*, South East Queensland Catchments Limited, Brisbane, viewed 13/04/2015, <http://www.lockyervalley.qld.gov.au/images/PDF/plan_and_build/Environment/living%20in%20the%20lockyer.pdf>

Government, Q 2015, *Fire danger rating*, Queensland Government, viewed 15/04/2015, <https://www.qld.gov.au/emergency/safety/fire-danger.html>

Group, CBD 2015, *Types of Concrete Bridges*, Concrete Bridge Development Group, viewed 09/03/2015, <http://www.cbdg.org.uk/intro3.asp>

Hanes, R 2012, *prestressed girder box for bridge by Rogers Hanes*, viewed 13/04/2015, <http://www.rogershanes.com/prestress-concrete-girder-box-for-bridge/prestressed-girder-box-for-bridge-by-rogers-hanes/>

Honert, RCvd & McAneney, J 2011, 'The 2011 Brisbane Floods: Causes, Impacts and Implications', viewed 09/03/2015, <https://www.riskfrontiers.com/pdf/water-03-01149.pdf>

Iqbal, S 2013, *What is scouring, Bridge Scouring? How to calculate Scour Depth?*, Civil Engineering Blog, viewed 17/04/2015, <http://www.iamcivilengineer.com/2013/12/what-is-scouring-bridge-scouring-how-to.html>

Johnson, P 2015, *Bridge Scour and Stream Stability*, Department of Civil and Environmental Engineering, PennState University, viewed 17/04/2015, <http://www.personal.psu.edu/faculty/p/a/paj6/Research.html>

LaViolette, M, Wipf, T, Lee, Y-S, Bigelow, J & Phares, B 2007, *BRIDGE CONSTRUCTION PRACTICES USING INCREMENTAL LAUNCHING*, National Cooperative Highway Research Progran, Washington D.C, USA, <http://onlinepubs.trb.org/onlinepubs/archive/NotesDocs/20-07(229)_FR.pdf>

Leeson, D, Fulmer, C & Heron, K 2014, 'Flood Resilient Bridge Design: Case Studies From Challenging Design Environments', presented at *9th Austroads Bridge Conference*, Sydney, New South Wales, viewed 29/05/15, <http://www.arrb.com.au/admin/file/content128/c6/11431_CF_Flood%20resilient%20Bridge%20Design;%20case-%20studies%20from%20challenging%20design%20environments.pdf>.

Library, LE 2015, *Glossary of Bridge Terminology*, University of Iowa Libraries, viewed 16/04/2015, <http://sdrc.lib.uiowa.edu/eng/bridges/WaddellGlossary/gloss.htm>

LUSAS 2013, *Case Study: Dee River Crossing*, viewed 13/04/2015, <http://www.lusas.com/case/bridge/deeriver.html>

Maeseele, M 2011, *Lockyer to face $1b flood bill*, The Queensland Times, viewed 13/04/2015, <http://www.qt.com.au/news/ipswich-lockyer-to-face-1b-flood-bill/758634/>

n.a *Lockyer Valley and Toowoomba*, <http://www.floodcommission.qld.gov.au/__data/assets/pdf_file/0004/8788/QFCI-Interim-Report-Chapter-7-Lockyer-Valley-and-Toowoomba.pdf>

Navy, I 2014, *Latest Update on Cyclone Hudhud*, Indian Navy, India, viewed 16/04/2015, <http://www.indiannavy.nic.in/press-release/latest-update-cyclone-hudhud>

NSW, RaTAo 2008, *Timber Bridge Manual*, 1 edn, Bridge Engineering Technology Branch Roads and Traffic Authority of NSW, viewed 07/03/2015 <http://www.rms.nsw.gov.au/documents/projects/key-build-programs/maintenance/tbm-1.pdf>

PERI 2015, *Motorway bridge over the Rio Sordo*, PERI Group, viewed 5/4/2015, <http://www.peri.com.kw/projects/projects/civil-engineering-projects/motorway_bridge_rio_sordo.cfm>

Pritchard, R 2013, *2011 to 2012 Queensland floods and cyclone events:*

Lessons learnt for bridge transport infastructure, Institution of Engineers Australia, viewed 29/05/15, <http://dx.dol.org/10.7158/S13-009.2013.14.2>

Pujol 2015, *Reinforced concrete pre-slab*, viewed 13/04/2015, <http://www.archiexpo.com/prod/pujol/reinforced-concrete-pre-slab-89366-915540.html>

QDMR 2003, *Case Study: Comparison of DMR practices and application of FRP technology (first draft)*,

Queensland, TSo 2014, *Regional First Home Owner Grant - Map of eligible areas*, Queensland Government, viewed 13/04/2015, <https://www.osr.qld.gov.au/historical-information/information-bul/fhog-boost/regional-fhog.shtml>

REIDsteel 2015, *50m Span Steel Bridge Construction Project*, John REID & Sons Ltd, England, viewed 14/04/2015, <http://www.steel-bridges.com/existingbridge6258.html?id=21>

Rohleder, W 2015, *Segmental Bridge Technology – Established and Evolving*, The State University of New York, New York, USA, viewed 14/04/2015, <http://mceer.buffalo.edu/education/bridge_speaker_series/2010-2011/presentations/Rohleder_presentation.pdf>

Saskatchewan, Uo 2015, *Hydrostatic force*, College of Arts & Science, Saskatchewan, viewed 05/09/2015, <http://physics.usask.ca/~chang/course/ep324/lecture/lecture8.pdf>

Seaperch 2015, *What is Bouyancy?*, Seaperch, viewed 12/08/2015, <http://www.phillyseaperch.org/uploads/9/1/0/6/9106381/buoyancy_for_ms.pdf>

Skwirk 2015, *Bushfires and bushfires in Australia*, Skwirk Online Education, viewed 15/04/2015, <http://www.skwirk.com/p-c_s-57_u-479_t-1306_c-5027/qld/sose-geography/disasters/natural-hazards/bushfires-and-bushfires-in-australia>

Standards, A 2004a, *AS 5100.1 - 2004*, Bridge Design, Part 1: Scope and General Principles, Standards Australia, Australia, viewed 09/03/2015, <http://www.saiglobal.com/PDFTemp/osu-2015-03-09/8267909466/5100.1-2004(+A1).pdf>

Standards, A 2004b, *AS 5100.2 - 2004*, Bridge Design, Part 2: Design Loads, Standards Australia, Australia, viewed 8/05/2015, <http://www.saiglobal.com/PDFTemp/osu-2015-05-08/3768016978/5100.2-2004(+A1).pdf>

SteelConstruction.info 2015, Steel construction.info, viewed 06/03/2015, <http://www.steelconstruction.info/Bridges>

Strand7 2015, *Strand7 linear static solver*, Strand7 Pty. Ltd., Sydney, Australia, viewed 2/06/15, <http://www.strand7.com/html/linearstatic.htm>

The Highways Agency, TSODD, The Welsh Office, The Department of the Environment for Northern Ireland 1994, *Design Manual for Roads and Bridges* The Design of Highway Bridges for Hydraulic Action, viewed 21/08/15, <

Toolbox, TE 2015, *Impact force*, The Engineering Toolbox, viewed 02/09/2015, <http://www.engineeringtoolbox.com/impact-force-d_1780.html>

USQ 2014, *CIV3506 - Concrete Structures*, Studybook, University of Southern Queensland, University of Southern Queensland, viewed 06/03/2015 <http://www.usq.edu.au/>

U.S. Department of Transportation 2011, *Bridge Preservation Guide*, Maintaining a State of Good Repair Using Cost Effective Investment Strategies, The Federal Highway Administration, USA, viewed 09/03/2015, <http://www.fhwa.dot.gov/bridge/preservation/guide/guide.pdf>.

APPENDICES

Appendix A – Project Specifications

University of Southern Queensland

SCHOOL OF CIVIL ENGINEERING AND SURVEYING

ENG 4111/4112 Research Project

PROJECT SPECIFICATION

FOR:	Bradley Jordan
TOPIC:	Analysis of bridges subjected to flood loadings based on different design standards
SUPERVISORS:	Weena Lokuge & Karu Karunasena
ENROLLMENT:	ENG4111 – S1, ONC, 2015 ENG4112 – S2, ONC, 2015
PROJECT AIM:	This project aims at simulating the behaviour of bridges subjected to flood loadings from different available design standards
SPONSORSHIP:	None
PROGRAMME:	**Issue B, June 2015**

1) Research literature and background information relating to the different types of bridges, including the different construction practices used, as well as natural disasters
2) Research and compare bridge design standards from around the world and identify flood loadings and load combinations that need to be taken into consideration for the design of a bridge in areas prone to flooding
3) Simulate the behaviour of a small, simple bridge subjected to the identified flood loadings
4) Identify a more complicated, realistic bridge in the Lockyer Valley Region that is prone to extreme flooding events and collect available data on the bridge
5) Simulate the behaviour of the bridge subjected to different flood loadings from the available design standards
6) Draw appropriate conclusions as to how the Australian Bridge Design Standards perform in a flooding event in comparison to different standards around the world
7) Make recommendations for to the Australian bridge design standards, AS5100 based on these results

Appendix B – Flood frequency analysis data for Tenthill Creek

Streamflow data from 1968 to 2015:

Time and Date	Max Discharge (Cumecs)	Quality code
1/01/1968 0:00		255
1/01/1969 0:00		255
1/01/1970 0:00		255
1/01/1971 0:00	901.602	9
1/01/1972 0:00	49.552	9
1/01/1973 0:00		255
1/01/1974 0:00		255
1/01/1975 0:00	69.84	9
1/01/1976 0:00	519.112	9
1/01/1977 0:00	73.845	9
1/01/1978 0:00	1.388	9
1/01/1979 0:00	17.657	59
1/01/1980 0:00	0	15
1/01/1981 0:00	311.638	60
1/01/1982 0:00		255
1/01/1983 0:00		255
1/01/1984 0:00	40.007	9
1/01/1985 0:00	23.625	60
1/01/1986 0:00	0.001	15
1/01/1987 0:00	10.503	30
1/01/1988 0:00	432.8	60
1/01/1989 0:00	95.65	60
1/01/1990 0:00	56.304	30
1/01/1991 0:00	846.621	60
1/01/1992 0:00	213	59
1/01/1993 0:00	1.93	59
1/01/1994 0:00	0	10
1/01/1995 0:00	11.687	30
1/01/1996 0:00	936.276	60
1/01/1997 0:00	9.002	30
1/01/1998 0:00	0	10
1/01/1999 0:00	17.37	59
1/01/2000 0:00	0.482	60
1/01/2001 0:00	273.925	60
1/01/2002 0:00	0	10
1/01/2003 0:00	0	10
1/01/2004 0:00	6.71	20

1/01/2005 0:00	85.42	30
1/01/2006 0:00	0	15
1/01/2007 0:00	11.765	30
1/01/2008 0:00	109.805	30
1/01/2009 0:00	3.992	20
1/01/2010 0:00	1176.461	60
1/01/2011 0:00	1098.644	60
1/01/2012 0:00	31.328	30
1/01/2013 0:00	1359.358	60
1/01/2014 0:00	35.118	30
1/01/2015 0:00		255

The quality code variables are given below:

Variables:
100 - Stream Water Level (Metres)
140 - Stream Discharge (Cumecs)
Qualities:
9 - CITEC - Normal Reading
10 - Good
15 - Water level below threshold (no flow)
20 - Fair
30 - Poor
59 - CITEC - Derived Height
60 - Estimate
255 - No data exists

The details of the flood frequency analysis are given below:

Formulas
AEP = (m-0.4)/(n+0.2)
ARI = 1/AEP
Mean (M) = ΣX/N
Standard Deviation (S) = [Σ(X-M)^2/(N-1)]^0.5
Skew (G) = ((N*Σ(X-M)^3)/((N-1)(N-2)*S^3)
Log(Q_Y) = M + Ky*S
Q_Y = 10^Log(Q_Y)
Log(CL5) = Log(Q_Y) + 1.645*(δ*S/sqrt(N))
CL5 = 10^Log(CL5)
Log(CL95) = Log(Q_Y) - 1.645*(δ*S/sqrt(N))
CL95 = 10^Log(CL95)

Flood frequency analysis table 1:

Rank	Discharge (m^3/s)	AEP	AEP %	ARI	Z	X = LOG(Q)	(X-M)^2	(X-M)^3
1	1359.358	0.017544	1.754386	57	2.107345	3.133333847	2.29931117	3.486556
2	1176.461	0.046784	4.678363	21.375	1.676873	3.070577535	2.11292871	3.071336
3	1098.644	0.076023	7.602339	13.15385	1.432339	3.040856988	2.027408944	2.886769
4	936.276	0.105263	10.52632	9.5	1.25212	2.971403891	1.834448159	2.48461
5	901.602	0.134503	13.45029	7.434783	1.105355	2.955014866	1.790321579	2.395502
6	846.621	0.163743	16.37427	6.107143	0.979191	2.927689037	1.717942775	2.251713
7	519.112	0.192982	19.29825	5.181818	0.866958	2.715261068	1.206208398	1.324749
8	432.8	0.222222	22.22222	4.5	0.76471	2.636287252	1.038975295	1.059029
9	311.638	0.251462	25.1462	3.976744	0.669896	2.493650409	0.768540702	0.673752
10	273.925	0.280702	28.07018	3.5625	0.580758	2.43763167	0.67345952	0.552672
11	213	0.309942	30.99415	3.226415	0.496016	2.328379603	0.506081035	0.360023
12	109.805	0.339181	33.91813	2.948276	0.414699	2.040622116	0.179467664	0.076029
13	95.65	0.368421	36.84211	2.714286	0.336038	1.980684974	0.132277034	0.048109
14	85.42	0.397661	39.76608	2.514706	0.259406	1.931559567	0.098956607	0.031129
15	73.845	0.426901	42.69006	2.342466	0.184271	1.868321095	0.063169392	0.015877
16	69.84	0.45614	45.61404	2.192308	0.110162	1.844104231	0.051582747	0.011715
17	56.304	0.48538	48.53801	2.060241	0.036655	1.750539249	0.017836504	0.002382
18	49.552	0.51462	51.46199	1.943182	-0.03665	1.695061188	0.006095754	0.000476
19	40.007	0.54386	54.38596	1.83871	-0.11016	1.602135986	0.000220519	-3.3E-06
20	35.118	0.573099	57.30994	1.744898	-0.18427	1.545529774	0.005105974	-0.00036
21	31.328	0.602339	60.23392	1.660194	-0.25941	1.49593267	0.014653879	-0.00177
22	23.625	0.631579	63.15789	1.583333	-0.33604	1.373371817	0.05934781	-0.01446
23	17.657	0.660819	66.08187	1.513274	-0.4147	1.246916917	0.136951034	-0.05068
24	17.37	0.690058	69.00585	1.449153	-0.49602	1.239799818	0.142269322	-0.05366
25	11.765	0.719298	71.92982	1.390244	-0.58076	1.070591932	0.298546343	-0.16312
26	11.687	0.748538	74.8538	1.335938	-0.6699	1.067703044	0.30171163	-0.16573
27	10.503	0.777778	77.77778	1.285714	-0.76471	1.021313365	0.35482574	-0.21136
28	9.002	0.807018	80.70175	1.23913	-0.86696	0.954339009	0.439100871	-0.29097
29	6.71	0.836257	83.62573	1.195804	-0.97919	0.82672252	0.624516172	-0.49353
30	3.992	0.865497	86.54971	1.155405	-1.10535	0.601190533	1.03184018	-1.04814
31	1.93	0.894737	89.47368	1.117647	-1.25212	0.285557309	1.772702029	-2.36023
32	1.388	0.923977	92.39766	1.082278	-1.43234	0.142389466	2.174434572	-3.20641
33	0.482	0.953216	95.32164	1.04908	-1.67687	-0.316952962	3.740119429	-7.23316
34	0.001	0.982456	98.24561	1.017857	-2.10734	-3	21.31655858	-98.4182
						54.97751979	48.93791607	-92.9794

Flood frequency analysis table 2:

ARI	AEP (%)	Ky (G=-0.3)	LOG(Q_Y)	Q_Y	δ	Log CL5	CL5	Log CL95	CL95
1.010101	99	-3.416	-2.5429212	0.002865	7.37095	-0.01062	0.975847	-5.07522	8.41E-06
1.052632	95	-1.967	-0.7783704	0.166583	3.49915	0.423769	2.653193	-1.98051	0.010459
1.111111	90	-1.327	0.0010032	1.002313	2.32555	0.79995	6.308848	-0.79794	0.159242
1.25	80	-0.668	0.8035146	6.360842	1.73395	1.399216	25.07357	0.207813	1.613663
2	50	0.261	1.9348242	86.06453	1.35145	2.399117	250.6786	1.470531	29.54821
5	20	0.813	2.607034	404.6076	0.6445	2.828453	673.6792	2.385615	243.0048
10	10	0.982	2.8128374	649.8863	1.22595	3.234015	1714.015	2.39166	246.411
20	5	1.075	2.9260901	843.5098	1.94175	3.593182	3919.059	2.258998	181.5509
50	2	1.141	3.006463	1014.993	2.70105	3.934414	8598.32	2.078512	119.8154
100	1	1.1685	3.0399517	1096.356	3.12545	4.113706	12992.89	1.966198	92.51195
200	0.5	1.1855	3.0606539	1149.884	3.4422	4.243228	17507.65	1.87808	75.52312
500	0.2	1.198	3.075876	1190.902	3.73365	4.358578	22833.8	1.793174	62.11177

Required statistical inputs:

Mean (M)	1.616985876	
Standard Deviation (S)	1.217771388	
Skew (G)	-1.657694572	<== interpolate between g=-1.6 and -1.7
N	34	

Normal probability scale for FFA plot:

Y	Z-value	Y-zero
99	-2.3263479	1
95	-1.6448536	1
90	-1.2815516	1
80	-0.8416212	1
50	0	1
20	0.8416212	1
10	1.2815516	1
5	1.6448536	1
2	2.0537489	1
1	2.3263479	1
0.5	2.5758293	1
0.2	2.8781617	1

Appendix C – Detailed calculations

Parametric study calculations

50 year ARI:

According to the Department of Transport and Main Roads, the maximum recorded flooding event occurred in 1887 with the maximum flow velocity being 2.32 m/s. By using PDF X-Change viewer, the channel area for this flooding event was determined to be 605.16 m^2. Therefore, the discharge during this flooding event is:

$$Q = AV = 2.32 * 605.16 = 1403.97\ m^3/s$$

Using this data, the slope of the channel can be determined by using Manning's equation for open channel flow. This equation takes the following form:

$$V = \frac{1}{n} R^{\frac{2}{3}} S^{\frac{1}{2}}$$

Where:

n is the Manning's coefficient, which can be obtained from table 3.1:

Surface Material	Manning's Roughness Coefficient - *n* -
Asbestos cement	0.011
Asphalt	0.016
Brass	0.011
Brick	0.015
Canvas	0.012
Cast-iron, new	0.012
Clay tile	0.014
Concrete - steel forms	0.011
Concrete (Cement) - finished	0.012
Concrete - wooden forms	0.015
Concrete - centrifugally spun	0.013
Copper	0.011
Corrugated metal	0.022
Earth, smooth	0.018
Earth channel - clean	0.022
Earth channel - gravelly	0.025
Earth channel - weedy	0.030
Earth channel - stony, cobbles	0.035
Floodplains - pasture, farmland	0.035
Floodplains - light brush	0.050
Floodplains - heavy brush	0.075
Floodplains - trees	0.15
Galvanized iron	0.016
Glass	0.010
Gravel, firm	0.023
Lead	0.011
Masonry	0.025
Metal - corrugated	0.022
Natural streams - clean and straight	0.030
Natural streams - major rivers	0.035
Natural streams - sluggish with deep pools	0.040
Natural channels, very poor condition	0.060
Plastic	0.009
Polyethylene PE - Corrugated with smooth inner walls	0.009 - 0.015
Polyethylene PE - Corrugated with corrugated inner walls	0.018 - 0.025
Polyvinyl Chloride PVC - with smooth inner walls	0.009 - 0.011
Rubble Masonry	0.017
Steel - Coal-tar enamel	0.010
Steel - smooth	0.012
Steel - New unlined	0.011
Steel - Riveted	0.019
Vitrified Sewer	0.013 - 0.015
Wood - planed	0.012
Wood - unplaned	0.013
Wood stove pipe, small diameter	0.011 - 0.012
Wood stove pipe, large diameter	0.012 - 0.013

(Toolbox 2015)

Based on the images of the channel above, it can be seen that the channel can be classified as “Earth channel – weedy”, which yields a Manning’s coefficient, n = 0.03

S is the slope of the channel

R is the hydraulic radius, which is given by the equation:

$$R = \frac{A}{P}$$

Where:

A = wetted area. For the maximum flooding event, A = 605.16m^2

P = wetted perimeter. By using the "perimeter" tool in PDF X-change viewer, P = 293.54m

Therefore, the hydraulic radius is:

$$R = \frac{A}{P} = \frac{605.16}{293.54} = 2.0616m$$

Now, using the above equation, the approximate slope of the channel can be determined by working backwards. Rearranging for the slope and solving, the equation for the slope of a channel is:

$$S = \left(VNR^{\frac{3}{2}}\right)^2 = \left(2.32 * 0.03 * 2.0616^{\frac{3}{2}}\right)^2 = 0.042445 = 4.2445\%\ grade$$

By looking at the RL's in figure 3.12, it can be seen that the bed level is situated at approximately 15.3 metres below the soffit level of the girders. An estimate for the channel cross-sectional area can be made. By importing the ground profile into PDF X-change viewer and using the "area" measuring tool, the approximate area was found to be:

$$Channel\ area = 670.41m^2$$

Now the maximum velocities for the corresponding ARI's can be determined.

$$Max\ V\ (ARI\ 100) = \frac{1900}{670.41} = 2.834\ m/s$$

$$Max\ V\ (ARI\ 500) = \frac{2300}{670.41} = 3.282\ m/s$$

Therefore, assuming the 50 year ARI velocity as the minimum velocity, the velocity ranges for each ARI is:

$$V\ (ARI\ 50) = 2.32\ m/s$$

$$V\ (ARI\ 100) = 2.32 - 2.834\ m/s$$

$$V\ (ARI\ 500) = 2.32 - 3.43\ m/s$$

Now that the velocity ranges have been determined, the only parameter that is left to determine is the flood depths. The assumed flood depths for the simulation are given below:

Realistically, the increased water level will increase the cross-sectional area and will decrease the velocity as a result to produce the same discharge. Assuming the width of the section above the bridge deck is constant, new velocities can be calculated. This is shown below:

$$New\ V\ (100\ year\ ARI) = \frac{1900}{670.41 + (1 * 82.15)} = 2.525\ m/s$$

$$New\ V\ (500\ year\ ARI) = \frac{2200}{670.41 + (2.5 * 82.15)} = 2.512\ m/s$$

AS5100 load calculations

<u>Full submergence</u>

Drag force

Worst-case velocity scenarios

Pier

$$F_{du} = 0.5 * C_d * V_u^2 * A_d$$

Cd = 1.4

V50 = 2.32m/s

V100 = 2.834m/s

V500 = 3.43m/s

(pier) Ad1 = 685*(9820+1219-3370) *10^-6 = 5.25m^2

(headstock, full submergence) Ad2 = ((1067+685)/2*1676)*10^-6 = 1.47m^2

(headstock, partial submergence) Ad3 = ((887.85+685)/2)*890*10^-6 = 0.70m^2

Therefore, the drag forces are:

AEP	**Drag force (kN)**	**Drag Pressure (kPa)**
1 in 50 (Ad1)	19.78	3.77

1 in 50 (Ad3)	2.64	
1 in 100 (Ad1)	29.52	5.62
1 in 100 (Ad2)	8.26	
1 in 500 (Ad1)	43.24	8.24
1 in 500 (Ad2)	12.11	

Superstructures

$$F_{du} = 0.5 * C_d * V_u^2 * A_d$$

Relative submergence, $S_r = \frac{d_{wgs}}{d_{sp}}$

Proximity ratio, $P_r = \frac{y_{gs}}{d_{ss}}$

Sr = 1857/1857 = 1.00

Pr = (114.207-97.08)*1000/1857 = 9.22

So, Cd = 1.3

V100 = 2.834m/s

V500 = 3.43m/s

Ad = ((1372+485)*82150)*10^-6 = 152.55m^2

$$F_{du100} = 0.5 * 1.3 * 2.834^2 = 5.22\ kPa$$

$$F_{du500} = 0.5 * 1.3 * 3.43^2 * 152.55 = 7.65\ kPa$$

Worst-case flood height scenarios

Pier

$$F_{du} = 0.5 * C_d * V_u^2 * A_d$$

Cd = 1.4

V100 = 2.525m/s

V500 = 2.512m/s

(pier) Ad1 = 685*(9820+1219-3370) *10^-6 = 5.25m^2 (headstock, full submergence) Ad2 = ((1067+685)/2*1676)*10^-6 = 1.47m^2

Therefore, the drag forces are:

AEP	Drag force (kN)	Drag Pressure (kPa)
1 in 100 (Ad1)	23.43	4.46
1 in 100 (Ad2)	6.56	
1 in 500 (Ad1)	23.19	4.42
1 in 500 (Ad2)	6.49	

Superstructures

$$F_{du} = 0.5 * C_d * V_u^2 * A_d$$

Relative submergence, $S_r = \frac{d_{wgs}}{d_{sp}}$

Proximity ratio, $P_r = \frac{y_{gs}}{d_{ss}}$

AEP	**Sr**	**Pr**	**Cd**	**V (m/s)**	**Ad (m^2)**
1 in 100	1.54	8.22	1.8	2.525	152.55
1 in 500	2.346	8.22	1.8	2.512	

$$F_{du100} = 0.5 * 1.8 * 2.525^2 = 5.74\ kPa$$

$$F_{du500} = 0.5 * 1.8 * 2.512^2 = 5.68\ kPa$$

Lift force

Worse-case velocity scenarios

Piers

$$F_{Lu}^* = 0.5 C_L V_u^2 A_L$$

Cl = 0.9 (assume $\theta_w < 30°$)

V50 = 2.32m/s

V100 = 2.834m/s

V500 = 3.43m/s

(pier) AL1 = 1524*(9820+1219-3370)*10^-6 = 11.69m^2 (headstock, partial submergence) AL2 = 790*9000*10^-6 = 7.11m^2

(headstock, full submergence) AL3 = 1676*9000*10^-6 = 15.084m^2

Therefore, the lift forces are:

AEP	Drag force (kN)	Drag Pressure (kPa)
1 in 50 (AL1)	28.31	2.42
1 in 50 (AL2)	17.22	
1 in 100 (AL1)	42.25	3.61
1 in 100 (AL3)	54.52	
1 in 500 (AL1)	61.89	5.29
1 in 500 (AL3)	79.86	

Superstructures

$$F_{Lu}^{*} = 0.5C_L V_u^2 A_L$$

Sr = 1,

C_L = -2,0.1

V100 = 2.834m/s

V500 = 3.43m/s

For downward lift force:

C_L = -2

A_L = (9210-2*(305))*82150*10^-6 = 706.49m^2

$$F_{Lu100}^{*} = 0.5 * -2 * 2.834^2 = -8.03\ kPa$$

$$F_{Lu500}^{*} = 0.5 * -2 * 3.43^2 = -11.76\ kPa$$

For upward lift force:

C_L = 0.1

(girder) AL1 = 635*27383.33*10^-6 = 17.39m^2

(deck, outside) AL2 = 400.5*82150*10^-6 = 32.9m^2

Therefore, the lift forces are:

AEP	Drag force (kN)	Drag Pressure (kPa)
1 in 100 (AL1)	6.98	0.40
1 in 100 (AL2)	13.21	
1 in 500 (AL1)	10.23	0.59
1 in 500 (AL2)	19.35	

Worse-case flood height scenarios

Piers

$$F_{Lu}^{*} = 0.5 C_L V_u^2 A_L$$

Cl = 0.9 (assume $\theta_w < 30°$)

V100 = 2.525m/s

V500 = 2.512m/s

(pier) AL1 = 1524*(9820+1219-3370)*10^-6 = 11.69m^2

(headstock, full submergence) AL3 = 1676*9000*10^-6 = 15.084m^2

Therefore, the lift forces are:

AEP	Drag force (kN)	Drag Pressure (kPa)
1 in 100 (AL1)	33.54	2.87
1 in 100 (AL3)	43.28	
1 in 500 (AL1)	33.19	2.84
1 in 500 (AL3)	42.83	

Superstructures

$$F_{Lu}^{*} = 0.5 C_L V_u^2 A_L$$

AEP	Sr	CL
1 in 100	1.54	-2,0.1
1 in 500	2.346	-1.3,0

V100 = 2.525m/s

V500 = 2.512m/s

For downward lift force:

C_{L100} = -2

C_{L500} = -1.3

(Deck, middle) A_{L1} = (9210-2*(305))*82150*10^-6 = 706.49m^2

(Deck, outside) A_{L2} = 305*82150*10^-6 = 25.06m^2

AEP	Lift force (kN)	Lift Pressure (kPa)
1 in 100 (AL1)	-4504.32	6.38
1 in 100 (AL2)	-159.77	
1 in 500 (AL1)	-2897.73	4.10
1 in 500 (AL2)	-102.79	

For upward lift force:

C_L = 0.1

(girder) AL1 = 635*27383.33*10^-6 = 17.39m^2

(deck, outside) AL2 = 400.5*82150*10^-6 = 32.9m^2

Therefore, the lift forces are:

AEP	Lift force (kN)	Lift Pressure (kPa)
1 in 100 (AL1)	5.54	0.32
1 in 100 (AL2)	10.49	

Debris force

Worse-case velocity scenario

Pier

$$F^*_{du} = 0.5C_d V_u^2 A_{deb}$$

Vu50^2*y = 2.32^2*(111.56-97.08) = 77.94

Cd1 = 2.45

Vu100^2*y = 2.834^2*(114.207-97.08) = 97.34

Cd2 = 2.2

Vu500^2*y = 3.43^2*(114.207-97.08) = 201.50

Cd3 = 1.7

Adeb = 3*20 = 60m^2 (maximum usable dimensions)

$$F^*_{du50} = 0.5 * 2.45 * 2.32^2 = 6.59\ kPa$$

$$F^*_{du100} = 0.5 * 2.2 * 2.834^2 = 9.84\ kPa$$

$$F^*_{du500} = 0.5 * 1.7 * 3.43^2 = 14.41\ kPa$$

Superstructures

$$F^*_{du} = 0.5 C_d V_u^2 A_{deb}$$

Pr = 8.22

F100 = 2.834/(9.81*(114.207-97.08)) = 0.22

Cd100 = 1.8

F500 = 3.43/(9.81*(114.207-97.08)) = 0.26

Cd500 = 1.65

Adeb = 60m^2

$$F^*_{du100} = 0.5 * 1.8 * 2.834^2 = 7.23\ kPa$$

$$F^*_{du500} = 0.5 * 1.65 * 3.43^2 = 9.71\ kPa$$

Worse-case flood height scenario

Pier

$$F^*_{du} = 0.5 C_d V_u^2 A_{deb}$$

Vu100^2*y = 2.525^2*(115.207-97.08) = 97.34

Cd2 = 2.1

Vu500^2*y = 2.512^2*(116.707-97.08) = 201.50

Cd3 = 2.05

Adeb = 3*20 = 60m^2 (maximum usable dimensions)

$$F^*_{du100} = 0.5 * 2.1 * 2.525^2 = 6.69\ kPa$$

$$F^*_{du500} = 0.5 * 2.05 * 2.512^2 = 6.47\ kPa$$

Superstructures

$$F^*_{du} = 0.5 C_d V_u^2 A_{deb}$$

Pr = 8.22

F100 = 2.525/(9.81*(115.207-97.08)) = 0.2

Cd100 = 1.9

F500 = 2.512/(9.81*(116.707-97.08)) = 0.2

Cd500 = 1.9

Adeb = 60m^2

$$F^*_{du100} = 0.5 * 1.9 * 2.525^2 = 6.057 kPa$$

$$F^*_{du500} = 0.5 * 1.9 * 2.512^2 = 6.0 kPa$$

Log forces

$$F^*_{Lu} = \frac{0.5 m V_u^2}{s}$$

Assume log has a minimum mass, m = 2000kg.

Stopping distance, s = 75mm

Worse-case velocity scenarios

The channel is very wide, so assume it can hold 3 logs of this size. Apply 1 log force at each pier and another at the middle girder.

$$F_{Lu50}^{*} = \frac{0.5 * 2000 * 2.32^2}{0.075} = \frac{71.765\ kN}{0.3848m^2} = 186.50\ kPa$$

For 100 and 500 year ARI, apply

$$F_{Lu100}^{*} = \frac{0.5 * 2000 * 2.834^2}{0.075} = \frac{107.09\ kN}{0.3848m^2} = 278.30\ kPa$$

$$F_{Lu500}^{*} = \frac{0.5 * 2000 * 3.43^2}{0.075} = \frac{156.865\ kN}{0.3848m^2} = 407.65\ kPa$$

Worse-case flood height scenarios

$$F_{Lu100}^{*} = \frac{0.5 * 2000 * 2.525^2}{0.075} = \frac{85.008\ kN}{0.3848m^2} = 220.91\ kPa$$

$$F_{Lu500}^{*} = \frac{0.5 * 2000 * 2.512^2}{0.075} = \frac{84.135\ kN}{0.3848m^2} = 218.65\ kPa$$

Buoyancy

Headstock

Partially submerged:

Fb = ρgV = 1000*9.81*6.23 = 61.80kN/6.165 = 10.02kPa

Fully submerged:

Fb = ρgV = 1000*9.81*(1.676*9*(1.067+0.685)/2) = 129.63kN/6.165 = 21.027kPa

Girders

Fb = ρgV = 1000*9.81*27.383*(0.483*0.152+0.635*0.24+0.635*0.152+(0.483+0.152)/2*0.165+(0.635+0.152)/22*0.18) = 119.69kN/17.39 = 6.88kPa for each girder

Deck

Fb = ρgV = 1000*9.81*82.15*(0.305*0.485*2+8.6*0.18) = 1485.94kN/756.6 = 1.964kPa

First segment is between edge of the deck and the closest edge of the girders

Second segment is between the girders

Hydrostatic thrust

For partial submergence, using excel:

Flood level = 11877mm

For the piers:

Piers			
Element	Centroid location (y)	Distance to centroid from flood level (h)	Rectangular pressure prism (kPa)
1	10790.8	1086.20	10.66
2	10294.4	1582.60	15.53
3	9798	2079.00	20.39
4	9301.6	2575.40	25.26
5	8805.2	3071.80	30.13
6	8308.8	3568.20	35.00
7	7812.4	4064.60	39.87
8	7316	4561.00	44.74
9	6819.6	5057.40	49.61
10	6323.2	5553.80	54.48
11	5826.8	6050.20	59.35
12	5330.4	6546.60	64.22
13	4834	7043.00	69.09
14	4337.6	7539.40	73.96
15	3841.2	8035.80	78.83
16	3344.8	8532.20	83.70
17	2848.4	9028.60	88.57

Where:

y = vertical centroid location from the origin point

h = flood level – y

Therefore, using P = ρgh, the pressures for each element could be calculated.

Headstocks						
Element	a	b	Centroid	Centroid location (y)	Distance to centroid from flood level (h)	Rectangular pressure prism (kPa)
1	780.5	876	205.47	11671.53	205.47	2.02
2	685	780.5	204.95	11253.05	623.95	6.12

The same method was used for the headstocks as well, however the elements are trapezoidal, and therefore the centroid was calculated using the following formula:

$$\frac{h(2a+b)}{3(a+b)}$$

Where the dimensions were as follows:

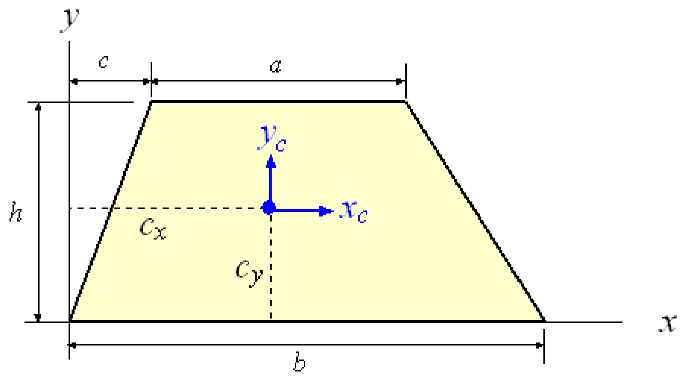

(efunda 2015)

The same method has been used for the other submergence conditions, as shown below.

For full submergence:

Flood level = 14772mm

For the piers:

Piers			
Element	Centroid location (y)	Distance to centroid from flood level (h)	Rectangular pressure prism (kPa)
1	10790.8	3981.2	39.06
2	10294.4	4477.6	43.93
3	9798	4974	48.79
4	9301.6	5470.4	53.66
5	8805.2	5966.8	58.53
6	8308.8	6463.2	63.40
7	7812.4	6959.6	68.27
8	7316	7456	73.14
9	6819.6	7952.4	78.01
10	6323.2	8448.8	82.88
11	5826.8	8945.2	87.75
12	5330.4	9441.6	92.62
13	4834	9938	97.49
14	4337.6	10434.4	102.36
15	3841.2	10930.8	107.23
16	3344.8	11427.2	112.10
17	2848.4	11923.6	116.97

For the headstocks:

Headstock						
Element	a	b	Centroid	Centroid location (y)	Distance to centroid from flood level (h)	Rectangular pressure prism (kPa)
1	971.5	1067	206.23	12508.77	2263.23	22.20
2	876	971.5	205.89	12090.11	2681.89	26.31
3	780.5	876	205.47	11671.53	3100.47	30.42
4	685	780.5	204.95	11253.05	3518.95	34.52

For the girders:

Girders							
Element	a	b	h	Centroid	Centroid location	Distance to centroid from flood level (h)	Rectangular pressure prism (kPa)
1	N/A	N/A	N/A	N/A	14211.00	561.00	5.50
2	152	483	165	68.17	14066.83	705.17	6.92
3	N/A	N/A	N/A	N/A	13811.25	960.75	9.42
4	N/A	N/A	N/A	N/A	13493.75	1278.25	12.54
5	152	635	180	71.59	13166.59	1605.41	15.75
6	N/A	N/A	N/A	N/A	13005.00	1767.00	17.33

For the deck:

Deck			
Element	Centroid location (y)	Distance to centroid from flood level (h)	Rectangular pressure prism (kPa)
1	14619.5	152.5	1.50
2	14377	395	3.87

For full submergence + 1m:

Flood level = 15772

For the piers:

Piers			
Element	Centroid location (y)	Distance to centroid from flood level (h)	Rectangular pressure prism (kPa)
1	10790.8	4981.2	48.87
2	10294.4	5477.6	53.74
3	9798	5974	58.60
4	9301.6	6470.4	63.47
5	8805.2	6966.8	68.34
6	8308.8	7463.2	73.21
7	7812.4	7959.6	78.08
8	7316	8456	82.95
9	6819.6	8952.4	87.82
10	6323.2	9448.8	92.69
11	5826.8	9945.2	97.56
12	5330.4	10441.6	102.43
13	4834	10938	107.30
14	4337.6	11434.4	112.17
15	3841.2	11930.8	117.04
16	3344.8	12427.2	121.91
17	2848.4	12923.6	126.78

For the headstocks:

Headstock						
Element	a	b	Centroid	Centroid location (y)	Distance to centroid from flood level (h)	Rectangular pressure prism (kPa)
1	971.5	1067	206.23	12508.77	3263.23	32.01
2	876	971.5	205.89	12090.11	3681.89	36.12
3	780.5	876	205.47	11671.53	4100.47	40.23
4	685	780.5	204.95	11253.05	4518.95	44.33

For the girders:

Girders							
Element	a	b	h	Centroid	Centroid location	Distance to centroid from flood level (h)	Rectangular pressure prism (kPa)
1	N/A	N/A	N/A	N/A	14211	1561	15.31
2	152	483	165	68.17	14066.83	1705.17	16.73
3	N/A	N/A	N/A	N/A	13811.25	1960.75	19.23
4	N/A	N/A	N/A	N/A	13493.75	2278.25	22.35
5	152	635	180	71.59	13166.59	2605.41	25.56
6	N/A	N/A	N/A	N/A	13005.00	2767.00	27.14

For the deck:

Deck			
Element	Centroid location (y)	Distance to centroid from flood level (h)	Rectangular pressure prism (kPa)
1	14619.5	1152.5	11.31
2	14377	1395	13.68

Also, there will be water pressure on the top of the deck from the extra water. This will create a uniform pressure distribution of $\rho gh = 9.81*1 = 9.81$kPa in the negative Y direction.

For full submergence + 2.5m:

Flood level = 17272mm

For the piers:

Piers			
Element	Centroid location (y)	Distance to centroid from flood level (h)	Rectangular pressure prism (kPa)
1	10790.8	6481.2	63.58
2	10294.4	6977.6	68.45
3	9798	7474	73.32
4	9301.6	7970.4	78.19
5	8805.2	8466.8	83.06
6	8308.8	8963.2	87.93
7	7812.4	9459.6	92.80
8	7316	9956	97.67
9	6819.6	10452.4	102.54
10	6323.2	10948.8	107.41
11	5826.8	11445.2	112.28
12	5330.4	11941.6	117.15
13	4834	12438	122.02
14	4337.6	12934.4	126.89
15	3841.2	13430.8	131.76
16	3344.8	13927.2	136.63
17	2848.4	14423.6	141.50

For the headstocks:

Headstock						
Element	a	b	Centroid	Centroid location (y)	Distance to centroid from flood level (h)	Rectangular pressure prism (kPa)
1	971.5	1067	206.23	12508.77	4763.23	46.73
2	876	971.5	205.89	12090.11	5181.89	50.83
3	780.5	876	205.47	11671.53	5600.47	54.94
4	685	780.5	204.95	11253.05	6018.95	59.05

For the girders:

Girders							
Element	a	b	h	Centroid	Centroid location	Distance to centroid from flood level (h)	Rectangular pressure prism (kPa)
1	N/A	N/A	N/A	N/A	14211.00	3061.00	30.03
2	152	483	165	68.17	14066.83	3205.17	31.44
3	N/A	N/A	N/A	N/A	13811.25	3460.75	33.95
4	N/A	N/A	N/A	N/A	13493.75	3778.25	37.06
5	152	635	180	71.59	13166.59	4105.41	40.27
6	N/A	N/A	N/A	N/A	13005.00	4267.00	41.86

For the deck:

Deck			
Element	Centroid location (y)	Distance to centroid from flood level (h)	Rectangular pressure prism (kPa)
1	14619.5	2652.5	26.02
2	14377	2895	28.40

Also, there will be water pressure on the top of the deck from the extra water. This will create a uniform pressure distribution of $\rho gh = 9.81*2.5 = 24.525$kPa in the negative Y direction.

Overall, this method of calculating the hydrostatic pressure is not 100% accurate as it is not accounting for the triangular pressure distribution on top of each of these rectangular pressure prisms, however, since the difference in height levels is below 500mm, the pressure difference would be quite small and it can be assumed that it will have a negligible effect, therefore it is an accurate method for this instance.

Partial submergence

In the event of partial submergence, traffic loads must be taken into account.

The most likely and most critical traffic scenario is the "M1600 moving traffic load", provided in clause 6.2.3 of AS5100.

The M1600 moving traffic load accounts for the loads applied by a moving stream of traffic. The load is assumed to act within a standard design lane with a width of 3.2m, as shown in the figure below:

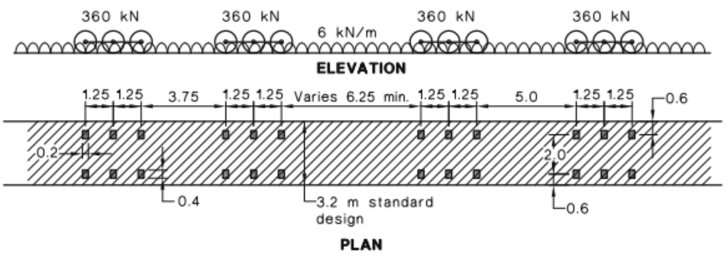

(Standards 2004b)

As shown in the figure above, the applied traffic loads can be taken as a 360kN load acting over an area of 2.5m x 2m, as well as a line load of 6kN/m acting through the centre of the lane. For Tenthill Bridge, there are 2 standard design lanes, therefore table 6.6 shall be taken into account.

TABLE 6.6

ACCOMPANYING LANE FACTORS

Standard design lane number, n	Accompanying lane factor, ALF_i
1 lane loaded	1.0
2 lanes loaded	1.0 for first lane; and 0.8 for second lane
3 or more lanes loaded	1.0 for first lane; 0.8 for second lane; and 0.4 for third and subsequent lanes

NOTES:

1 First lane—the loaded lane giving the largest effect.

2 Second lane—the loaded lane giving the second largest effect.

(Standards 2004b)

It is more likely that one lane will be loaded, rather than both lanes being loaded simultaneously. Furthermore, the most critical effect that the traffic loading will have on the bridge is when the downstream end is loaded (which will contribute to overturning), hence only the downstream lane will be loaded for the simulation.

Following clause 6.7, a dynamic load allowance shall be taken into consideration to account for the interaction between moving vehicles and the bridge structure. The dynamic load allowance can be obtained from table 6.7.2, as seen below:

TABLE 6.7.2

DYNAMIC LOAD ALLOWANCE (α)

Loading	Dynamic load allowance (α)
W80 wheel load	0.4
A160 axle load	0.4
M1600 tri-axle group (see Note 2)	0.35
M1600 load (see Note 2)	0.30
S1600 load (see Note 2)	0
HLP loading	0.1

NOTES:

1 Dynamic load allowance is not required for centrifugal forces, braking forces or pedestrian load.

2 Including the UDL component of the traffic load.

(Standards 2004b)

As the M1600 load is the only load being taken into account, α = 0.3, hence:

$$M1600\ load = (1+\alpha) * load\ factor * action\ under\ consideration$$

Where:

Load factor = 1.0

TABLE 6.10(A)

LOAD FACTORS FOR DESIGN ROAD TRAFFIC LOADS

Traffic load	Limit state	
	Ultimate	Serviceability
W80 wheel load	1.8	1.0
A160 axle load	1.8	1.0
M1600 moving traffic load	1.8	1.0
S1600 stationary traffic load	1.8	1.0
Heavy load platform load	1.5	1.0

Hence,

$$Total\ traffic\ load = 1.3 * M1600\ load$$

BA59/94 load calculations

Drag force on piers:

$$F_D = \frac{C_D \rho U_o^2}{2000}$$

Where:

Uo = 2.512m/s

ρ = 1000kg/m^3

C_D = 0.4

$$F_D = \frac{0.4 * 1000 * 2.512^2}{2000} = 1.262\ kPa$$

Lift force on piers:

$$F_L = \frac{C_L \rho U_o^2}{2000}$$

Where:

C_L = 0.8

$$F_L = \frac{0.8 * 1000 * 2.512^2}{2000} = 2.524\ kPa$$

Drag force on superstructures:

$$F_d = \frac{C_d \rho U_o^2}{2000}$$

C_d = 2.2

$$F_d = \frac{2.2 * 1000 * 2.512^2}{2000} = 6.941\ kPa$$

Log force:

$$F = \frac{mv^2}{2d}$$

Where:

m = 2000kg

v = 2.512m/s

d = 0.075m

$$F = \frac{2000 * 2.512^2}{2 * 0.075} = 84.135\ kN$$

Debris force:

$$P = 0.517U_o^2$$

Where:

U_o = 2.512m/s

$$P = 0.517 * 2.512^2 = 3.262\ kPa$$

AASHTO load calculations

Drag force on piers:

$$F_d^* = \frac{C_D V^2}{2}$$

Where:

C_D = 1.4

V = 2.512m/s

$$F_d^* = \frac{1.4 * 2.512^2}{2} = \quad 4.417\ kPa$$

Lift force on piers:

$$F_L^* = \frac{C_L V^2}{2}$$

Where:

C_L = 1.0 (θ>30 degrees)

$$F_L^* = \frac{1 * 2.512^2}{2} = 3.155\ kPa$$

Debris force:

$$F_d^* = \frac{C_D V^2}{2}$$

$C_D = 0.5$

$$F_d^* = \frac{0.5 * 2.512^2}{2} = 1.577\ kPa$$

Indian Code of Practice calculations

$$P = 52KV^2 * \frac{9.81}{1000}$$

Where:

V = sqrt(2)*2.512 = 3.553m/s

K = 1.5

$$P = 52 * 1.5 * 3.553^2 * \frac{9.81}{1000} = 9.659\ kPa$$

This needs to be broken up into a longitudinal (drag) and lateral (lift) component. This can be done by simple trigonometry.

Assuming the angle between the centreline of the pier and the direction of the water flow is 30 degrees:

$$Drag\ force = 9.659 * \cos(30) = 8.365\ kPa$$

$$Lift\ force = 9.659 * \sin(30) = 4.8295\ kPa$$

Appendix D – Flood load values

AS5100 flood loads

The different loads are shown in the tables below.

For 50 year ARI:

Force type	Force value	Force direction
Drag force	3.77 kPa	Negative X-direction
Lift force	2.42 kPa	+- Z-direction
Debris force	6.59 kPa	Negative X-direction
Log force	186.50 kPa	Negative X-direction
Buoyancy	10.02 kPa	Positive Y-direction
Hydrostatic thrust	2.01 – 88.57 kPa	+- X and Z direction
Traffic load (wheel forces)	78 kN per wheel	Negative Y-direction
Traffic load 2 (strip load)	13.89 5kPa	Negative Y-direction

For 100 year ARI:

Force type	Force value	Force direction	Component the force is acting on	Worse-case velocity of flood height scenario
Drag force	5.62 kPa	Negative X-direction	Piers	Velocity scenario
Drag force	5.22 kPa	Negative X-direction	Superstructures	Velocity scenario
Drag force	4.46 kPa	Negative X-direction	Piers	Flood height scenario
Drag force	5.74 kPa	Negative X-direction	Superstructures	Flood height scenario
Lift force	3.61 kPa	+- Z-direction	Piers	Velocity scenario
Lift force	0.4 kPa	Positive Y-direction	Superstructures	Velocity scenario

Lift force	8.03 kPa	Negative Y-direction	Superstructures	Velocity scenario
Lift force	2.87 kPa	+- Z-direction	Piers	Flood height scenario
Lift force	0.32 kPa	Positive Y-direction	Superstructures	Flood height scenario
Lift force	6.38 kPa	Negative Y-direction	Superstructures	Flood height scenario
Debris force	9.84 kPa	Negative X-direction	Piers	Velocity scenario
Debris force	7.23 kPa	Negative X-direction	Superstructures	Velocity scenario
Debris force	6.69 kPa	Negative X-direction	Piers	Flood height scenario
Debris force	6.057 kPa	Negative X-direction	Superstructures	Flood height scenario
Log force	278.30 kPa	Negative X-direction	Superstructures + piers	Velocity scenario
Log force	220.91 kPa	Negative X-direction	Superstructures + piers	Flood height scenario
Buoyancy	21.027 kPa	Positive Y-direction	Headstock	n/a
Buoyancy	6.88 kPa	Positive Y-direction	Girders	n/a
Buoyancy	1.964 kPa	Positive Y-direction	Deck	n/a
Hydrostatic thrust	1-49 – 3.87 kPa	+- X-direction	Deck	Velocity scenario
Hydrostatic thrust	5.5 – 17.33 kPa	+- X-direction	Girders	Velocity scenario
Hydrostatic thrust	22.2 – 34.52 kPa	+-X and Z-direction	Headstocks	Velocity scenario

Hydrostatic thrust	39.05 – 116.97 kPa	+- X and Z-direction	Piers	Velocity scenario
Hydrostatic thrust	11.3 – 13.68 kPa	+- X-direction	Deck	Flood height scenario
Hydrostatic thrust	15.31 – 27.14 kPa	+- X-direction	Girders	Flood height scenario
Hydrostatic thrust	32.01 – 44.33 kPa	+- X and Z-direction	Headstocks	Flood height scenario
Hydrostatic thrust	48.86 – 126.78 kPa	+- X and Z direction	Piers	Flood height scenario

For 500 year ARI:

Force type	**Force value**	**Force direction**	**Component the force is acting on**	**Worse-case velocity of flood height scenario**
Drag force	8.24 kPa	Negative X-direction	Piers	Velocity scenario
Drag force	7.65 kPa	Negative X-direction	Superstructures	Velocity scenario
Drag force	4.42 kPa	Negative X-direction	Piers	Flood height scenario
Drag force	5.68 kPa	Negative X-direction	Superstructures	Flood height scenario
Lift force	5.29 kPa	+- Z-direction	Piers	Velocity scenario
Lift force	0.59 kPa	Positive Y-direction	Superstructures	Velocity scenario
Lift force	11.76 kPa	Negative Y-direction	Superstructures	Velocity scenario
Lift force	2.84 kPa	+- Z-direction	Piers	Flood height scenario
Lift force	0 kPa	Positive Y-direction	Superstructures	Flood height scenario
Lift force	4.10 kPa	Negative Y-direction	Superstructures	Flood height scenario

Debris force	14.41 kPa	Negative X-direction	Piers	Velocity scenario
Debris force	9.71 kPa	Negative X-direction	Superstructures	Velocity scenario
Debris force	6.47 kPa	Negative X-direction	Piers	Flood height scenario
Debris force	6.0 kPa	Negative X-direction	Superstructures	Flood height scenario
Log force	407.65 kPa	Negative X-direction	Superstructures + piers	Velocity scenario
Log force	218.65 kPa	Negative X-direction	Superstructures + piers	Flood height scenario
Buoyancy	21.027 kPa	Positive Y-direction	Headstock	n/a
Buoyancy	6.88 kPa	Positive Y-direction	Girders	n/a
Buoyancy	1.964 kPa	Positive Y-direction	Deck	n/a
Hydrostatic thrust	1-49 – 3.87 kPa	+- X-direction	Deck	Velocity scenario
Hydrostatic thrust	5.5 – 17.33 kPa	+- X-direction	Girders	Velocity scenario
Hydrostatic thrust	22.2 – 34.52 kPa	+-X and Z-direction	Headstocks	Velocity scenario
Hydrostatic thrust	39.05 – 116.97 kPa	+- X and Z-direction	Piers	Velocity scenario
Hydrostatic thrust	26.02 – 28.39 kPa	+- X-direction and –Y-direction	Deck	Flood height scenario

Hydrostatic thrust	30.02 – 41.85 kPa	+- X-direction	Girders	Flood height scenario
Hydrostatic thrust	46.72 – 59.04 kPa	+- X and Z-direction	Headstocks	Flood height scenario
Hydrostatic thrust	63.58 – 141.49 kPa	+- X and Z direction	Piers	Flood height scenario

BA59/94 flood loads

Force type	**Force value**	**Force direction**	**Bridge component the forces act on**
Drag force	1.262 kPa	Negative X-direction	Piers
Lift force	2.524 kPa	+-Z-direction	Piers
Drag force	6.941 kPa	Negative X-direction	Superstructures
Debris force	3.262 kPa	Negative X-direction	Superstructures
Log force	84.135 kN	Negative X-direction	Piers and girders
Buoyancy	21.027 kPa	Positive Y-direction	Headstock
Buoyancy	6.88 kPa	Positive Y-direction	Girders
Buoyancy	1.964 kPa	Positive Y-direction	Deck
Hydrostatic thrust	26.02 – 28.39 kPa	+- X-direction and –Y-direction	Deck
Hydrostatic thrust	30.02 – 41.85 kPa	+- X-direction	Girders

Hydrostatic thrust	46.72 – 59.04 kPa	+- X and Z-direction	Headstocks
Hydrostatic thrust	63.58 – 141.49 kPa	+- X and Z direction	Piers

AASHTO

Force type	**Force value**	**Force direction**	**Bridge component the forces act on**
Drag force	4.417 kPa	Negative X-direction	Piers
Lift force	3.155 kPa	+-Z-direction	Piers
Debris force	1.577 kPa	Negative X-direction	Superstructures
Buoyancy	21.027 kPa	Positive Y-direction	Headstock
Buoyancy	6.88 kPa	Positive Y-direction	Girders
Buoyancy	1.964 kPa	Positive Y-direction	Deck
Hydrostatic thrust	26.02 – 28.39 kPa	+- X-direction and –Y-direction	Deck
Hydrostatic thrust	30.02 – 41.85 kPa	+- X-direction	Girders
Hydrostatic thrust	46.72 – 59.04 kPa	+- X and Z-direction	Headstocks
Hydrostatic thrust	63.58 – 141.49 kPa	+- X and Z direction	Piers

Indian Code of Practice

Force type	**Force value**	**Force direction**	**Bridge component the forces act on**
Drag force	8.365 kPa	Negative X-direction	Piers
Lift force	4.8925 kPa	+-Z-direction	Piers
Buoyancy	21.027 kPa	Positive Y-direction	Headstock
Buoyancy	6.88 kPa	Positive Y-direction	Girders
Buoyancy	1.964 kPa	Positive Y-direction	Deck
Hydrostatic thrust	26.02 – 28.39 kPa	+- X-direction and –Y-direction	Deck
Hydrostatic thrust	30.02 – 41.85 kPa	+- X-direction	Girders
Hydrostatic thrust	46.72 – 59.04 kPa	+- X and Z-direction	Headstocks
Hydrostatic thrust	63.58 – 141.49 kPa	+- X and Z direction	Piers

Appendix E – Tenthill bridge Strand7 model results figures

The deflected shape of the Tenthill Bridge model are shown below, set at 5% displacement scale:

AS5100 results

XYZ displacement figures:

Load combination cases 1 and 2:

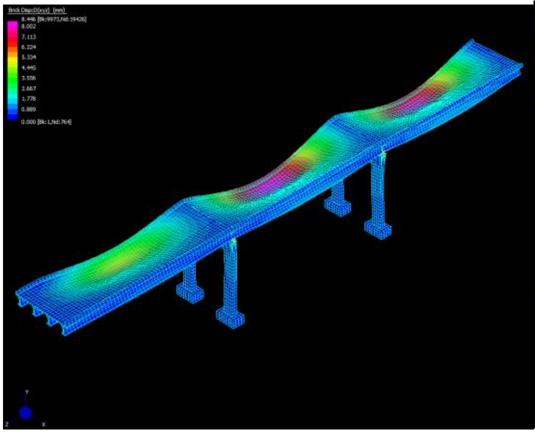

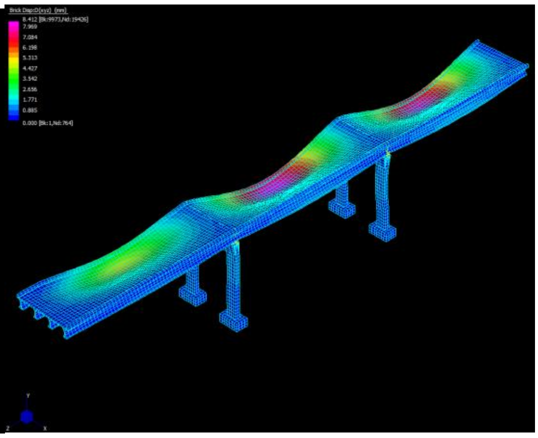

Load combinations 3 and 4:

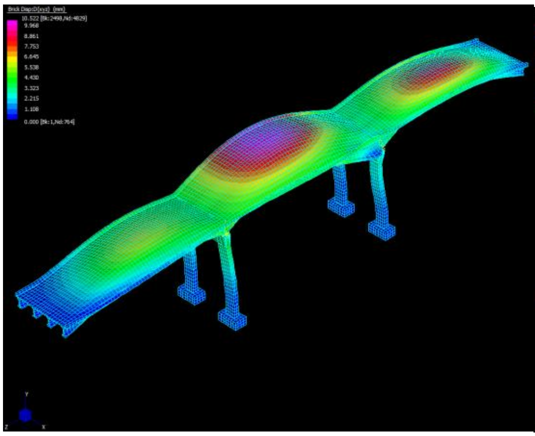

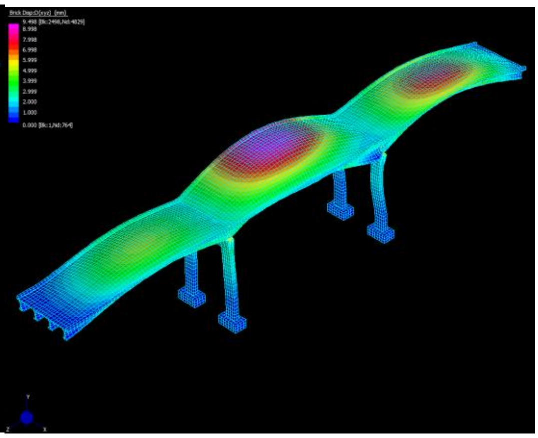

Load combinations 5 and 6:

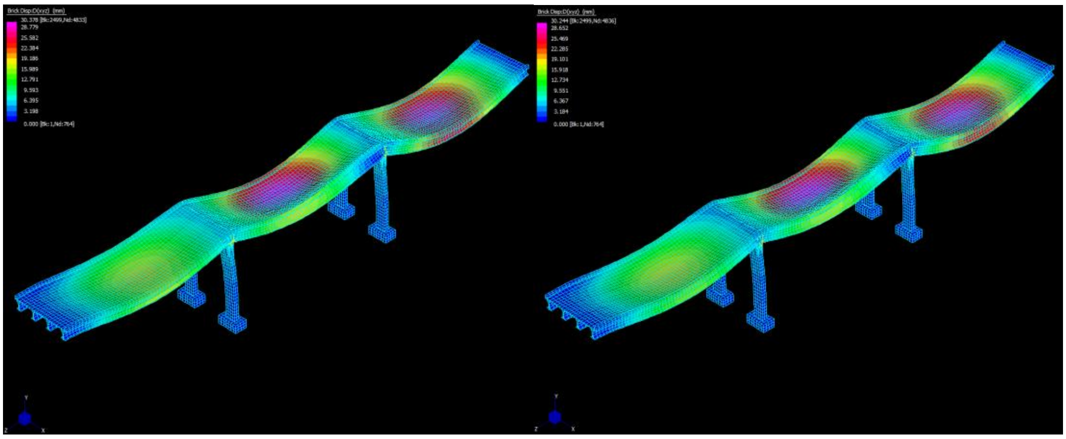

Load combinations 7 and 8:

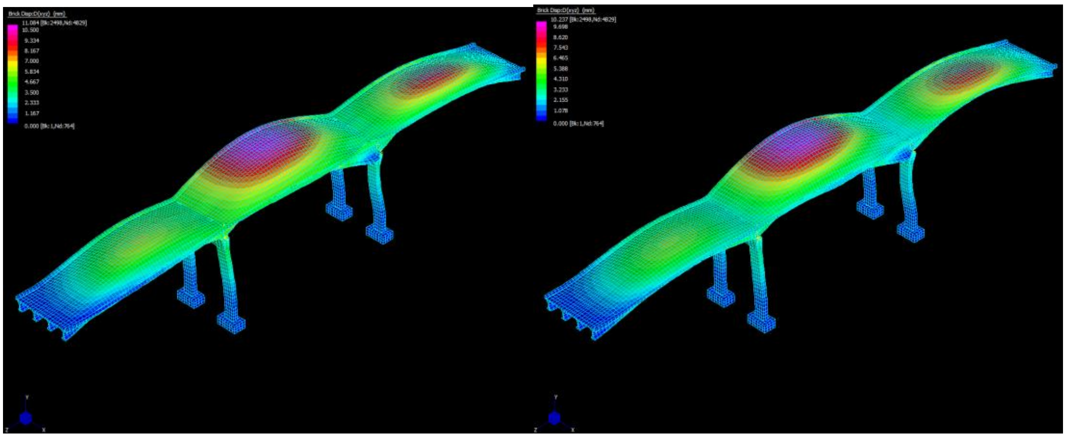

Load combinations 9 and 10:

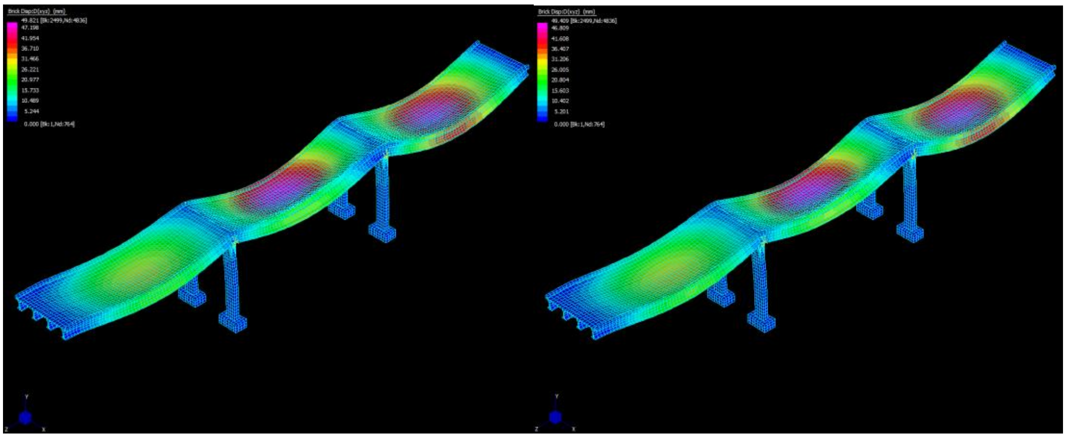

Mean XYZ stress concentration:

Load combinations 1 and 2:

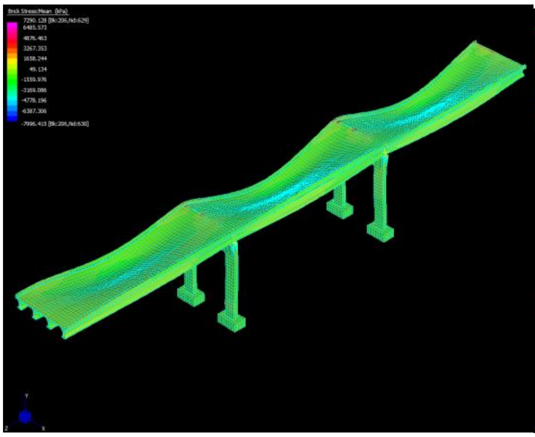 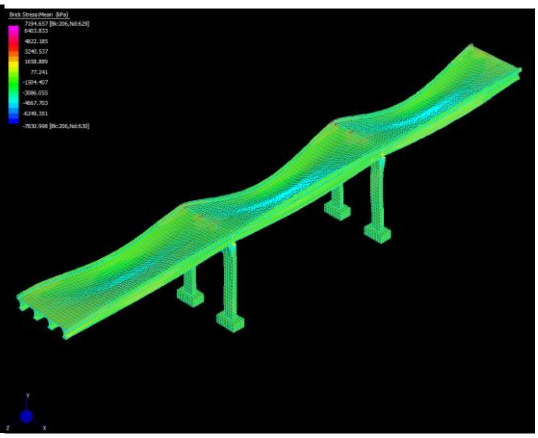

Load combinations 3 and 4:

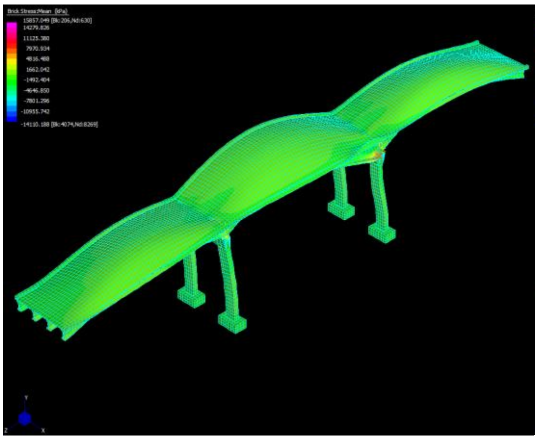 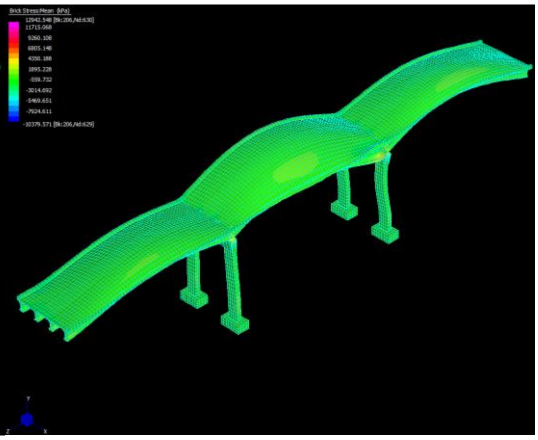

Load combinations 5 and 6:

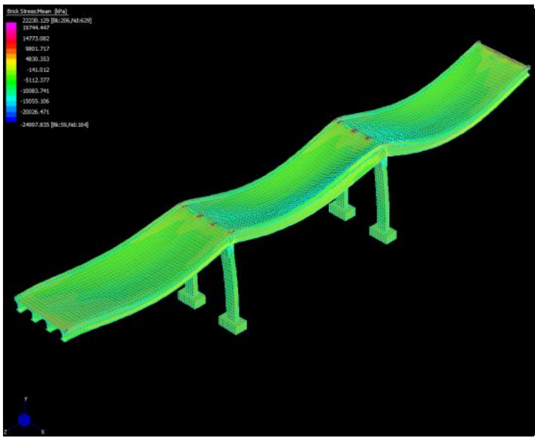 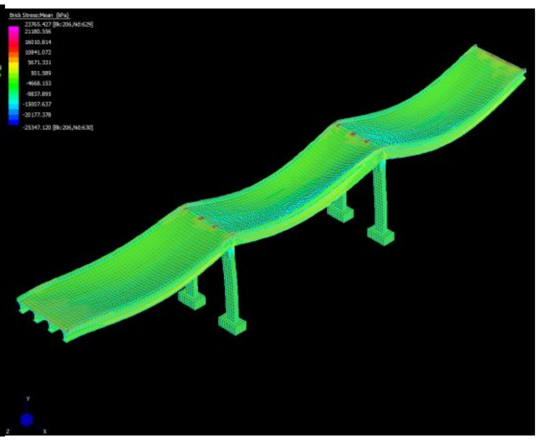

Load combinations 7 and 8:

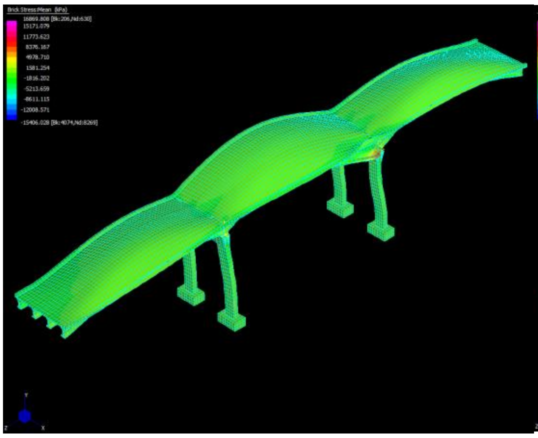
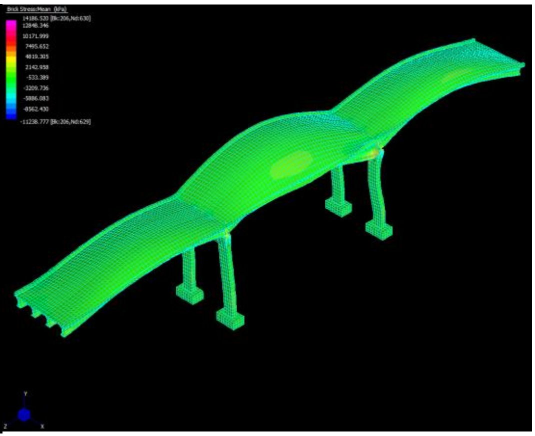

Load combinations 9 and 10:

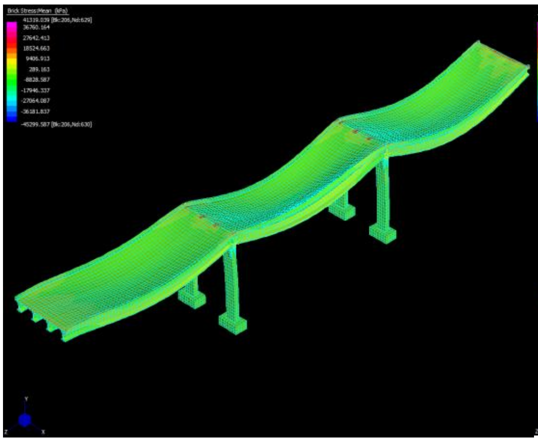
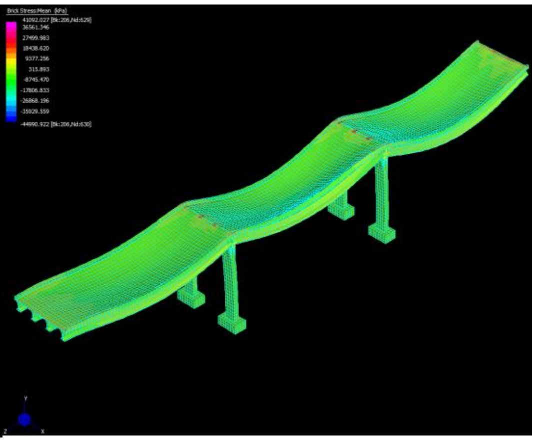

BA 59/94 results

XYZ displacement results:

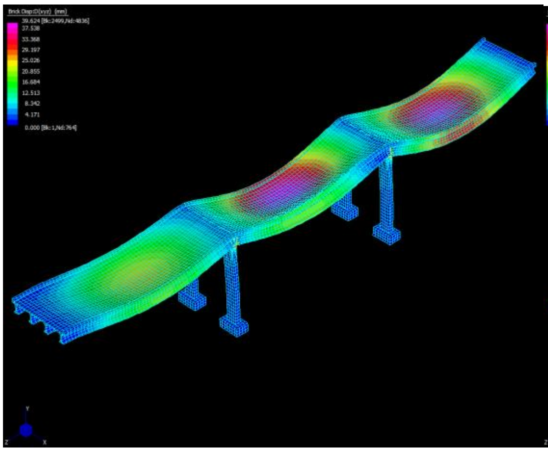
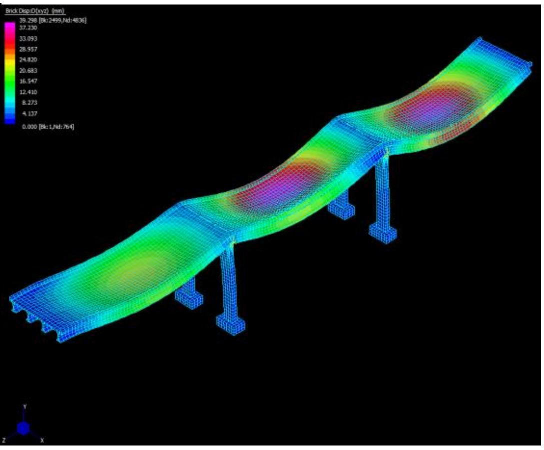

Mean stress concentration results:

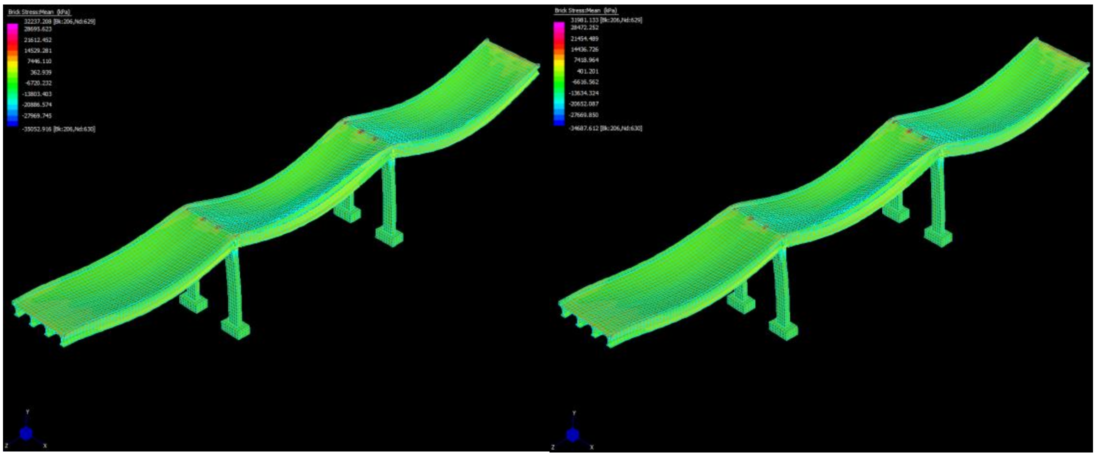

AASHTO results

Displacement results:

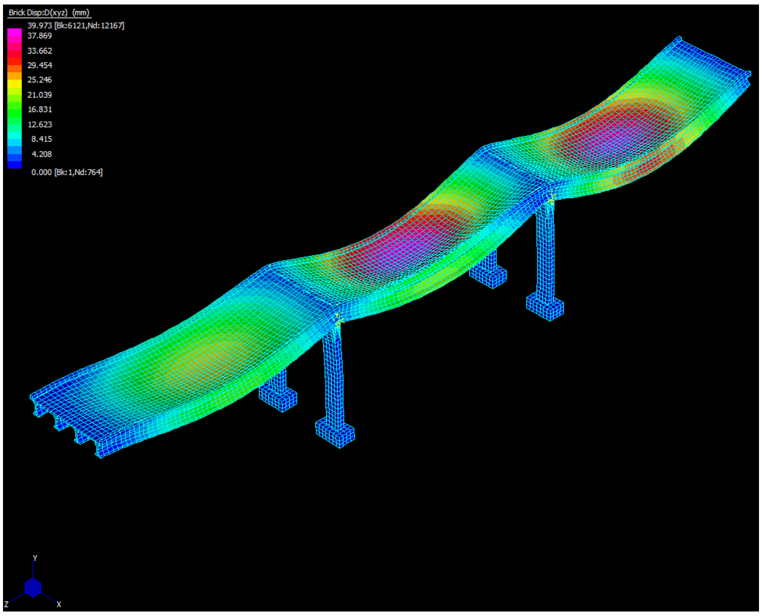

Stress concentration results:

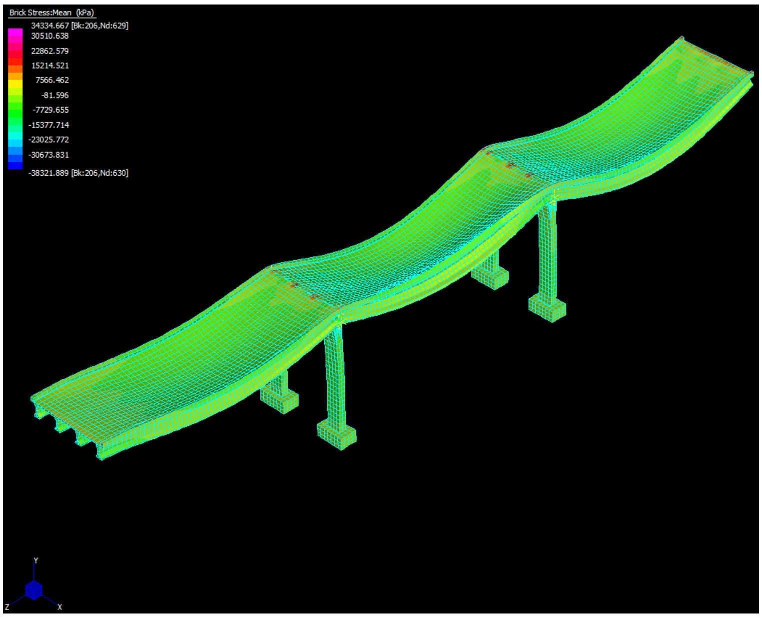

Indian Code of Practice Results:

Displacement results:

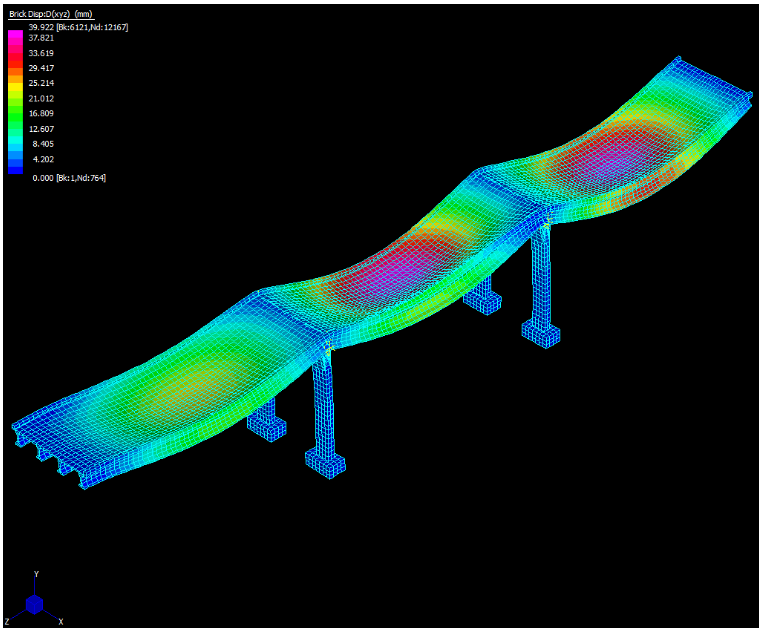

Stress concentration results:

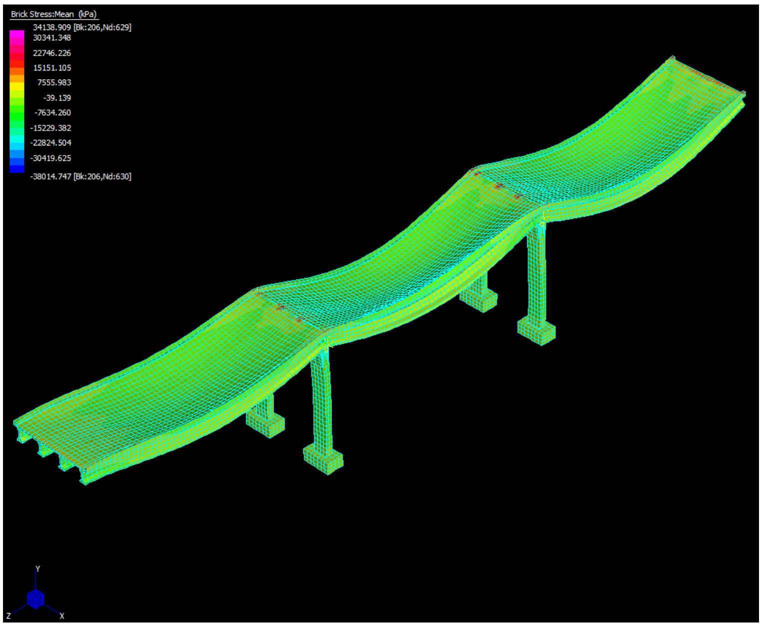
Brick Stress:Mean (kPa)
34138.909 [Bk:206,Nd:629]
30341.348
22746.226
15151.105
7555.983
-39.139
-7634.260
-15229.382
-22824.504
-30419.625
-38014.747 [Bk:206,Nd:630]
Y
Z
X

Appendix F – Resource Requirements

Resources that will be utilised in this project consists of project specific software including:

- Licenses and software locks
- A computer capable of running the required software and reading the data

The project specific software utilised in this project consists of Strand7. The University of Southern Queensland has access to the required software and the associated licenses and software locks, therefore the simulations will be run on the computers located in Z-block at USQ. Due to a limited amount of access time (8:00am to 5:00pm) to the computer laboratories during the day, after-hours access was granted to the author (8:00am to 12:00am). The networked computer laboratories used for this project are:

- Z308 – CATLab: CAD laboratory
- Z310/Z311 – General-purpose PC workstations

Appendix G – Risk Assessment

The risks associated with the activity are minimal from a physical point of view. A possible physical risk could be staring at a computer screen for extended periods of time which could result in eye strain, fatigue and/or stress. This could be avoided by taking regular breaks, as well as having plenty of water and food available.

The risks of damage are somewhat more prevalent as the computer software, hardware and data files could be damaged. The strategies for avoiding these situations are as follows:

- All of the data and files used in the project will be copied to an external hard drive that is stored at the home of the author. Therefore if any data is lost or corrupt, the data and files can be easily re-obtained.

Furthermore, as the simulations will be run on the Universities computers, there could be unexpected hardware, network access, software and printing problems. If any problems are to arise, they will be reported to the ICT Help Desk.